LAMONT-DOHERTY GEOLOGICAL OBSERVATORY

OF COLUMBIA UNIVERSITY

PALISADES, NEW YORK

Results of IPOD Site Survey Aboard R/V VEMA Cruise 3206

PART A: DATA REPORT

William J. Ludwig and Philip D. Rabinowitz

Technical Report No. CU-1-75

International Phase of Ocean Drilling Grant 25905

of National Science Foundation Subcontract UC-NSF-C842-2

Preface

The International Phase of Ocean Drilling (IPOD) sponsored by the National Science Foundation is the fourth phase of the Deep-Sea Drilling Project. The IPOD site survey management is situated at Lamont-Doherty Geological Observatory of Columbia University under the general supervision of Dr. Marcus Langseth. The site surveying was done under a sub-contract from Scripps Institute of Oceanography (International Phase of Ocean Drilling Grant 25905 of the National Science Foundation Grant UC-NSF-842-2).

We wish to thank the officers crew and scientific staff aboard R/V VEMA for their cooperation in gathering the data.

SHIPBOARD PARTICIPANTS

VEMA 3206
Dakar to San Juan

CREW

Cunningham, Peter	Master
Nass, Kerry	2nd Officer
Schnare, Thomas	3rd Officer
Johnson, Robert	Radio Officer
Williams, William	Bosun
Walker, Thomas	O.S.
Nicholson, Allan	O.S.
Himmelman, Eric	O.S.
Boehner, Martin	O.S.
Griswold, William	O.S.
Roache, David	O.S.
Pentz, Clarence	Chief Engineer
Rent, William	2nd Engineer
Knickle, Clyde	3rd Engineer
Murphy, Alphonse	Oiler
Hull, Joseph	Chief Steward
Forde, Ivan	Cook
Edwards, George	Messman
Creaser, Thomas	Messman

SCIENTISTS

Ludwig, William	Chief-Scientist
Carpenter, George	Asst. Chief Scientist
Ongley, Lois	T'grad
Hubbard, Arthur	Ocean Bott. Seismic
Brock, Robert	E.T.
Antle, Michael	Airgun
Bogart, Richard	Camera
Brown, Walter	Computer Tech.
Gutierrez, Carlos	E.T.
Holland, David	E.T.
Knickle, Lloyd	Coring Bosun
Paisley-Smith, Van	Gravity
Pratt, David	Core Describer

TABLE OF CONTENTS

Introduction

The purpose of this report is to present the underway geophysical measurements (navigation, bathymetric, gravimetric, geomagnetic, seismic reflection and sonobuoy refraction) as well as station data (coring, heat flow, bottom photography) collected aboard R/V VEMA during cruise 3206. The cruise was devoted to surveying two sites (sites 7 and 8) for the International Phase of Ocean Drilling (IPOD) program.

Site 8 is the VEMA fracture zone which offsets the mid-Atlantic ridge about 300 km at 11°N. Site 7 is situated in the region of the oldest magnetic anomalies seaward of the Cretaceous quiet zone in the eastern North Atlantic (anomalies 31 to 34; 75 to ∿81 m.y.b.p.). Site 7 was chosen to lie along the same synthetic flow line and same age but on the opposite side of the ridge as site 3 (surveyed aboard R/V VEMA cruise 3207).

Two seismic refraction experiments were made on site 7 by shooting a start-shaped pattern of shots to three ocean bottom seismometers (OBS) in a triangular array. One OBS star experiment was carried out in site 8 as well as refraction profiles with extended range sonobuoys. The results of these seismic experiments as well as the interpretation of the data obtained on sites 7 and 8 will be presented in forthcoming reports.

Instrumentation

The Navy satellite navigation system (Guier, 1966) was used to obtain frequent and precise fixes. The ship's electromagnetic (E-M) log and gyrocompass were used to interpolate the ship's track between satellite fixes by employing the computer techniques of Talwani (1969). These interpolated ship positions should be generally accurate to better than 0.5 nautical mile.

Both 12 kHz and 3.5 kHz transducers were used with a redesigned Westrex Mark V recorder for the precision depth measurements. Relative

and techniques used to measure temperature and conductivity in the deep sea, the reader is referred to Gerard et al. (1960) and Langseth (1965).

The Ewing-Thorndike deep-sea camera used on this cruise was similar to that described by Thorndike (1959).

SECTION 1

UNDERWAY GEOPHYSICAL DATA

PART A: Navigation

PART B: Bathymetric, geomagnetic and gravity profiles

PART C: Seismic Reflection Records

PART D: Sonobuoy Results

PART A

Navigation

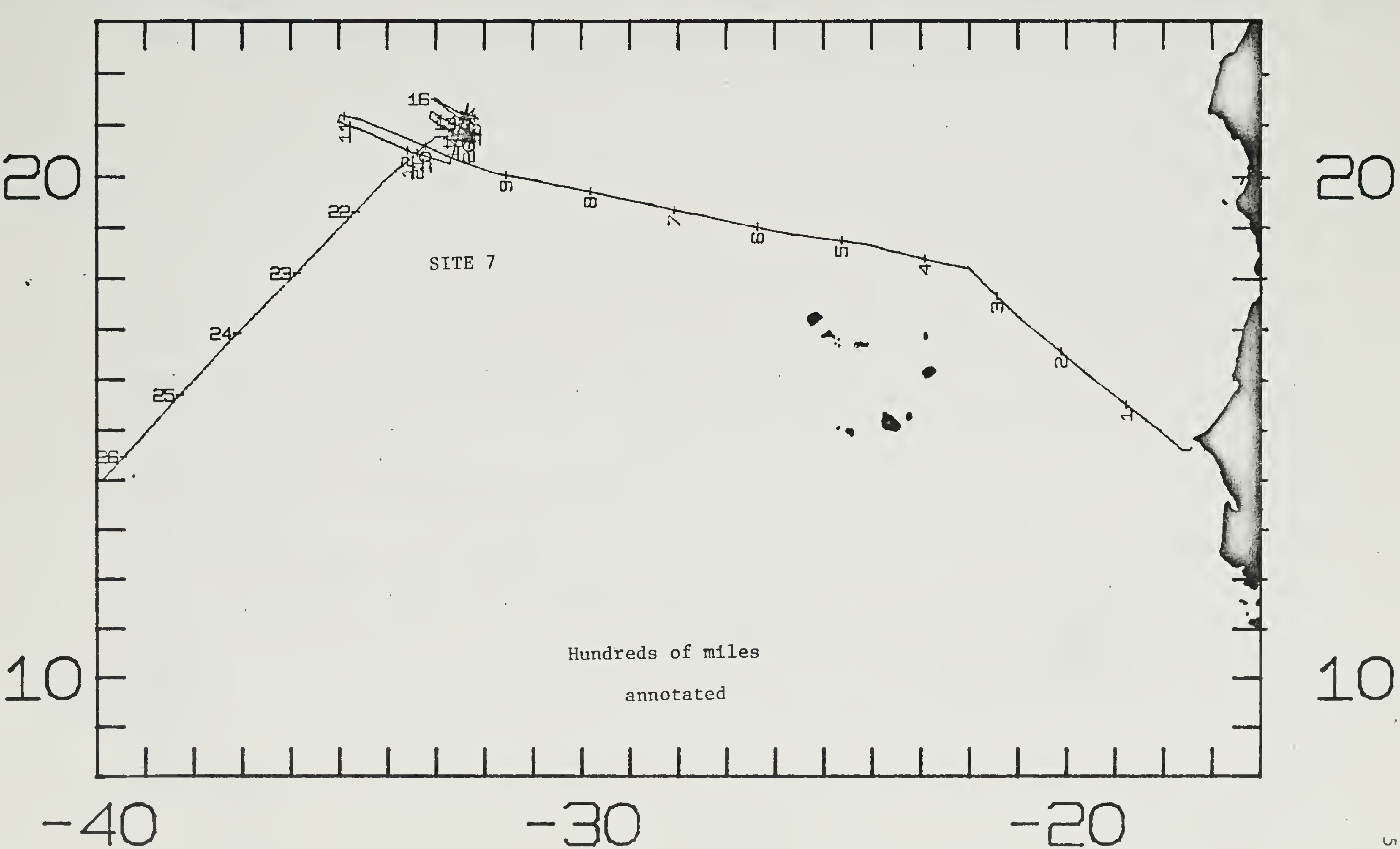

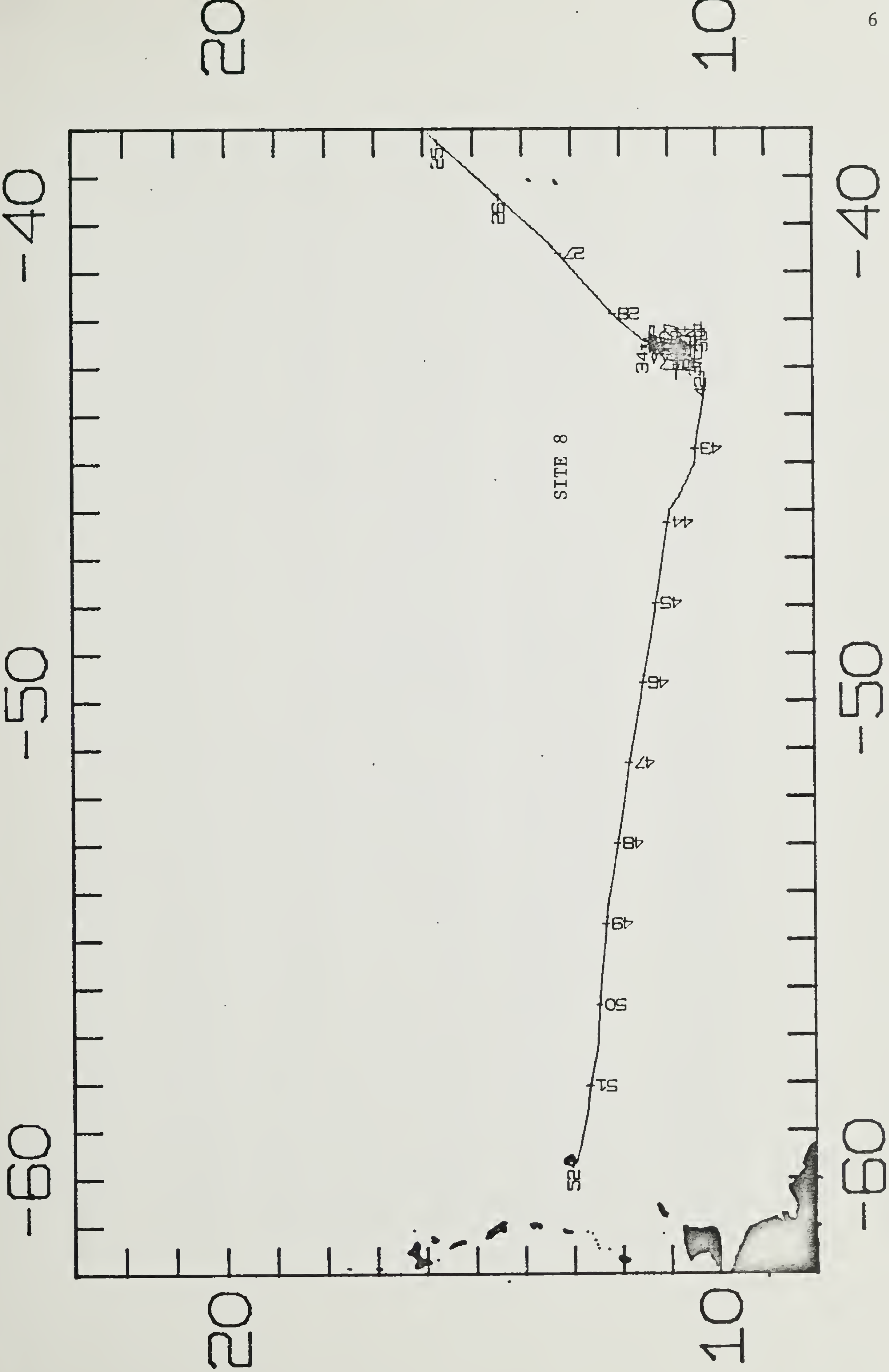
-60
-50
-40
20
10
SITE 8
25
26
27
28
34
42
43
44
45
46
47
48
49
50
51
52

DAY	MON	YEAR	TZ	TIME	LATITUDE	LONGITUDE	DISTANCE	SPEED	COURSE
18	2	1975	0.0	1338	14 39.7	-17 24.8	0.0	8.2	179
18	2	1975	0.0	1346	14 38.6	-17 24.8	1.1	7.5	216
18	2	1975	0.0	1350	14 38.2	-17 25.1	1.6	6.0	238
18	2	1975	0.0	1355	14 37.9	-17 25.5	2.1	8.6	216
18	2	1975	0.0	14 9	14 36.3	-17 26.8	4.1	8.1	269
18	2	1975	0.0	15 0	14 36.2	-17 33.8	11.0	3.6	267
18	2	1975	0.0	1530	14 36.1	-17 35.7	12.8	6.7	310
18	2	1975	0.0	1548	14 37.4	-17 37.3	14.8	7.9	312
18	2	1975	0.0	1734	14 46.7	-17 48.1	28.8	8.0	310
18	2	1975	0.0	1830	14 51.5	-17 54.1	36.3	8.2	310
18	2	1975	0.0	1836	14 52.0	-17 54.7	37.1	8.0	308
18	2	1975	0.0	1948	14 58.0	-18 2.5	46.7	7.1	344
18	2	1975	0.0	20 0	14 59.3	-18 3.0	48.1	8.2	308
18	2	1975	0.0	21 2	15 4.6	-18 9.8	56.6	7.9	307
18	2	1975	0.0	2224	15 11.1	-18 18.8	67.4	7.7	309
18	2	1975	0.0	2250	15 13.2	-18 21.5	70.8	8.0	307
18	2	1975	0.0	23 0	15 14.0	-18 22.6	72.1	8.0	307
19	2	1975	1.0	1 0	15 28.4	-18 42.5	96.1	7.9	307
19	2	1975	1.0	140	15 31.6	-18 46.8	101.4	7.8	309
19	2	1975	1.0	210	15 34.0	-18 50.0	105.3	7.7	308
19	2	1975	1.0	358	15 42.6	-19 1.2	119.1	7.3	308
19	2	1975	1.0	4 0	15 42.8	-19 1.4	119.3	7.3	308
19	2	1975	1.0	7 0	15 56.1	-19 19.3	141.1	7.2	308
19	2	1975	1.0	7 6	15 56.6	-19 19.9	141.9	7.4	306
19	2	1975	1.0	750	15 59.8	-19 24.5	147.3	7.9	308
19	2	1975	1.0	820	16 2.2	-19 27.7	151.2	7.5	312
19	2	1975	1.0	838	16 3.7	-19 29.4	153.4	7.6	311
19	2	1975	1.0	9 0	16 5.5	-19 31.6	156.2	4.4	308
19	2	1975	1.0	946	16 7.6	-19 34.4	159.6	7.4	311
19	2	1975	1.0	1026	16 10.8	-19 38.3	164.5	7.7	310
19	2	1975	1.0	12 0	16 18.6	-19 47.9	176.5	7.5	310
19	2	1975	1.0	1358	16 28.1	-19 59.7	191.4	7.6	310
19	2	1975	1.0	15 0	16 33.2	-20 6.0	199.2	8.4	310
19	2	1975	1.0	1540	16 36.8	-20 10.4	204.9	8.0	310
19	2	1975	1.0	18 0	16 48.8	-20 25.4	223.6	7.8	310
19	2	1975	1.0	1832	16 51.5	-20 28.7	227.7	8.0	309
19	2	1975	1.0	21 0	17 3.9	-20 44.8	247.5	8.0	309
19	2	1975	1.0	22 4	17 9.3	-20 51.8	256.1	7.8	311
19	2	1975	1.0	2245	17 12.8	-20 56.0	261.4	7.6	315
19	2	1975	1.0	23 4	17 14.5	-20 57.7	263.8	7.9	314
19	2	1975	1.0	2348	17 18.6	-21 2.1	269.6	7.8	314
20	2	1975	1.0	0 0	17 19.7	-21 3.3	271.2	7.8	314
20	2	1975	1.0	052	17 24.3	-21 8.3	277.9	8.0	314
20	2	1975	1.0	122	17 27.1	-21 11.4	281.9	7.7	313
20	2	1975	1.0	3 0	17 35.8	-21 21.0	294.5	7.7	313
20	2	1975	1.0	3 2	17 36.0	-21 21.2	294.8	7.9	315
20	2	1975	1.0	448	17 45.8	-21 31.7	308.8	7.9	316
20	2	1975	1.0	6 0	17 52.6	-21 38.6	318.2	7.7	316
20	2	1975	1.0	618	17 54.2	-21 40.3	320.6	7.7	316
20	2	1975	1.0	8 6	18 4.2	-21 50.4	334.4	7.7	314

DAY	MON	YEAR	TZ	TIME	LATITUDE	LONGITUDE	DISTANCE	SPEED	COURSE
20	2	1975	1.0	9 0	18 8.9	-21 55.7	341.3	7.9	314
20	2	1975	1.0	920	18 10.8	-21 57.7	343.9	7.5	312
20	2	1975	1.0	945	18 12.9	-22 0.1	347.1	8.2	281
20	2	1975	1.0	11 6	18 14.9	-22 11.5	358.1	8.8	281
20	2	1975	1.0	12 0	18 16.4	-22 19.7	366.0	8.9	281
20	2	1975	1.0	1237	18 17.5	-22 25.3	371.5	6.1	280
20	2	1975	1.0	1249	18 17.7	-22 26.6	372.7	8.9	281
20	2	1975	1.0	13 6	18 18.2	-22 29.2	375.2	8.7	282
20	2	1975	1.0	1444	18 21.2	-22 43.8	389.4	8.7	284
20	2	1975	1.0	1555	18 23.7	-22 54.3	399.7	4.5	284
20	2	1975	1.0	1624	18 24.2	-22 56.6	401.9	8.6	284
20	2	1975	1.0	1632	18 24.5	-22 57.7	403.0	9.1	285
20	2	1975	1.0	1742	18 27.3	-23 8.5	413.6	8.8	284
20	2	1975	1.0	19 0	18 30.1	-23 20.2	425.1	8.9	284
20	2	1975	1.0	1930	18 31.1	-23 24.8	429.5	8.7	285
20	2	1975	1.0	2010	18 32.7	-23 30.7	435.3	8.9	280
20	2	1975	1.0	2056	18 33.9	-23 37.8	442.2	8.5	288
20	2	1975	1.0	22 0	18 36.6	-23 47.0	451.3	8.6	288
20	2	1975	1.0	2244	18 38.5	-23 53.3	457.6	8.3	283
21	2	1975	1.0	0 0	18 41.0	-24 4.1	468.2	8.1	281
21	2	1975	1.0	020	18 41.5	-24 7.0	470.9	8.3	278
21	2	1975	1.0	148	18 43.1	-24 19.7	483.1	8.7	279
21	2	1975	1.0	220	18 43.8	-24 24.6	487.7	8.6	277
21	2	1975	1.0	3 0	18 44.5	-24 30.5	493.4	8.6	277
21	2	1975	1.0	532	18 47.2	-24 53.3	515.2	8.9	278
21	2	1975	1.0	6 0	18 47.8	-24 57.7	519.3	8.9	278
21	2	1975	1.0	756	18 50.2	-25 15.7	536.5	8.9	279
21	2	1975	1.0	830	18 51.0	-25 20.9	541.5	8.8	279
21	2	1975	1.0	935	18 52.4	-25 30.9	551.1	5.2	279
21	2	1975	1.0	950	18 52.6	-25 32.2	552.4	1.2	278
21	2	1975	1.0	958	18 52.7	-25 32.4	552.5	0.8	243
21	2	1975	1.0	1142	18 52.0	-25 33.7	553.9	1.7	281
21	2	1975	1.0	1217	18 52.2	-25 34.7	554.9	4.7	282
21	2	1975	1.0	1348	18 53.7	-25 42.1	562.1	8.9	282
21	2	1975	1.0	14 4	18 54.1	-25 44.6	564.4	8.6	280
21	2	1975	1.0	1536	18 56.5	-25 58.4	577.7	8.5	282
21	2	1975	1.0	1730	18 59.9	-26 15.0	593.8	8.3	282
21	2	1975	1.0	1842	19 2.0	-26 25.3	603.7	8.4	279
21	2	1975	1.0	2030	19 4.5	-26 41.1	618.9	8.8	282
21	2	1975	1.0	2136	19 6.4	-26 51.1	628.6	8.7	283
21	2	1975	1.0	2314	19 9.7	-27 5.7	642.7	8.7	284
21	2	1975	1.0	2330	19 10.3	-27 8.1	645.0	9.0	284
22	2	1975	2.0	026	19 14.3	-27 25.9	662.3	8.7	282
22	2	1975	2.0	1 0	19 15.4	-27 31.0	667.3	8.7	282
22	2	1975	2.0	158	19 17.1	-27 39.7	675.7	8.8	275
22	2	1975	2.0	214	19 17.3	-27 42.2	678.0	8.8	282
22	2	1975	2.0	344	19 20.0	-27 55.8	691.1	8.5	282
22	2	1975	2.0	4 0	19 20.5	-27 58.2	693.4	8.5	282
22	2	1975	2.0	530	19 23.2	-28 11.4	706.2	8.4	283
22	2	1975	2.0	7 0	19 26.1	-28 24.5	718.8	8.3	283

DAY	MON	YEAR	TZ	TIME	LATITUDE	LONGITUDE	DISTANCE	SPEED	COURSE
22	2	1975	2.0	716	19 26.6	-28 26.7	721.1	8.7	285
22	2	1975	2.0	750	19 27.9	-28 31.8	726.0	8.9	281
22	2	1975	2.0	10 0	19 31.7	-28 51.8	745.2	8.5	281
22	2	1975	2.0	12 0	19 35.0	-29 9.5	762.3	8.1	281
22	2	1975	2.0	1212	19 35.3	-29 11.2	763.9	8.6	282
22	2	1975	2.0	1358	19 38.6	-29 26.9	779.0	8.5	283
22	2	1975	2.0	15 0	19 40.6	-29 36.0	787.8	9.3	283
22	2	1975	2.0	1528	19 41.6	-29 40.4	792.1	8.7	280
22	2	1975	2.0	1654	19 43.8	-29 53.5	804.6	8.8	282
22	2	1975	2.0	18 0	19 45.9	-30 3.6	814.3	8.7	282
22	2	1975	2.0	1840	19 47.2	-30 9.5	820.1	8.9	282
22	2	1975	2.0	1916	19 48.3	-30 15.1	825.4	8.5	279
22	2	1975	2.0	21 0	19 50.7	-30 30.6	840.2	8.6	279
22	2	1975	2.0	21 4	19 50.8	-30 31.2	840.7	8.4	284
22	2	1975	2.0	23 0	19 54.6	-30 47.9	856.9	8.6	281
22	2	1975	2.0	2312	19 55.0	-30 49.7	858.7	8.8	286
22	2	1975	2.0	2334	19 55.8	-30 53.0	861.9	8.7	281
23	2	1975	2.0	0 0	19 56.5	-30 57.0	865.7	8.7	281
23	2	1975	2.0	122	19 58.7	-31 9.4	877.5	8.5	279
23	2	1975	2.0	248	20 0.7	-31 22.2	889.8	8.4	279
23	2	1975	2.0	3 0	20 1.0	-31 24.0	891.5	8.6	279
23	2	1975	2.0	434	20 3.0	-31 38.1	904.9	8.6	283
23	2	1975	2.0	6 0	20 5.8	-31 50.9	917.3	8.6	291
23	2	1975	2.0	7 6	20 9.2	-32 0.3	926.7	9.0	292
23	2	1975	2.0	8 0	20 12.2	-32 8.3	934.8	8.5	292
23	2	1975	2.0	828	20 13.7	-32 12.3	938.8	8.0	289
23	2	1975	2.0	920	20 16.0	-32 19.2	945.7	4.0	288
23	2	1975	2.0	945	20 16.5	-32 20.9	947.3	0.9	278
23	2	1975	2.0	1012	20 16.6	-32 21.4	947.8	0.3	223
23	2	1975	2.0	1058	20 16.4	-32 21.5	948.0	0.7	276
23	2	1975	2.0	1142	20 16.4	-32 22.1	948.5	6.2	290
23	2	1975	2.0	1154	20 16.9	-32 23.3	949.8	7.8	290
23	2	1975	2.0	1246	20 19.2	-32 30.1	956.5	8.8	291
23	2	1975	2.0	13 0	20 19.9	-32 32.1	958.6	8.7	291
23	2	1975	2.0	1432	20 24.6	-32 45.5	972.0	8.8	295
23	2	1975	2.0	16 0	20 30.2	-32 58.0	985.0	8.9	295
23	2	1975	2.0	1620	20 31.5	-33 0.9	987.9	9.0	293
23	2	1975	2.0	1752	20 36.8	-33 14.5	1001.7	8.7	292
23	2	1975	2.0	19 0	20 40.5	-33 24.3	1011.6	8.6	294
23	2	1975	2.0	1938	20 42.7	-33 29.6	1017.0	7.9	293
23	2	1975	2.0	2154	20 49.7	-33 47.2	1034.9	8.5	294
23	2	1975	2.0	22 0	20 50.1	-33 48.0	1035.8	8.9	292
24	2	1975	2.0	030	20 58.3	-34 10.0	1057.9	8.6	293
24	2	1975	2.0	1 0	20 59.9	-34 14.3	1062.2	8.8	293
24	2	1975	2.0	154	21 3.0	-34 22.1	1070.1	8.7	293
24	2	1975	2.0	311	21 7.4	-34 33.2	1081.3	8.7	284
24	2	1975	2.0	338	21 8.3	-34 37.2	1085.2	8.0	281
24	2	1975	2.0	6 0	21 12.0	-34 57.1	1104.1	7.6	207
24	2	1975	2.0	7 6	21 4.5	-35 1.1	1112.5	6.5	115
24	2	1975	2.0	726	21 3.6	-34 59.0	1114.6	8.4	112

DAY	MON	YEAR	TZ	TIME	LATITUDE	LONGITUDE	DISTANCE	SPEED	COURSE
24	2	1975	2.0	9 8	20 58.3	-34 44.8	1128.9	8.4	107
24	2	1975	2.0	10 0	20 56.1	-34 37.3	1136.2	8.1	107
24	2	1975	2.0	1012	20 55.6	-34 35.7	1137.8	8.0	112
24	2	1975	2.0	1052	20 53.6	-34 30.3	1143.2	8.0	114
24	2	1975	2.0	12 0	20 50.0	-34 21.4	1152.3	7.9	114
24	2	1975	2.0	1216	20 49.1	-34 19.4	1154.4	7.8	115
24	2	1975	2.0	14 2	20 43.3	-34 6.1	1168.1	7.5	113
24	2	1975	2.0	15 0	20 40.5	-33 59.0	1175.3	7.4	113
24	2	1975	2.0	1526	20 39.2	-33 55.8	1178.5	7.5	115
24	2	1975	2.0	17 2	20 34.1	-33 44.1	1190.6	7.9	112
24	2	1975	2.0	18 0	20 31.3	-33 36.6	1198.2	7.0	111
24	2	1975	2.0	19 0	20 28.7	-33 29.6	1205.3	6.7	105
24	2	1975	2.0	1926	20 28.0	-33 26.6	1208.1	7.0	108
24	2	1975	2.0	1945	20 27.3	-33 24.4	1210.4	8.0	108
24	2	1975	2.0	2046	20 24.8	-33 16.1	1218.5	7.8	107
24	2	1975	2.0	2112	20 23.9	-33 12.6	1221.9	7.5	108
24	2	1975	2.0	22 0	20 22.0	-33 6.5	1227.9	7.9	108
24	2	1975	2.0	2230	20 20.8	-33 2.5	1231.9	7.7	103
24	2	1975	2.0	2310	20 19.7	-32 57.1	1237.0	7.6	107
24	2	1975	2.0	2320	20 19.3	-32 55.8	1238.3	7.9	107
25	2	1975	2.0	1 0	20 15.4	-32 42.5	1251.4	7.8	27
25	2	1975	2.0	1 6	20 16.1	-32 42.1	1252.2	8.3	19
25	2	1975	2.0	244	20 29.0	-32 37.4	1265.8	8.2	14
25	2	1975	2.0	4 0	20 39.0	-32 34.8	1276.1	8.3	14
25	2	1975	2.0	430	20 43.1	-32 33.7	1280.3	8.6	17
25	2	1975	2.0	7 0	21 3.6	-32 27.2	1301.7	8.6	17
25	2	1975	2.0	758	21 11.6	-32 24.6	1310.0	8.5	18
25	2	1975	2.0	8 8	21 12.9	-32 24.2	1311.4	8.5	35
25	2	1975	2.0	857	21 18.6	-32 19.9	1318.4	7.1	219
25	2	1975	2.0	9 4	21 17.9	-32 20.4	1319.2	9.0	216
25	2	1975	2.0	956	21 11.6	-32 25.4	1327.0	4.5	216
25	2	1975	2.0	1010	21 10.8	-32 26.1	1328.0	1.1	212
25	2	1975	2.0	11 8	21 9.9	-32 26.7	1329.1	0.7	253
25	2	1975	2.0	1256	21 9.5	-32 27.9	1330.3	1.3	202
25	2	1975	2.0	1312	21 9.2	-32 28.1	1330.7	0.8	167
25	2	1975	2.0	1330	21 9.0	-32 28.0	1330.9	4.7	169
25	2	1975	2.0	1350	21 7.5	-32 27.7	1332.4	7.0	96
25	2	1975	2.0	1432	21 7.0	-32 22.4	1337.4	6.8	91
25	2	1975	2.0	1449	21 6.9	-32 20.4	1339.3	7.8	350
25	2	1975	2.0	1512	21 9.9	-32 20.9	1342.3	7.8	225
25	2	1975	2.0	1532	21 8.0	-32 22.9	1344.9	7.3	91
25	2	1975	2.0	16 0	21 8.0	-32 19.2	1348.3	7.4	350
25	2	1975	2.0	1616	21 9.9	-32 19.6	1350.3	7.9	345
25	2	1975	2.0	1624	21 10.9	-32 19.9	1351.3	8.2	230
25	2	1975	2.0	1644	21 9.2	-32 22.1	1354.1	5.9	88
25	2	1975	2.0	1712	21 9.3	-32 19.2	1356.8	3.2	325
25	2	1975	2.0	18 2	21 11.4	-32 20.8	1359.5	2.3	326
25	2	1975	2.0	1811	21 11.7	-32 21.0	1359.8	3.8	200
25	2	1975	2.0	1850	21 9.4	-32 21.9	1362.3	1.8	106
25	2	1975	2.0	1921	21 9.2	-32 21.0	1363.2	0.5	206

DAY	MON	YEAR	TZ	TIME	LATITUDE		LONGITUDE		DISTANCE	SPEED	COURSE
25	2	1975	2.0	1946	21	9.0	-32	21.1	1363.4	0.2	207
25	2	1975	2.0	2024	21	8.9	-32	21.1	1363.5	0.6	237
25	2	1975	2.0	2124	21	8.5	-32	21.7	1364.2	0.7	348
25	2	1975	2.0	2131	21	8.6	-32	21.7	1364.2	7.8	23
25	2	1975	2.0	2145	21	10.3	-32	21.0	1366.1	0.7	348
25	2	1975	2.0	22 0	21	10.4	-32	21.0	1366.2	3.6	0
25	2	1975	2.0	22 8	21	10.9	-32	21.0	1366.7	7.4	2
25	2	1975	2.0	2230	21	13.6	-32	20.9	1369.4	8.3	3
25	2	1975	2.0	2310	21	19.1	-32	20.6	1374.9	7.3	4
25	2	1975	2.0	2355	21	24.6	-32	20.2	1380.4	6.2	197
26	2	1975	2.0	018	21	22.3	-32	20.9	1382.8	7.8	198
26	2	1975	2.0	2 0	21	9.8	-32	25.2	1396.0	8.0	198
26	2	1975	2.0	220	21	7.2	-32	26.1	1398.7	6.8	198
26	2	1975	2.0	3 6	21	2.2	-32	27.8	1404.0	7.4	35
26	2	1975	2.0	429	21	10.7	-32	21.6	1414.2	0.3	353
26	2	1975	2.0	5 7	21	10.9	-32	21.6	1414.4	7.4	43
26	2	1975	2.0	550	21	14.7	-32	17.7	1419.7	7.0	48
26	2	1975	2.0	646	21	19.1	-32	12.5	1426.2	7.9	197
26	2	1975	2.0	838	21	5.0	-32	17.1	1441.0	8.1	200
26	2	1975	2.0	9 0	21	2.2	-32	18.3	1444.0	8.0	200
26	2	1975	2.0	957	20	55.1	-32	21.1	1451.6	6.3	356
26	2	1975	2.0	1018	20	57.3	-32	21.3	1453.8	7.7	0
26	2	1975	2.0	1148	21	8.9	-32	21.2	1465.4	7.4	321
26	2	1975	2.0	12 6	21	10.6	-32	22.7	1467.6	6.6	314
26	2	1975	2.0	1314	21	15.8	-32	28.5	1475.1	3.8	114
26	2	1975	2.0	1320	21	15.7	-32	28.1	1475.5	6.9	112
26	2	1975	2.0	1618	21	8.0	-32	7.6	1496.1	7.6	274
26	2	1975	2.0	1740	21	8.7	-32	18.7	1506.5	7.6	284
26	2	1975	2.0	18 5	21	9.5	-32	22.0	1509.6	7.8	268
26	2	1975	2.0	1858	21	9.2	-32	29.4	1516.5	7.1	267
26	2	1975	2.0	1912	21	9.2	-32	31.1	1518.2	8.7	113
26	2	1975	2.0	2018	21	5.5	-32	21.7	1527.7	9.0	114
26	2	1975	2.0	2112	21	2.1	-32	13.8	1535.9	7.4	315
26	2	1975	2.0	2122	21	3.0	-32	14.7	1537.1	9.1	320
26	2	1975	2.0	2142	21	5.3	-32	16.8	1540.1	6.8	299
26	2	1975	2.0	22 4	21	6.5	-32	19.1	1542.6	0.6	357
26	2	1975	2.0	2342	21	7.4	-32	19.2	1543.5	1.1	22
27	2	1975	2.0	033	21	8.3	-32	18.8	1544.5	2.9	335
27	2	1975	2.0	058	21	9.4	-32	19.3	1545.7	2.1	169
27	2	1975	2.0	116	21	8.7	-32	19.2	1546.3	0.5	325
27	2	1975	2.0	122	21	8.8	-32	19.2	1546.4	7.2	244
27	2	1975	2.0	148	21	7.4	-32	22.2	1549.5	7.5	17
27	2	1975	2.0	2 3	21	9.2	-32	21.6	1551.4	0.5	325
27	2	1975	2.0	222	21	9.3	-32	21.7	1551.5	6.8	224
27	2	1975	2.0	242	21	7.7	-32	23.4	1553.8	0.5	325
27	2	1975	2.0	248	21	7.8	-32	23.5	1553.8	7.5	38
27	2	1975	2.0	314	21	10.3	-32	21.3	1557.1	0.5	325
27	2	1975	2.0	342	21	10.5	-32	21.4	1557.3	3.7	301
27	2	1975	2.0	355	21	10.9	-32	22.2	1558.1	7.5	299
27	2	1975	2.0	5 2	21	14.9	-32	30.0	1566.5	7.9	295

DAY	MON	YEAR	TZ	TIME	LATITUDE	LONGITUDE	DISTANCE	SPEED	COURSE
27	2	1975	2.0	530	21 16.5	-32 33.6	1570.2	7.9	301
27	2	1975	2.0	648	21 21.8	-32 43.1	1580.4	7.9	298
27	2	1975	2.0	724	21 24.0	-32 47.6	1585.2	6.7	299
27	2	1975	2.0	830	21 27.6	-32 54.6	1592.6	7.9	300
27	2	1975	2.0	921	21 30.9	-33 0.8	1599.3	4.9	180
27	2	1975	2.0	950	21 28.5	-33 0.8	1601.7	7.7	126
27	2	1975	2.0	1120	21 21.9	-32 50.8	1613.1	8.5	125
27	2	1975	2.0	1130	21 21.1	-32 49.5	1614.5	8.2	127
27	2	1975	2.0	1426	21 6.7	-32 28.9	1638.6	7.9	132
27	2	1975	2.0	1430	21 6.4	-32 28.5	1639.1	7.8	132
27	2	1975	2.0	1730	20 50.8	-32 9.9	1662.4	8.1	196
27	2	1975	2.0	1830	20 43.0	-32 12.3	1670.5	4.7	194
27	2	1975	2.0	1846	20 41.8	-32 12.6	1671.8	4.2	198
27	2	1975	2.0	1854	20 41.2	-32 12.8	1672.4	0.7	196
27	2	1975	2.0	2032	20 40.2	-32 13.1	1673.5	0.5	225
27	2	1975	2.0	2058	20 40.0	-32 13.3	1673.7	1.3	275
27	2	1975	2.0	2117	20 40.0	-32 13.7	1674.1	4.0	293
27	2	1975	2.0	2130	20 40.4	-32 14.6	1675.0	7.8	297
27	2	1975	2.0	2238	20 44.4	-32 23.0	1683.8	8.3	297
28	2	1975	2.0	026	20 51.3	-32 37.3	1698.8	8.0	300
28	2	1975	2.0	030	20 51.5	-32 37.8	1699.3	8.2	300
28	2	1975	2.0	144	20 56.6	-32 47.2	1709.5	8.0	297
28	2	1975	2.0	222	20 58.9	-32 52.0	1714.5	7.7	303
28	2	1975	2.0	330	21 3.7	-32 59.9	1723.3	7.8	303
28	2	1975	2.0	435	21 8.3	-33 7.5	1731.8	6.8	16
28	2	1975	2.0	545	21 15.9	-33 5.2	1739.7	6.0	114
28	2	1975	2.0	6 0	21 15.2	-33 3.7	1741.2	7.8	121
28	2	1975	2.0	634	21 13.0	-32 59.7	1745.6	7.6	123
28	2	1975	2.0	746	21 8.1	-32 51.5	1754.6	7.7	118
28	2	1975	2.0	822	21 5.9	-32 47.1	1759.2	8.3	117
28	2	1975	2.0	9 0	21 3.5	-32 42.1	1764.5	8.1	114
28	2	1975	2.0	928	21 2.0	-32 38.4	1768.2	9.3	113
28	2	1975	2.0	956	21 0.3	-32 34.2	1772.6	8.8	111
28	2	1975	2.0	1028	20 58.6	-32 29.5	1777.2	9.0	116
28	2	1975	2.0	1050	20 57.2	-32 26.3	1780.5	8.1	120
28	2	1975	2.0	1222	20 50.9	-32 14.8	1793.0	7.2	121
28	2	1975	2.0	1251	20 49.1	-32 11.6	1796.5	1.6	32
28	2	1975	2.0	1310	20 49.5	-32 11.3	1797.0	2.2	100
28	2	1975	2.0	1321	20 49.4	-32 10.9	1797.4	3.5	263
28	2	1975	2.0	1332	20 49.4	-32 11.6	1798.0	4.4	266
28	2	1975	2.0	1355	20 49.3	-32 13.4	1799.7	1.6	10
28	2	1975	2.0	1420	20 49.9	-32 13.2	1800.4	2.4	170
28	2	1975	2.0	15 0	20 48.3	-32 13.0	1802.0	0.9	252
28	2	1975	2.0	1516	20 48.3	-32 13.2	1802.2	1.3	260
28	2	1975	2.0	1530	20 48.2	-32 13.5	1802.5	4.5	267
28	2	1975	2.0	1612	20 48.1	-32 16.9	1805.7	1.2	338
28	2	1975	2.0	1651	20 48.8	-32 17.2	1806.4	3.0	205
28	2	1975	2.0	1710	20 47.9	-32 17.7	1807.4	1.3	260
28	2	1975	2.0	1722	20 47.9	-32 17.9	1807.7	1.2	236
28	2	1975	2.0	19 8	20 46.6	-32 19.8	1809.8	0.4	235

DAY	MON	YEAR	TZ	TIME	LATITUDE	LONGITUDE	DISTANCE	SPEED	COURSE
28	2	1975	2.0	1936	20 46.6	-32 20.0	1810.0	6.2	62
28	2	1975	2.0	1942	20 46.8	-32 19.4	1810.6	6.6	53
28	2	1975	2.0	1948	20 47.2	-32 18.8	1811.3	1.0	335
28	2	1975	2.0	20 0	20 47.4	-32 18.9	1811.5	7.3	1
28	2	1975	2.0	2136	20 59.1	-32 18.7	1823.1	6.9	359
28	2	1975	2.0	2152	21 0.9	-32 18.7	1824.9	5.7	359
28	2	1975	2.0	22 0	21 1.7	-32 18.7	1825.7	7.7	199
28	2	1975	2.0	2338	20 49.8	-32 23.2	1838.3	7.7	198
1	3	1975	2.0	0 0	20 47.1	-32 24.1	1841.1	7.5	198
1	3	1975	2.0	052	20 41.0	-32 26.3	1847.5	4.9	46
1	3	1975	2.0	132	20 43.3	-32 23.8	1850.8	6.6	46
1	3	1975	2.0	238	20 48.3	-32 18.1	1858.1	6.0	43
1	3	1975	2.0	3 0	20 49.9	-32 16.5	1860.3	7.3	43
1	3	1975	2.0	4 4	20 55.6	-32 10.8	1868.1	7.2	197
1	3	1975	2.0	422	20 53.6	-32 11.5	1870.2	9.2	200
1	3	1975	2.0	510	20 46.6	-32 14.2	1877.6	8.9	200
1	3	1975	2.0	545	20 41.8	-32 16.1	1882.8	8.4	194
1	3	1975	2.0	647	20 33.3	-32 18.3	1891.5	5.3	355
1	3	1975	2.0	658	20 34.3	-32 18.4	1892.5	7.6	358
1	3	1975	2.0	822	20 44.9	-32 18.9	1903.1	7.0	20
1	3	1975	2.0	845	20 47.4	-32 17.9	1905.8	8.6	319
1	3	1975	2.0	850	20 48.0	-32 18.4	1906.6	8.8	314
1	3	1975	2.0	918	20 50.8	-32 21.5	1910.7	7.8	318
1	3	1975	2.0	948	20 53.7	-32 24.3	1914.6	7.8	320
1	3	1975	2.0	10 9	20 55.8	-32 26.2	1917.3	5.7	102
1	3	1975	2.0	1034	20 55.3	-32 23.7	1919.7	6.8	109
1	3	1975	2.0	1128	20 53.3	-32 17.5	1925.8	6.8	111
1	3	1975	2.0	1230	20 50.8	-32 10.5	1932.8	7.1	110
1	3	1975	2.0	1330	20 48.4	-32 3.4	1939.9	7.0	267
1	3	1975	2.0	1422	20 48.0	-32 9.9	1945.9	7.8	270
1	3	1975	2.0	1530	20 48.1	-32 19.3	1954.7	7.6	270
1	3	1975	2.0	1653	20 48.1	-32 30.6	1965.2	5.6	111
1	3	1975	2.0	1930	20 42.8	-32 15.9	1980.0	5.9	111
1	3	1975	2.0	2022	20 41.0	-32 10.8	1985.1	7.1	312
1	3	1975	2.0	2028	20 41.4	-32 11.3	1985.8	9.0	316
1	3	1975	2.0	2042	20 42.9	-32 12.9	1987.9	8.6	314
1	3	1975	2.0	2130	20 47.7	-32 18.2	1994.8	1.8	298
1	3	1975	2.0	2214	20 48.3	-32 19.5	1996.1	1.3	262
1	3	1975	2.0	2250	20 48.2	-32 20.3	1996.9	0.2	282
1	3	1975	2.0	2330	20 48.3	-32 20.5	1997.0	5.0	84
1	3	1975	2.0	2352	20 48.5	-32 18.6	1998.9	4.3	110
2	3	1975	2.0	0 0	20 48.3	-32 18.0	1999.4	0.2	282
2	3	1975	2.0	226	20 48.4	-32 18.6	2000.0	0.8	241
2	3	1975	2.0	330	20 48.0	-32 19.4	2000.8	0.4	237
2	3	1975	2.0	457	20 47.7	-32 19.9	2001.4	2.2	145
2	3	1975	2.0	516	20 47.1	-32 19.5	2002.1	4.4	74
2	3	1975	2.0	535	20 47.5	-32 18.0	2003.5	5.2	2
2	3	1975	2.0	610	20 50.5	-32 17.9	2006.5	5.4	350
2	3	1975	2.0	722	20 56.9	-32 19.1	2013.0	5.1	191
2	3	1975	2.0	756	20 54.1	-32 19.7	2015.9	6.4	177

DAY	MON	YEAR	TZ	TIME	LATITUDE	LONGITUDE	DISTANCE	SPEED	COURSE
2	3	1975	2.0	832	20 50.3	-32 19.5	2019.7	5.7	177
2	3	1975	2.0	946	20 43.3	-32 19.1	2026.7	3.9	52
2	3	1975	2.0	1036	20 45.3	-32 16.4	2029.9	3.5	24
2	3	1975	2.0	1056	20 46.4	-32 15.9	2031.1	6.9	271
2	3	1975	2.0	12 5	20 46.5	-32 24.4	2039.1	9.1	271
2	3	1975	2.0	1226	20 46.5	-32 27.8	2042.2	9.4	271
2	3	1975	2.0	1326	20 46.7	-32 37.9	2051.7	9.2	271
2	3	1975	2.0	15 0	20 46.9	-32 53.4	2066.1	9.7	271
2	3	1975	2.0	1512	20 46.9	-32 55.4	2068.1	9.8	264
2	3	1975	2.0	1536	20 46.5	-32 59.6	2072.0	9.7	231
2	3	1975	2.0	1732	20 34.7	-33 15.0	2090.6	9.3	229
2	3	1975	2.0	1830	20 28.8	-33 22.3	2099.6	9.1	229
2	3	1975	2.0	1918	20 24.0	-33 28.2	2106.9	9.1	228
2	3	1975	2.0	1952	20 20.5	-33 32.2	2112.1	9.5	230
2	3	1975	2.0	2110	20 12.5	-33 42.3	2124.4	9.0	229
2	3	1975	2.0	2130	20 10.6	-33 44.7	2127.4	9.4	229
2	3	1975	2.0	22 0	20 7.5	-33 48.5	2132.1	9.3	228
3	3	1975	2.0	0 0	19 55.2	-34 3.4	2150.8	9.0	224
3	3	1975	2.0	136	19 44.7	-34 13.9	2165.2	9.5	223
3	3	1975	2.0	3 0	19 34.9	-34 23.5	2178.5	9.7	223
3	3	1975	2.0	520	19 18.2	-34 39.8	2201.2	9.3	224
3	3	1975	2.0	6 0	19 13.7	-34 44.4	2207.4	9.4	224
3	3	1975	2.0	7 6	19 6.2	-34 51.9	2217.8	9.5	226
3	3	1975	2.0	822	18 57.8	-35 1.0	2229.8	9.6	224
3	3	1975	2.0	9 0	18 53.4	-35 5.4	2235.9	9.6	224
3	3	1975	2.0	926	18 50.4	-35 8.5	2240.0	9.6	225
3	3	1975	2.0	950	18 47.7	-35 11.3	2243.9	9.6	222
3	3	1975	2.0	10 8	18 45.5	-35 13.3	2246.8	9.6	223
3	3	1975	2.0	1134	18 35.4	-35 23.2	2260.5	9.6	224
3	3	1975	2.0	12 0	18 32.4	-35 26.3	2264.7	9.4	224
3	3	1975	2.0	1322	18 23.2	-35 35.8	2277.6	9.6	223
3	3	1975	2.0	1418	18 16.6	-35 42.2	2286.6	9.5	222
3	3	1975	2.0	15 0	18 11.7	-35 46.9	2293.2	9.4	222
3	3	1975	2.0	16 4	18 4.2	-35 54.0	2303.3	9.4	225
3	3	1975	2.0	18 0	17 51.4	-36 7.6	2321.5	9.5	225
3	3	1975	2.0	1832	17 47.8	-36 11.4	2326.6	9.0	226
3	3	1975	2.0	20 2	17 38.5	-36 21.6	2340.0	9.2	222
3	3	1975	2.0	2050	17 33.1	-36 26.8	2347.4	8.9	223
3	3	1975	2.0	21 0	17 32.0	-36 27.9	2348.9	8.9	223
3	3	1975	2.0	2146	17 27.0	-36 32.8	2355.7	9.5	225
3	3	1975	2.0	23 2	17 18.6	-36 41.7	2367.7	9.2	225
4	3	1975	2.0	0 0	17 12.3	-36 48.2	2376.5	9.3	225
4	3	1975	2.0	230	16 55.8	-37 5.4	2399.8	9.0	222
4	3	1975	2.0	3 0	16 52.5	-37 8.5	2404.3	9.1	222
4	3	1975	2.0	326	16 49.5	-37 11.2	2408.2	8.8	222
4	3	1975	2.0	4 2	16 45.6	-37 14.9	2413.5	5.4	222
4	3	1975	2.0	416	16 44.7	-37 15.8	2414.7	9.1	222
4	3	1975	2.0	422	16 44.0	-37 16.4	2415.7	4.8	222
4	3	1975	2.0	448	16 42.4	-37 17.9	2417.7	8.9	222
4	3	1975	2.0	650	16 29.0	-37 30.4	2435.7	9.3	222

DAY	MON	YEAR	TZ	TIME	LATITUDE	LONGITUDE	DISTANCE	SPEED	COURSE
4	3	1975	2.0	730	16 24.4	-37 34.7	2441.9	9.2	222
4	3	1975	2.0	838	16 16.7	-37 42.0	2452.4	9.3	223
4	3	1975	2.0	9 2	16 13.9	-37 44.6	2456.1	9.4	223
4	3	1975	2.0	1030	16 3.8	-37 54.4	2469.9	9.4	223
4	3	1975	2.0	1046	16 1.9	-37 56.2	2472.4	9.3	224
4	3	1975	2.0	12 0	15 53.7	-38 4.5	2483.9	9.2	224
4	3	1975	2.0	1230	15 50.4	-38 7.8	2488.5	8.6	223
4	3	1975	2.0	1322	15 44.9	-38 13.0	2495.9	8.9	223
4	3	1975	2.0	1416	15 39.1	-38 18.7	2503.9	9.2	223
4	3	1975	2.0	15 0	15 34.1	-38 23.5	2510.7	9.2	223
4	3	1975	2.0	15 8	15 33.2	-38 24.4	2511.9	9.5	222
4	3	1975	2.0	1742	15 15.0	-38 41.1	2536.3	9.1	222
4	3	1975	2.0	18 0	15 13.0	-38 43.1	2539.0	9.2	222
4	3	1975	2.0	1930	15 2.8	-38 52.7	2552.8	9.7	223
4	3	1975	2.0	20 2	14 59.1	-38 56.3	2557.9	9.1	219
4	3	1975	2.0	2038	14 54.8	-38 59.9	2563.4	9.2	222
4	3	1975	2.0	21 0	14 52.3	-39 2.3	2566.8	9.3	222
4	3	1975	2.0	2212	14 44.0	-39 10.0	2578.0	9.2	224
4	3	1975	2.0	2354	14 32.7	-39 21.3	2593.7	9.7	222
5	3	1975	2.0	0 0	14 32.0	-39 22.0	2594.7	9.5	222
5	3	1975	2.0	140	14 20.2	-39 32.9	2610.5	9.3	222
5	3	1975	2.0	3 0	14 11.0	-39 41.4	2622.8	9.9	222
5	3	1975	2.0	418	14 1.5	-39 50.2	2635.7	9.8	222
5	3	1975	2.0	6 0	13 49.0	-40 1.7	2652.3	9.1	222
5	3	1975	2.0	714	13 40.7	-40 9.3	2663.5	9.4	224
5	3	1975	2.0	915	13 27.1	-40 22.8	2682.4	9.6	228
5	3	1975	2.0	934	13 25.0	-40 25.1	2685.4	9.3	232
5	3	1975	2.0	956	13 22.9	-40 27.8	2688.9	9.3	227
5	3	1975	2.0	1138	13 12.1	-40 39.7	2704.6	9.5	228
5	3	1975	2.0	12 0	13 9.8	-40 42.3	2708.1	9.4	228
5	3	1975	2.0	1324	13 1.0	-40 52.3	2721.2	9.6	230
5	3	1975	2.0	1412	12 56.0	-40 58.3	2728.9	9.2	229
5	3	1975	2.0	15 0	12 51.2	-41 4.1	2736.3	9.1	229
5	3	1975	2.0	1558	12 45.4	-41 11.0	2745.1	9.4	227
5	3	1975	2.0	18 0	12 32.4	-41 25.1	2764.2	9.5	227
5	3	1975	2.0	1842	12 27.8	-41 30.1	2770.8	9.5	228
5	3	1975	2.0	2058	12 13.5	-41 46.6	2792.4	9.1	227
5	3	1975	2.0	21 0	12 13.3	-41 46.8	2792.7	9.2	227
5	3	1975	2.0	2116	12 11.6	-41 48.6	2795.1	9.4	226
5	3	1975	2.0	2236	12 2.9	-41 58.0	2807.7	9.4	221
5	3	1975	2.0	23 2	11 59.9	-42 0.7	2811.8	9.2	219
6	3	1975	3.0	030	11 42.3	-42 15.4	2834.5	9.2	219
6	3	1975	3.0	230	11 28.0	-42 27.4	2853.0	8.2	185
6	3	1975	3.0	545	11 1.4	-42 29.9	2879.7	8.0	177
6	3	1975	3.0	734	10 46.9	-42 29.1	2894.2	8.8	170
6	3	1975	3.0	746	10 45.2	-42 28.8	2896.0	7.5	171
6	3	1975	3.0	830	10 39.7	-42 27.9	2901.5	5.2	31
6	3	1975	3.0	920	10 43.5	-42 25.7	2905.9	5.9	11
6	3	1975	3.0	942	10 45.6	-42 25.3	2908.0	3.2	92
6	3	1975	3.0	952	10 45.6	-42 24.7	2908.6	3.7	108

DAY	MON	YEAR	TZ	TIME	LATITUDE	LONGITUDE	DISTANCE	SPEED	COURSE
6	3	1975	3.0	10 2	10 45.4	-42 24.2	2909.2	1.4	246
6	3	1975	3.0	1130	10 44.5	-42 26.0	2911.2	0.9	302
6	3	1975	3.0	1242	10 45.1	-42 26.9	2912.3	3.8	14
6	3	1975	3.0	13 0	10 46.2	-42 26.7	2913.4	6.3	9
6	3	1975	3.0	14 2	10 52.7	-42 25.6	2919.9	7.0	6
6	3	1975	3.0	1540	11 4.1	-42 24.4	2931.4	8.3	297
6	3	1975	3.0	1654	11 8.8	-42 33.7	2941.7	8.0	294
6	3	1975	3.0	1830	11 13.9	-42 45.7	2954.5	8.1	294
6	3	1975	3.0	1945	11 18.0	-42 55.2	2964.7	4.3	78
6	3	1975	3.0	2054	11 19.0	-42 50.2	2969.6	6.0	83
6	3	1975	3.0	2122	11 19.3	-42 47.4	2972.4	6.3	88
6	3	1975	3.0	22 5	11 19.5	-42 42.8	2977.0	6.7	171
6	3	1975	3.0	2230	11 16.7	-42 42.3	2979.7	6.3	89
6	3	1975	3.0	2258	11 16.8	-42 39.3	2982.7	7.3	89
7	3	1975	3.0	128	11 17.1	-42 20.7	3000.9	4.7	98
7	3	1975	3.0	130	11 17.0	-42 20.5	3001.1	7.5	94
7	3	1975	3.0	312	11 16.1	-42 7.6	3013.8	6.0	355
7	3	1975	3.0	314	11 16.2	-42 7.6	3014.0	8.3	354
7	3	1975	3.0	353	11 21.6	-42 8.2	3019.4	8.8	279
7	3	1975	3.0	436	11 22.6	-42 14.5	3025.7	9.3	269
7	3	1975	3.0	624	11 22.3	-42 31.6	3042.5	9.7	269
7	3	1975	3.0	630	11 22.3	-42 32.6	3043.4	9.7	269
7	3	1975	3.0	656	11 22.3	-42 36.9	3047.6	7.8	266
7	3	1975	3.0	730	11 22.0	-42 41.4	3052.0	7.0	119
7	3	1975	3.0	835	11 18.3	-42 34.7	3059.6	6.8	107
7	3	1975	3.0	9 4	11 17.3	-42 31.5	3062.9	6.6	103
7	3	1975	3.0	915	11 17.1	-42 30.3	3064.1	3.7	103
7	3	1975	3.0	931	11 16.8	-42 29.3	3065.0	0.1	222
7	3	1975	3.0	958	11 16.8	-42 29.3	3065.1	0.7	284
7	3	1975	3.0	1040	11 16.9	-42 29.8	3065.6	0.8	318
7	3	1975	3.0	1226	11 18.0	-42 30.8	3067.0	0.2	273
7	3	1975	3.0	1248	11 18.0	-42 30.8	3067.0	2.4	127
7	3	1975	3.0	13 2	11 17.6	-42 30.4	3067.6	6.3	126
7	3	1975	3.0	13 8	11 17.3	-42 29.9	3068.2	7.5	135
7	3	1975	3.0	1327	11 15.6	-42 28.2	3070.6	8.7	180
7	3	1975	3.0	1454	11 2.9	-42 28.2	3083.2	8.6	186
7	3	1975	3.0	1638	10 48.0	-42 29.7	3098.2	9.4	185
7	3	1975	3.0	1752	10 36.5	-42 30.8	3109.8	9.0	187
7	3	1975	3.0	1822	10 32.1	-42 31.3	3114.3	9.3	184
7	3	1975	3.0	19 0	10 26.2	-42 31.7	3120.1	8.9	184
7	3	1975	3.0	1948	10 19.1	-42 32.3	3127.3	8.7	188
7	3	1975	3.0	20 0	10 17.4	-42 32.5	3129.0	8.9	264
7	3	1975	3.0	20 8	10 17.3	-42 33.7	3130.2	9.0	275
7	3	1975	3.0	2150	10 18.7	-42 49.2	3145.5	7.7	353
7	3	1975	3.0	2354	10 34.4	-42 51.2	3161.3	8.6	3
8	3	1975	3.0	0 0	10 35.2	-42 51.1	3162.2	8.5	2
8	3	1975	3.0	034	10 40.1	-42 50.9	3167.0	8.4	358
8	3	1975	3.0	220	10 55.0	-42 51.5	3181.9	7.8	6
8	3	1975	3.0	230	10 56.3	-42 51.4	3183.2	7.8	6
8	3	1975	3.0	330	11 4.0	-42 50.5	3191.0	6.9	56

DAY	MON	YEAR	TZ	TIME	LATITUDE	LONGITUDE	DISTANCE	SPEED	COURSE
8	3	1975	3.0	430	11 7.9	-42 44.7	3197.9	7.5	56
8	3	1975	3.0	6 4	11 14.5	-42 34.8	3209.6	6.8	59
8	3	1975	3.0	719	11 19.0	-42 27.3	3218.2	3.7	57
8	3	1975	3.0	735	11 19.5	-42 26.5	3219.2	4.6	253
8	3	1975	3.0	752	11 19.1	-42 27.8	3220.5	4.7	249
8	3	1975	3.0	8 0	11 18.9	-42 28.4	3221.1	0.1	116
8	3	1975	3.0	852	11 18.8	-42 28.3	3221.2	0.9	266
8	3	1975	3.0	910	11 18.8	-42 28.6	3221.5	4.1	85
8	3	1975	3.0	916	11 18.9	-42 28.2	3221.9	4.2	334
8	3	1975	3.0	942	11 20.5	-42 29.0	3223.7	3.6	203
8	3	1975	3.0	10 4	11 19.3	-42 29.5	3225.0	3.3	184
8	3	1975	3.0	1032	11 17.7	-42 29.6	3226.5	3.6	20
8	3	1975	3.0	1052	11 18.9	-42 29.2	3227.7	2.2	22
8	3	1975	3.0	11 0	11 19.1	-42 29.1	3228.0	3.8	91
8	3	1975	3.0	1115	11 19.1	-42 28.1	3229.0	6.7	67
8	3	1975	3.0	1127	11 19.6	-42 26.8	3230.3	1.8	71
8	3	1975	3.0	1134	11 19.7	-42 26.6	3230.5	1.5	51
8	3	1975	3.0	1150	11 20.0	-42 26.3	3230.9	1.4	29
8	3	1975	3.0	12 0	11 20.2	-42 26.2	3231.1	3.9	217
8	3	1975	3.0	12 6	11 19.9	-42 26.4	3231.5	3.9	212
8	3	1975	3.0	1237	11 18.1	-42 27.5	3233.5	4.4	311
8	3	1975	3.0	1251	11 18.8	-42 28.3	3234.6	4.5	358
8	3	1975	3.0	13 0	11 19.5	-42 28.4	3235.2	1.3	65
8	3	1975	3.0	1312	11 19.6	-42 28.1	3235.5	4.9	83
8	3	1975	3.0	1322	11 19.7	-42 27.3	3236.3	5.3	91
8	3	1975	3.0	15 0	11 19.6	-42 18.5	3244.9	6.8	357
8	3	1975	3.0	1514	11 21.2	-42 18.6	3246.5	7.3	271
8	3	1975	3.0	17 0	11 21.3	-42 31.7	3259.4	7.3	271
8	3	1975	3.0	17 4	11 21.3	-42 32.2	3259.9	7.8	268
8	3	1975	3.0	1745	11 21.2	-42 37.7	3265.3	7.9	187
8	3	1975	3.0	1757	11 19.6	-42 37.9	3266.8	8.4	232
8	3	1975	3.0	1817	11 17.9	-42 40.1	3269.6	6.3	233
8	3	1975	3.0	1836	11 16.7	-42 41.8	3271.6	1.0	249
8	3	1975	3.0	1927	11 16.4	-42 42.5	3272.5	5.8	84
8	3	1975	3.0	21 0	11 17.3	-42 33.4	3281.5	8.6	253
8	3	1975	3.0	2130	11 16.1	-42 37.6	3285.8	9.3	257
8	3	1975	3.0	2210	11 14.6	-42 43.7	3292.0	7.1	252
8	3	1975	3.0	2217	11 14.4	-42 44.5	3292.8	7.2	88
8	3	1975	3.0	23 0	11 14.5	-42 39.2	3298.0	7.9	88
8	3	1975	3.0	2318	11 14.6	-42 36.8	3300.4	7.9	88
8	3	1975	3.0	2351	11 14.8	-42 32.3	3304.7	7.7	90
9	3	1975	3.0	048	11 14.8	-42 24.9	3312.0	7.4	92
9	3	1975	3.0	124	11 14.6	-42 20.4	3316.4	6.1	91
9	3	1975	3.0	130	11 14.6	-42 19.8	3317.0	7.8	296
9	3	1975	3.0	348	11 22.4	-42 36.3	3335.0	6.1	91
9	3	1975	3.0	6 0	11 22.3	-42 22.6	3348.4	6.0	91
9	3	1975	3.0	7 5	11 22.2	-42 16.0	3354.9	7.5	252
9	3	1975	3.0	842	11 18.5	-42 27.8	3367.1	7.4	206
9	3	1975	3.0	914	11 14.9	-42 29.5	3371.0	8.8	206
9	3	1975	3.0	932	11 12.6	-42 30.7	3373.7	7.2	213

DAY	MON	YEAR	TZ	TIME	LATITUDE	LONGITUDE	DISTANCE	SPEED	COURSE
9	3	1975	3.0	10 4	11 9.3	-42 32.9	3377.5	6.8	354
9	3	1975	3.0	11 0	11 15.6	-42 33.5	3383.9	7.6	357
9	3	1975	3.0	1120	11 18.2	-42 33.7	3386.4	7.7	359
9	3	1975	3.0	1230	11 27.1	-42 33.9	3395.4	5.9	4
9	3	1975	3.0	1323	11 32.3	-42 33.5	3400.6	6.8	161
9	3	1975	3.0	1450	11 23.0	-42 30.2	3410.4	8.0	160
9	3	1975	3.0	1515	11 19.9	-42 29.0	3413.8	8.0	158
9	3	1975	3.0	1616	11 12.3	-42 25.8	3421.9	7.0	156
9	3	1975	3.0	1720	11 5.4	-42 22.8	3429.4	5.7	6
9	3	1975	3.0	18 0	11 9.3	-42 22.3	3433.3	8.0	0
9	3	1975	3.0	1817	11 11.5	-42 22.3	3435.5	8.5	357
9	3	1975	3.0	1828	11 13.1	-42 22.4	3437.1	7.7	359
9	3	1975	3.0	1918	11 19.5	-42 22.5	3443.5	7.9	355
9	3	1975	3.0	2016	11 27.1	-42 23.1	3451.1	6.7	346
9	3	1975	3.0	2033	11 28.9	-42 23.6	3453.0	8.7	213
9	3	1975	3.0	2040	11 28.1	-42 24.2	3454.0	7.8	204
9	3	1975	3.0	21 6	11 25.0	-42 25.6	3457.4	7.6	208
9	3	1975	3.0	2150	11 20.1	-42 28.2	3463.0	0.5	309
9	3	1975	3.0	2356	11 20.8	-42 29.1	3464.1	0.8	270
10	3	1975	3.0	028	11 20.8	-42 29.6	3464.5	0.9	189
10	3	1975	3.0	044	11 20.5	-42 29.6	3464.8	4.0	150
10	3	1975	3.0	120	11 18.5	-42 28.4	3467.2	0.9	189
10	3	1975	3.0	216	11 17.7	-42 28.5	3468.0	0.2	255
10	3	1975	3.0	3 0	11 17.6	-42 28.6	3468.1	3.9	73
10	3	1975	3.0	325	11 18.1	-42 27.0	3469.7	0.2	255
10	3	1975	3.0	4 0	11 18.1	-42 27.1	3469.8	0.8	256
10	3	1975	3.0	546	11 17.7	-42 28.5	3471.2	0.9	229
10	3	1975	3.0	614	11 17.5	-42 28.8	3471.6	0.8	246
10	3	1975	3.0	8 0	11 16.9	-42 30.2	3473.1	2.2	266
10	3	1975	3.0	824	11 16.8	-42 31.1	3474.0	0.3	250
10	3	1975	3.0	846	11 16.8	-42 31.2	3474.1	7.2	271
10	3	1975	3.0	9 5	11 16.8	-42 33.5	3476.4	6.5	2
10	3	1975	3.0	935	11 20.1	-42 33.4	3479.6	6.1	89
10	3	1975	3.0	950	11 20.1	-42 31.9	3481.2	7.2	178
10	3	1975	3.0	10 8	11 17.9	-42 31.8	3483.3	7.6	180
10	3	1975	3.0	1050	11 12.6	-42 31.8	3488.6	5.5	93
10	3	1975	3.0	1058	11 12.6	-42 31.1	3489.4	6.0	1
10	3	1975	3.0	1120	11 14.8	-42 31.0	3491.6	5.9	60
10	3	1975	3.0	1140	11 15.8	-42 29.3	3493.5	6.5	54
10	3	1975	3.0	12 4	11 17.3	-42 27.2	3496.1	0.5	319
10	3	1975	3.0	1354	11 17.9	-42 27.7	3497.0	0.4	233
10	3	1975	3.0	14 5	11 17.9	-42 27.8	3497.0	8.0	252
10	3	1975	3.0	1523	11 14.7	-42 37.9	3507.5	7.7	163
10	3	1975	3.0	16 0	11 10.1	-42 36.5	3512.2	5.6	53
10	3	1975	3.0	1615	11 11.0	-42 35.4	3513.6	7.4	337
10	3	1975	3.0	1715	11 17.8	-42 38.3	3521.0	5.7	69
10	3	1975	3.0	1736	11 18.5	-42 36.4	3523.0	7.6	163
10	3	1975	3.0	1815	11 13.8	-42 34.9	3528.0	6.3	53
10	3	1975	3.0	1916	11 17.7	-42 29.6	3534.4	2.6	53
10	3	1975	3.0	1928	11 18.0	-42 29.2	3535.0	3.5	60

DAY	MON	YEAR	T?	TIME	LATITUDE	LONGITUDE	DISTANCE	SPEED	COURSE
10	3	1975	3.0	1950	11 18.6	-42 28.1	3536.2	4.9	207
10	3	1975	3.0	1958	11 18.0	-42 28.4	3536.9	5.7	210
10	3	1975	3.0	2018	11 16.4	-42 29.3	3538.8	4.3	3
10	3	1975	3.0	22 0	11 23.8	-42 28.9	3546.1	4.8	179
10	3	1975	3.0	2210	11 23.0	-42 28.9	3546.9	8.2	178
10	3	1975	3.0	2225	11 20.9	-42 28.8	3549.0	5.2	179
10	3	1975	3.0	2330	11 15.2	-42 28.7	3554.7	6.8	95
10	3	1975	3.0	2345	11 15.1	-42 27.0	3556.4	6.9	128
11	3	1975	3.0	052	11 10.3	-42 20.8	3564.0	7.3	134
11	3	1975	3.0	230	11 2.1	-42 12.0	3576.0	9.3	181
11	3	1975	3.0	530	10 34.1	-42 12.4	3604.0	9.2	181
11	3	1975	3.0	644	10 22.8	-42 12.6	3615.3	8.5	187
11	3	1975	3.0	7 0	10 20.5	-42 12.9	3617.6	8.0	167
11	3	1975	3.0	745	10 14.7	-42 11.5	3623.6	8.6	267
11	3	1975	3.0	845	10 14.3	-42 20.2	3632.2	6.3	353
11	3	1975	3.0	9 2	10 16.1	-42 20.4	3634.0	8.1	354
11	3	1975	3.0	922	10 18.8	-42 20.7	3636.7	8.2	357
11	3	1975	3.0	950	10 22.6	-42 21.0	3640.5	8.1	359
11	3	1975	3.0	1110	10 33.3	-42 21.1	3651.2	6.9	4
11	3	1975	3.0	12 0	10 39.1	-42 20.7	3657.0	7.1	146
11	3	1975	3.0	1234	10 35.8	-42 18.4	3661.0	8.9	152
11	3	1975	3.0	13 0	10 32.4	-42 16.6	3664.9	6.9	152
11	3	1975	3.0	1349	10 27.4	-42 13.9	3670.5	2.9	161
11	3	1975	3.0	14 0	10 26.9	-42 13.7	3671.1	0.9	265
11	3	1975	3.0	1430	10 26.9	-42 14.2	3671.5	3.9	264
11	3	1975	3.0	1438	10 26.8	-42 14.7	3672.0	7.9	263
11	3	1975	3.0	1745	10 23.9	-42 39.7	3696.8	4.9	41
11	3	1975	3.0	1920	10 29.7	-42 34.5	3704.5	5.0	59
11	3	1975	3.0	20 0	10 31.4	-42 31.6	3707.8	0.9	265
11	3	1975	3.0	2024	10 31.4	-42 32.0	3708.2	0.9	321
11	3	1975	3.0	2038	10 31.5	-42 32.1	3708.4	1.6	262
11	3	1975	3.0	2048	10 31.5	-42 32.4	3708.7	8.2	264
11	3	1975	3.0	2125	10 31.0	-42 37.6	3713.8	11.2	265
11	3	1975	3.0	2130	10 30.9	-42 38.5	3714.7	8.6	264
11	3	1975	3.0	2214	10 30.3	-42 44.9	3721.0	8.8	264
11	3	1975	3.0	2238	10 29.9	-42 48.5	3724.6	8.9	265
11	3	1975	3.0	2347	10 29.0	-42 58.9	3734.8	5.6	265
12	3	1975	3.0	0 0	10 28.9	-43 0.1	3736.1	3.1	255
12	3	1975	3.0	016	10 28.7	-43 0.9	3736.9	6.5	174
12	3	1975	3.0	027	10 27.5	-43 0.8	3738.1	6.3	93
12	3	1975	3.0	214	10 26.9	-42 49.3	3749.4	6.2	90
12	3	1975	3.0	330	10 26.9	-42 41.4	3757.2	6.4	90
12	3	1975	3.0	556	10 26.9	-42 25.4	3772.9	6.7	95
12	3	1975	3.0	624	10 26.6	-42 22.2	3776.0	6.3	91
12	3	1975	3.0	630	10 26.6	-42 21.6	3776.7	6.3	91
12	3	1975	3.0	758	10 26.5	-42 12.3	3785.9	6.9	88
12	3	1975	3.0	834	10 26.7	-42 8.1	3790.0	5.0	102
12	3	1975	3.0	854	10 26.3	-42 6.4	3791.7	8.5	184
12	3	1975	3.0	955	10 17.7	-42 7.1	3800.3	8.0	263
12	3	1975	3.0	1022	10 17.3	-42 10.7	3803.9	7.9	275

DAY	MON	YEAR	TZ	TIME	LATITUDE	LONGITUDE	DISTANCE	SPEED	COURSE
12	3	1975	3.0	12 5	10 18.4	-42 24.6	3817.5	7.6	356
12	3	1975	3.0	1251	10 24.2	-42 24.9	3823.3	2.9	345
12	3	1975	3.0	13 6	10 24.9	-42 25.1	3824.1	6.6	191
12	3	1975	3.0	1325	10 22.9	-42 25.5	3826.2	1.0	295
12	3	1975	3.0	1527	10 23.7	-42 27.3	3828.1	2.9	345
12	3	1975	3.0	1537	10 24.2	-42 27.4	3828.6	7.3	356
12	3	1975	3.0	1845	10 47.1	-42 29.0	3851.6	5.2	83
12	3	1975	3.0	21 0	10 48.5	-42 17.3	3863.2	7.6	275
12	3	1975	3.0	2125	10 48.8	-42 20.5	3866.4	8.6	275
12	3	1975	3.0	2150	10 49.0	-42 24.1	3870.0	8.9	271
12	3	1975	3.0	22 0	10 49.1	-42 25.6	3871.5	5.5	270
12	3	1975	3.0	2310	10 49.0	-42 32.2	3877.9	5.7	273
12	3	1975	3.0	2320	10 49.1	-42 33.2	3878.9	5.0	273
12	3	1975	3.0	2356	10 49.2	-42 36.2	3881.9	8.7	268
13	3	1975	3.0	018	10 49.2	-42 39.5	3885.1	7.3	352
13	3	1975	3.0	058	10 54.0	-42 40.1	3889.9	7.6	4
13	3	1975	3.0	217	11 4.0	-42 39.4	3900.0	6.9	84
13	3	1975	3.0	3 4	11 4.6	-42 33.9	3905.3	7.6	91
13	3	1975	3.0	5 0	11 4.4	-42 19.0	3920.0	7.6	91
13	3	1975	3.0	5 8	11 4.3	-42 18.0	3921.0	7.4	91
13	3	1975	3.0	642	11 4.1	-42 6.1	3932.6	8.0	183
13	3	1975	3.0	648	11 3.3	-42 6.2	3933.4	9.3	190
13	3	1975	3.0	720	10 58.5	-42 7.0	3938.4	9.5	196
13	3	1975	3.0	823	10 48.9	-42 9.8	3948.4	4.8	202
13	3	1975	3.0	836	10 47.9	-42 10.2	3949.4	3.1	186
13	3	1975	3.0	849	10 47.2	-42 10.3	3950.1	0.2	123
13	3	1975	3.0	932	10 47.1	-42 10.1	3950.2	0.9	247
13	3	1975	3.0	1050	10 46.7	-42 11.2	3951.4	1.4	274
13	3	1975	3.0	1112	10 46.7	-42 11.7	3951.9	6.2	13
13	3	1975	3.0	1120	10 47.5	-42 11.5	3952.7	5.8	15
13	3	1975	3.0	1142	10 49.6	-42 11.0	3954.8	1.3	254
13	3	1975	3.0	1350	10 48.8	-42 13.8	3957.7	7.7	269
13	3	1975	3.0	1442	10 48.6	-42 20.6	3964.4	8.2	270
13	3	1975	3.0	15 5	10 48.6	-42 23.8	3967.5	7.9	270
13	3	1975	3.0	1634	10 48.6	-42 35.7	3979.2	7.9	271
13	3	1975	3.0	1730	10 48.8	-42 43.2	3986.6	7.7	271
13	3	1975	3.0	1820	10 48.9	-42 49.8	3993.0	7.8	273
13	3	1975	3.0	1842	10 49.1	-42 52.7	3995.9	5.2	274
13	3	1975	3.0	19 0	10 49.2	-42 54.2	3997.5	8.1	273
13	3	1975	3.0	20 8	10 49.7	-43 3.5	4006.6	8.0	273
13	3	1975	3.0	21 0	10 50.1	-43 10.5	4013.5	7.1	272
13	3	1975	3.0	2140	10 50.3	-43 15.3	4018.2	5.9	87
13	3	1975	3.0	2218	10 50.5	-43 11.5	4022.0	7.9	92
13	3	1975	3.0	2248	10 50.4	-43 7.5	4025.9	7.4	89
14	3	1975	3.0	0 6	10 50.5	-42 57.7	4035.5	7.2	82
14	3	1975	3.0	022	10 50.8	-42 55.8	4037.5	7.3	95
14	3	1975	3.0	034	10 50.7	-42 54.3	4038.9	5.0	175
14	3	1975	3.0	050	10 49.3	-42 54.2	4040.2	2.9	105
14	3	1975	3.0	055	10 49.3	-42 53.9	4040.5	6.8	96
14	3	1975	3.0	2 0	10 48.5	-42 46.5	4047.9	6.9	96

DAY	MON	YEAR	TZ	TIME	LATITUDE	LONGITUDE	DISTANCE	SPEED	COURSE
14	3	1975	3.0	2 8	10 48.4	-42 45.5	4048.8	6.6	96
14	3	1975	3.0	317	10 47.7	-42 37.8	4056.4	1.8	114
14	3	1975	3.0	336	10 47.5	-42 37.3	4056.9	7.5	179
14	3	1975	3.0	540	10 32.0	-42 37.1	4072.4	6.4	94
14	3	1975	3.0	6 4	10 31.8	-42 34.5	4075.0	7.4	86
14	3	1975	3.0	632	10 32.1	-42 31.0	4078.4	7.0	89
14	3	1975	3.0	728	10 32.1	-42 24.4	4084.9	6.6	89
14	3	1975	3.0	8 0	10 32.2	-42 20.8	4088.4	6.3	8
14	3	1975	3.0	816	10 33.8	-42 20.6	4090.1	7.0	6
14	3	1975	3.0	844	10 37.1	-42 20.3	4093.4	7.1	358
14	3	1975	3.0	914	10 40.7	-42 20.4	4097.0	7.3	357
14	3	1975	3.0	955	10 45.6	-42 20.6	4101.9	3.2	347
14	3	1975	3.0	1010	10 46.4	-42 20.8	4102.8	1.2	310
14	3	1975	3.0	1032	10 46.7	-42 21.1	4103.2	0.8	239
14	3	1975	3.0	1146	10 46.2	-42 22.0	4104.2	1.8	277
14	3	1975	3.0	1213	10 46.3	-42 22.8	4105.0	5.8	295
14	3	1975	3.0	1223	10 46.7	-42 23.7	4106.0	9.3	298
14	3	1975	3.0	1348	10 52.9	-42 35.5	4119.1	9.8	298
14	3	1975	3.0	1415	10 55.0	-42 39.4	4123.5	9.4	305
14	3	1975	3.0	1548	11 3.4	-42 51.5	4138.0	8.4	303
14	3	1975	3.0	1711	11 9.7	-43 1.4	4149.6	7.8	190
14	3	1975	3.0	1756	11 3.9	-43 2.5	4155.5	9.3	182
14	3	1975	3.0	19 2	10 53.7	-43 2.7	4165.7	9.0	184
14	3	1975	3.0	1944	10 47.4	-43 3.2	4172.0	8.6	180
14	3	1975	3.0	20 0	10 45.1	-43 3.2	4174.2	8.9	180
14	3	1975	3.0	2048	10 38.0	-43 3.2	4181.4	8.9	186
14	3	1975	3.0	21 0	10 36.2	-43 3.4	4183.2	1.7	225
14	3	1975	3.0	21 1	10 36.2	-43 3.4	4183.2	8.7	186
14	3	1975	3.0	2325	10 15.4	-43 5.6	4204.1	8.0	269
15	3	1975	3.0	1 0	10 15.3	-43 18.5	4216.8	8.9	275
15	3	1975	3.0	230	10 16.4	-43 32.0	4230.2	9.0	275
15	3	1975	3.0	3 0	10 16.8	-43 36.6	4234.6	8.8	279
15	3	1975	3.0	518	10 19.9	-43 56.8	4254.8	8.9	282
15	3	1975	3.0	530	10 20.3	-43 58.6	4256.6	8.9	282
15	3	1975	3.0	728	10 23.8	-44 16.1	4274.2	8.6	282
15	3	1975	3.0	8 0	10 24.7	-44 20.7	4278.8	8.6	276
15	3	1975	3.0	10 0	10 26.5	-44 38.0	4295.9	5.2	278
15	3	1975	3.0	1013	10 26.6	-44 39.2	4297.0	1.6	293
15	3	1975	3.0	1054	10 27.1	-44 40.2	4298.1	0.5	262
15	3	1975	3.0	1215	10 27.0	-44 40.9	4298.8	3.8	271
15	3	1975	3.0	1224	10 27.0	-44 41.5	4299.4	8.0	271
15	3	1975	3.0	1240	10 27.0	-44 43.7	4301.6	8.4	276
15	3	1975	3.0	1254	10 27.2	-44 45.6	4303.5	8.8	272
15	3	1975	3.0	1430	10 27.7	-44 59.9	4317.5	8.2	296
15	3	1975	3.0	1440	10 28.3	-45 1.1	4318.9	8.5	295
15	3	1975	3.0	1644	10 35.7	-45 17.4	4336.5	8.5	296
15	3	1975	3.0	1730	10 38.6	-45 23.3	4342.9	8.6	296
15	3	1975	3.0	1830	10 42.4	-45 31.1	4351.5	0.7	248
15	3	1975	3.0	1831	10 42.4	-45 31.1	4351.5	8.5	296
15	3	1975	3.0	1930	10 46.1	-45 38.7	4359.9	8.6	303

DAY	MON	YEAR	TZ	TIME	LATITUDE	LONGITUDE	DISTANCE	SPEED	COURSE
15	3	1975	3.0	1940	10 46.9	-45 40.0	4361.3	8.8	304
15	3	1975	3.0	2110	10 54.2	-45 51.1	4374.5	9.0	305
15	3	1975	3.0	2126	10 55.5	-45 53.1	4376.9	8.4	305
15	3	1975	3.0	2215	10 59.5	-45 58.8	4383.8	8.7	279
15	3	1975	3.0	2256	11 0.5	-46 4.8	4389.7	8.9	280
16	3	1975	3.0	0 0	11 2.1	-46 14.3	4399.2	8.9	280
16	3	1975	3.0	010	11 2.3	-46 15.8	4400.6	8.6	280
16	3	1975	3.0	2 6	11 5.1	-46 32.5	4417.3	8.6	279
16	3	1975	3.0	3 0	11 6.3	-46 40.3	4425.1	8.8	279
16	3	1975	3.0	430	11 8.2	-46 53.6	4438.2	8.8	277
16	3	1975	3.0	6 0	11 9.8	-47 7.0	4451.4	8.7	277
16	3	1975	3.0	614	11 10.1	-47 9.0	4453.5	8.5	282
16	3	1975	3.0	640	11 10.8	-47 12.7	4457.2	8.6	276
16	3	1975	3.0	7 0	11 11.1	-47 15.6	4460.0	8.6	279
16	3	1975	3.0	846	11 13.4	-47 30.8	4475.1	8.7	278
16	3	1975	3.0	9 0	11 13.7	-47 32.9	4477.2	8.7	278
16	3	1975	3.0	10 2	11 15.0	-47 42.0	4486.2	8.9	279
16	3	1975	3.0	1148	11 17.6	-47 57.8	4501.9	9.2	279
16	3	1975	3.0	12 0	11 17.8	-47 59.7	4503.8	9.5	279
16	3	1975	3.0	1213	11 18.2	-48 1.8	4505.8	4.6	277
16	3	1975	3.0	1227	11 18.3	-48 2.8	4506.9	0.7	263
16	3	1975	3.0	1425	11 18.1	-48 4.3	4508.4	6.7	278
16	3	1975	3.0	1430	11 18.2	-48 4.9	4508.9	9.1	279
16	3	1975	3.0	1556	11 20.2	-48 18.1	4522.0	9.0	279
16	3	1975	3.0	1730	11 22.5	-48 32.2	4536.1	9.1	279
16	3	1975	3.0	18 6	11 23.3	-48 37.7	4541.5	9.0	280
16	3	1975	3.0	1954	11 26.2	-48 54.0	4557.7	8.8	280
16	3	1975	3.0	2030	11 27.1	-48 59.3	4563.0	9.1	280
16	3	1975	3.0	2318	11 31.6	-49 25.0	4588.6	9.4	280
16	3	1975	3.0	2330	11 31.9	-49 26.9	4590.5	8.9	280
17	3	1975	3.0	1 2	11 34.2	-49 40.7	4604.2	8.8	279
17	3	1975	3.0	230	11 36.3	-49 53.7	4617.1	9.8	279
17	3	1975	3.0	256	11 37.0	-49 58.0	4621.3	8.7	280
17	3	1975	3.0	340	11 38.1	-50 4.4	4627.7	9.0	280
17	3	1975	3.0	438	11 39.6	-50 13.1	4636.4	4.0	280
17	3	1975	3.0	526	11 40.2	-50 16.3	4639.6	4.4	280
17	3	1975	3.0	7 6	11 41.5	-50 23.7	4646.9	9.0	280
17	3	1975	3.0	738	11 42.3	-50 28.5	4651.7	9.1	280
17	3	1975	3.0	811	11 43.2	-50 33.5	4656.7	4.9	280
17	3	1975	3.0	851	11 43.8	-50 36.8	4660.0	8.7	280
17	3	1975	3.0	922	11 44.6	-50 41.3	4664.5	9.0	280
17	3	1975	3.0	952	11 45.4	-50 45.8	4668.9	9.0	281
17	3	1975	3.0	1056	11 47.2	-50 55.4	4678.5	9.2	279
17	3	1975	3.0	1138	11 48.2	-51 2.0	4685.0	9.1	280
17	3	1975	3.0	12 0	11 48.7	-51 5.3	4688.3	9.1	280
17	3	1975	3.0	1246	11 49.9	-51 12.4	4695.3	9.0	278
17	3	1975	3.0	1436	11 52.3	-51 29.0	4711.8	9.1	278
17	3	1975	3.0	15 0	11 52.9	-51 32.7	4715.4	6.0	277
17	3	1975	3.0	1642	11 54.2	-51 43.0	4725.6	9.3	278
17	3	1975	3.0	1656	11 54.5	-51 45.2	4727.7	9.2	277

DAY	MON	YEAR	TZ	TIME	LATITUDE	LONGITUDE	DISTANCE	SPEED	COURSE
17	3	1975	3.0	19 4	11 56.9	-52 5.1	4747.4	9.2	279
17	3	1975	3.0	1930	11 57.5	-52 9.1	4751.4	9.4	279
17	3	1975	3.0	2050	11 59.5	-52 21.7	4763.9	9.0	278
17	3	1975	3.0	2118	12 0.0	-52 26.0	4768.1	9.2	280
17	3	1975	3.0	2222	12 1.8	-52 35.9	4777.9	9.1	278
17	3	1975	3.0	2230	12 2.0	-52 37.1	4779.1	9.1	278
17	3	1975	3.0	23 6	12 2.8	-52 42.6	4784.6	9.3	280
18	3	1975	3.0	014	12 4.5	-52 53.3	4795.1	9.0	279
18	3	1975	4.0	030	12 6.2	-53 4.8	4806.5	9.1	279
18	3	1975	4.0	330	12 10.3	-53 32.2	4833.7	9.1	279
18	3	1975	4.0	338	12 10.5	-53 33.5	4834.9	9.1	280
18	3	1975	4.0	548	12 13.9	-53 53.4	4854.6	9.2	280
18	3	1975	4.0	630	12 15.0	-53 59.9	4861.1	9.3	280
18	3	1975	4.0	718	12 16.3	-54 7.4	4868.6	9.4	278
18	3	1975	4.0	734	12 16.7	-54 10.0	4871.1	9.1	281
18	3	1975	4.0	8 2	12 17.5	-54 14.2	4875.3	9.3	279
18	3	1975	4.0	815	12 17.8	-54 16.3	4877.3	9.2	274
18	3	1975	4.0	9 2	12 18.4	-54 23.6	4884.6	8.9	273
18	3	1975	4.0	950	12 18.7	-54 31.0	4891.7	8.6	275
18	3	1975	4.0	1054	12 19.6	-54 40.4	4900.9	9.0	274
18	3	1975	4.0	11 0	12 19.6	-54 41.3	4901.8	8.9	274
18	3	1975	4.0	12 0	12 20.3	-54 50.4	4910.7	0.1	191
18	3	1975	4.0	12 1	12 20.3	-54 50.4	4910.7	8.8	274
18	3	1975	4.0	1240	12 20.7	-54 56.2	4916.4	8.8	276
18	3	1975	4.0	15 0	12 22.8	-55 17.2	4937.1	8.7	276
18	3	1975	4.0	1652	12 24.5	-55 33.8	4953.4	8.0	275
18	3	1975	4.0	18 0	12 25.4	-55 43.1	4962.5	8.2	275
18	3	1975	4.0	1852	12 26.1	-55 50.3	4969.6	8.4	274
18	3	1975	4.0	2038	12 27.1	-56 5.5	4984.4	8.6	276
18	3	1975	4.0	21 0	12 27.4	-56 8.7	4987.6	8.7	276
18	3	1975	4.0	2116	12 27.7	-56 11.1	4989.9	8.3	275
18	3	1975	4.0	2220	12 28.4	-56 20.1	4998.8	8.2	276
18	3	1975	4.0	23 4	12 29.1	-56 26.3	5004.8	8.1	272
19	3	1975	4.0	0 0	12 29.3	-56 34.0	5012.4	8.0	272
19	3	1975	4.0	0 6	12 29.3	-56 34.9	5013.2	8.0	273
19	3	1975	4.0	150	12 30.1	-56 49.0	5027.1	8.0	272
19	3	1975	4.0	3 0	12 30.4	-56 58.6	5036.4	8.1	272
19	3	1975	4.0	4 0	12 30.6	-57 6.9	5044.6	8.5	277
19	3	1975	4.0	458	12 31.7	-57 15.3	5052.8	8.7	279
19	3	1975	4.0	622	12 33.5	-57 27.6	5064.9	8.6	287
19	3	1975	4.0	646	12 34.5	-57 31.0	5068.4	8.8	281
19	3	1975	4.0	7 0	12 34.9	-57 33.0	5070.4	8.8	281
19	3	1975	4.0	9 0	12 38.2	-57 50.8	5088.1	8.9	281
19	3	1975	4.0	910	12 38.5	-57 52.3	5089.5	3.8	283
19	3	1975	4.0	929	12 38.8	-57 53.5	5090.7	6.2	282
19	3	1975	4.0	940	12 39.0	-57 54.6	5091.9	5.9	279
19	3	1975	4.0	10 2	12 39.4	-57 56.8	5094.0	6.1	281
19	3	1975	4.0	1048	12 40.3	-58 1.5	5098.7	6.4	277
19	3	1975	4.0	12 0	12 41.3	-58 9.3	5106.4	6.1	277
19	3	1975	4.0	1332	12 42.4	-58 18.8	5115.7	6.2	276

DAY	MON	YEAR	TZ	TIME	LATITUDE	LONGITUDE	DISTANCE	SPEED	COURSE
19	3	1975	4.0	15 0	12 43.4	-58 28.1	5124.8	6.4	276
19	3	1975	4.0	16 4	12 44.1	-58 35.0	5131.6	6.2	277
19	3	1975	4.0	1630	12 44.4	-58 37.8	5134.3	6.0	282
19	3	1975	4.0	1812	12 46.6	-58 47.9	5144.5	6.0	282
19	3	1975	4.0	1930	12 48.2	-58 55.8	5152.3	6.4	283
19	3	1975	4.0	21 0	12 50.4	-59 5.5	5162.0	6.6	283
19	3	1975	4.0	2116	12 50.8	-59 7.2	5163.7	6.3	279
19	3	1975	4.0	2214	12 51.7	-59 13.4	5169.9	7.2	284
20	3	1975	4.0	040	12 56.0	-59 30.8	5187.4	4.8	284
20	3	1975	4.0	2 0	12 57.5	-59 37.2	5193.8	4.9	310
20	3	1975	4.0	242	12 59.8	-59 39.9	5197.2	2.8	292
20	3	1975	4.0	3 0	13 0.1	-59 40.7	5198.0	2.2	329
20	3	1975	4.0	438	13 3.2	-59 42.6	5201.6	2.1	165
20	3	1975	4.0	442	13 3.0	-59 42.6	5201.8	1.7	327
20	3	1975	4.0	517	13 3.9	-59 43.1	5202.8	2.1	165
20	3	1975	4.0	537	13 3.2	-59 42.9	5203.5	3.0	11
20	3	1975	4.0	650	13 6.7	-59 42.2	5207.1		

PART B

Bathymetric, Geomagnetic and Gravity profiles

All bathymetric, gravimetric, magnetic and navigational data were digitized and reduced with the aid of an IBM 1130 digital computer and on-line Calcomp plotter. The entire data processing procedure including program listings is given in Talwani (1969).

The profiles of topography are plotted at a vertical exaggeration of 100:1. The units of depth used are nominal fathoms (1/400 sec reflection time). Residual geomagnetic anomalies are plotted in gammas (10^5 gammas = 1 oersted). They are obtained by subtracting the regional magnetic field (Cain et al., 1964) from the observations of the total magnetic field. Free-air gravity anomalies are plotted in milligals (1 mgal = 10^{-3} cm/sec^2). The topographic, geomagnetic, and gravity profiles are plotted with respect to distance, which is annotated at intervals of 200 nautical miles near the bottom of each profile. In addition, tick marks shown above the distance scale indicate the distance at which any change in course or speed occurred. The corresponding course and speed between changes and the coordinates at the points of change are annotated above the distance scale listings. Navigational changes which occur too frequently to be annotated in the space available or only minor adjustments in course or speed are indicated only by tick marks. Listings of the entire detailed navigation as well as navigation plots appear in Part A. The course and speed apply to the time interval following each entry.

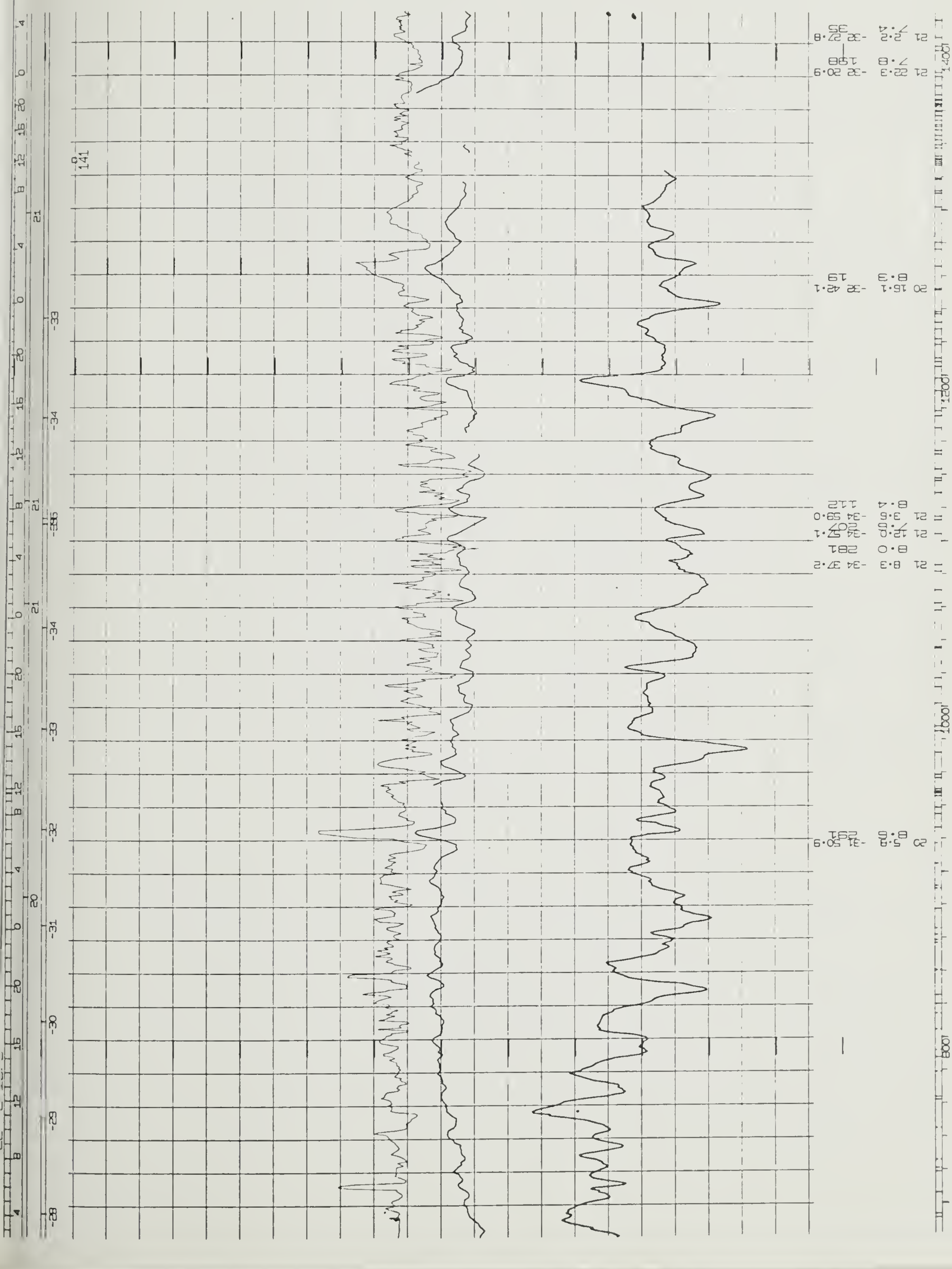

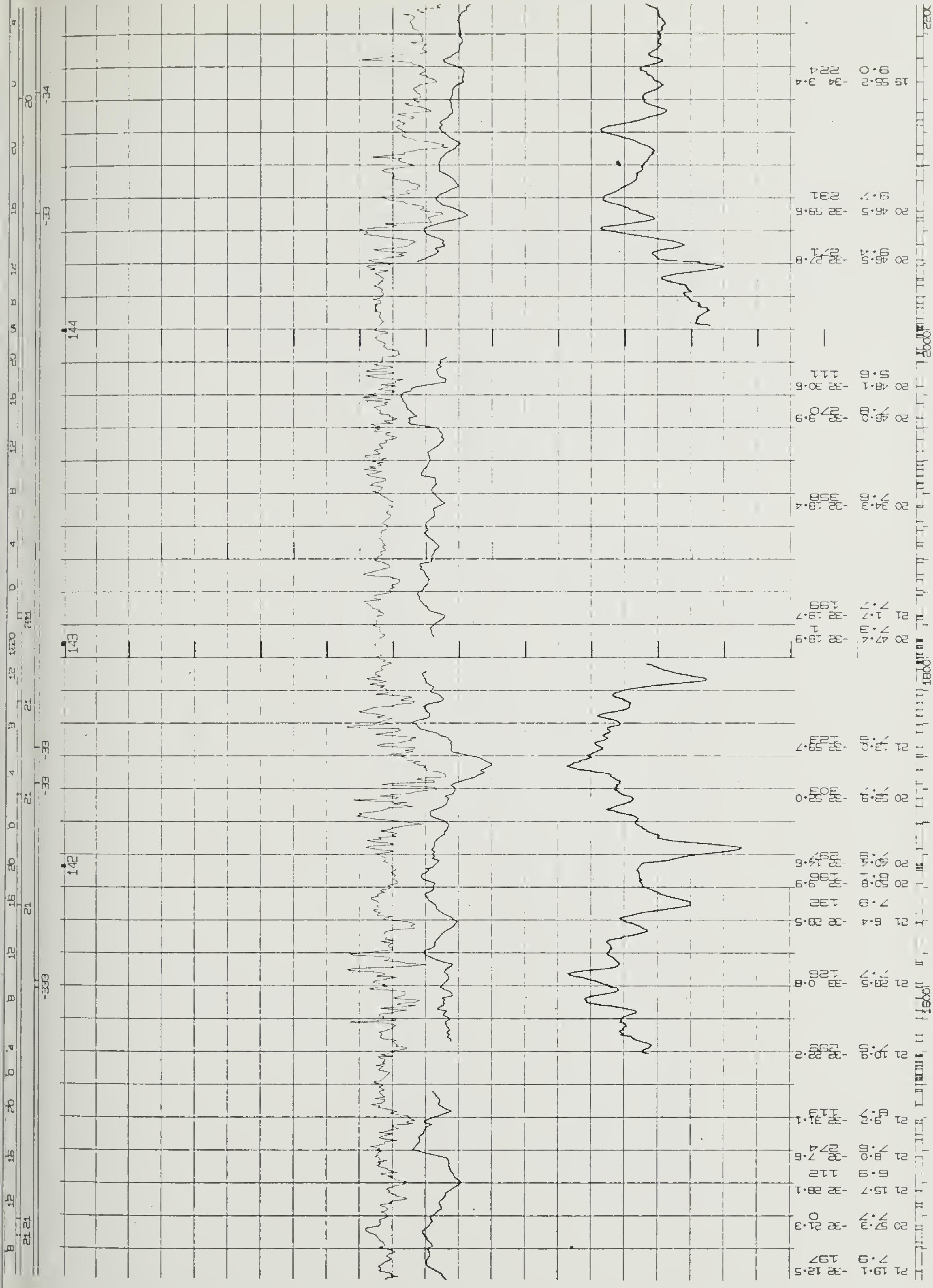

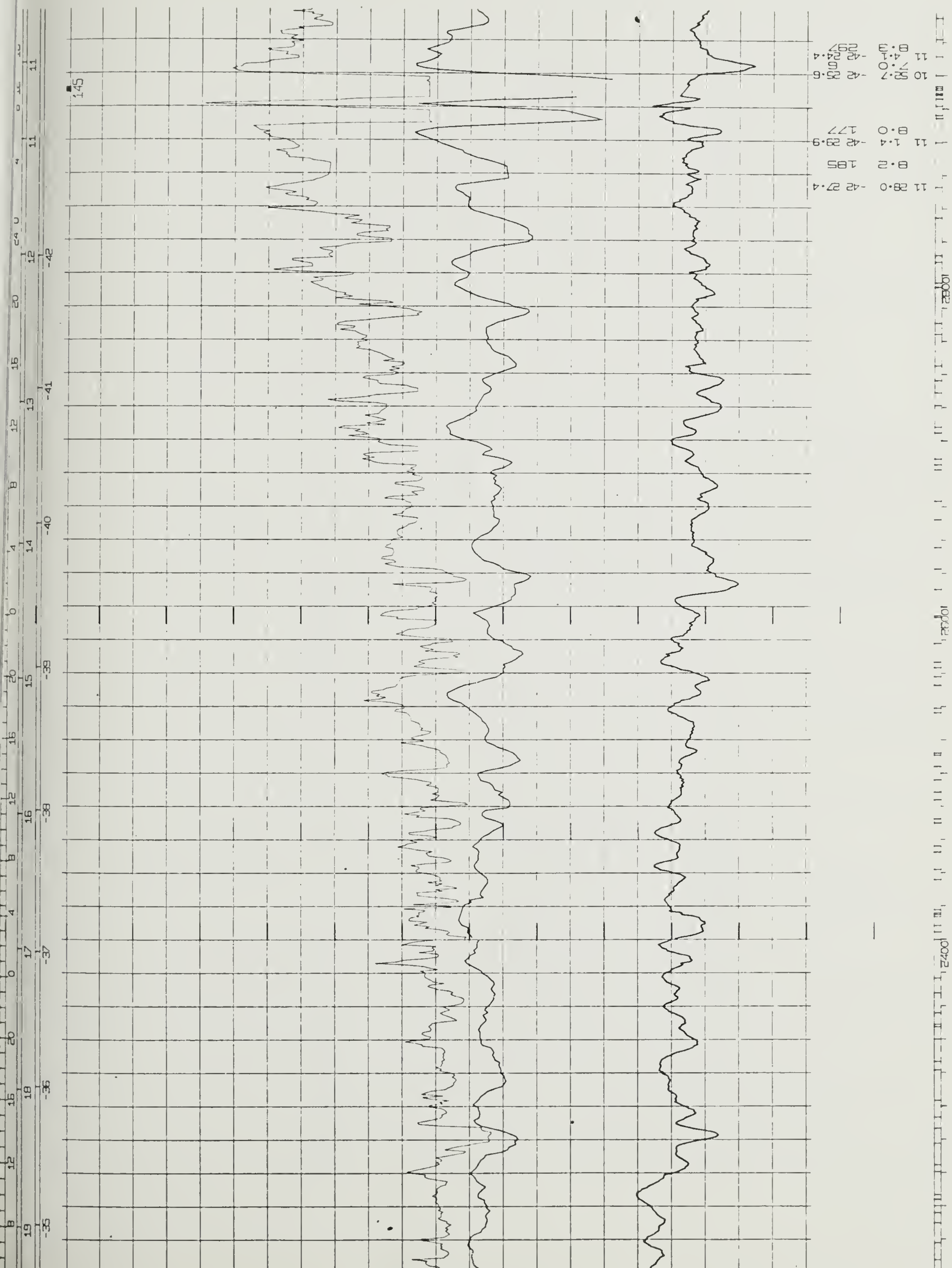

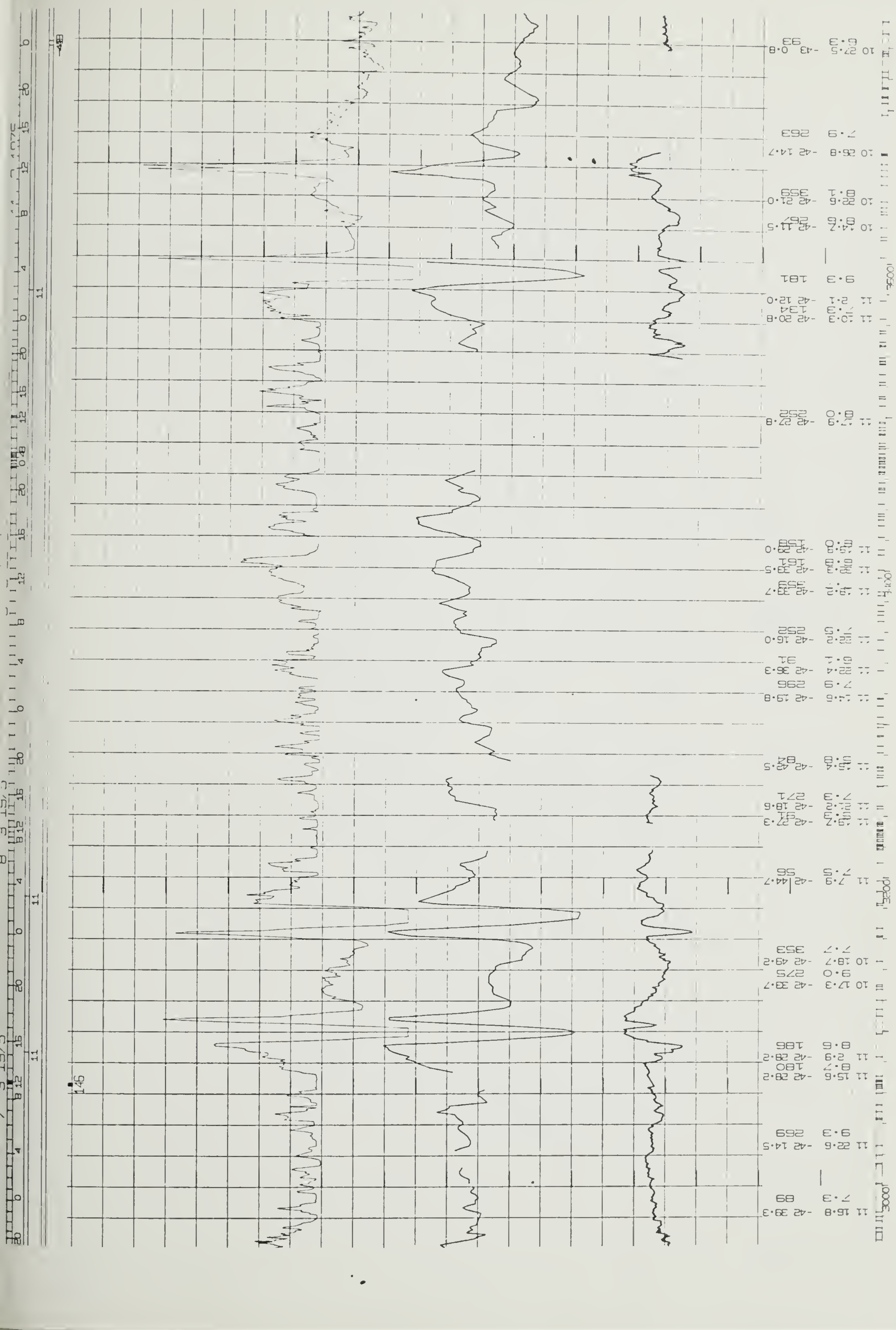

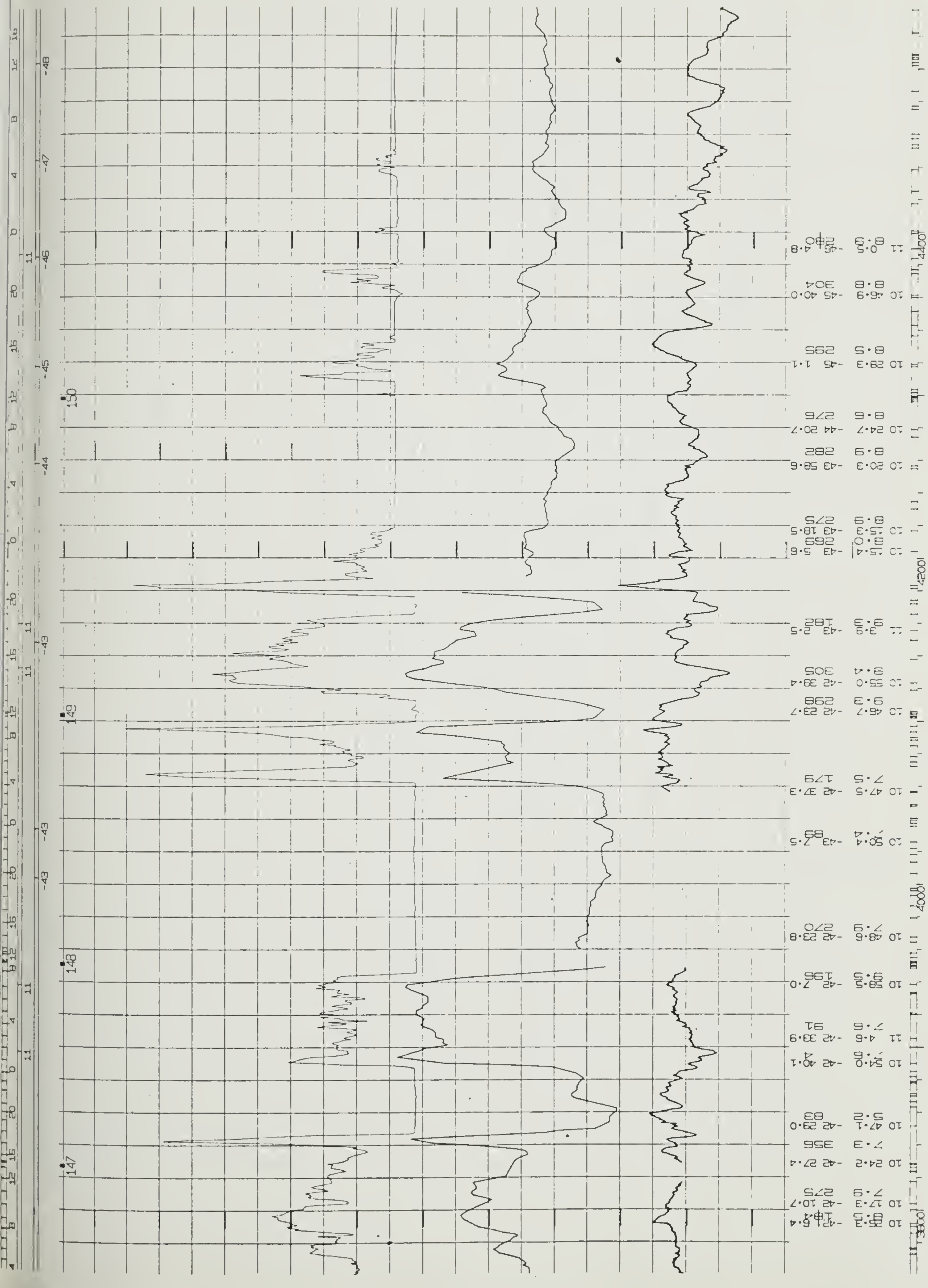

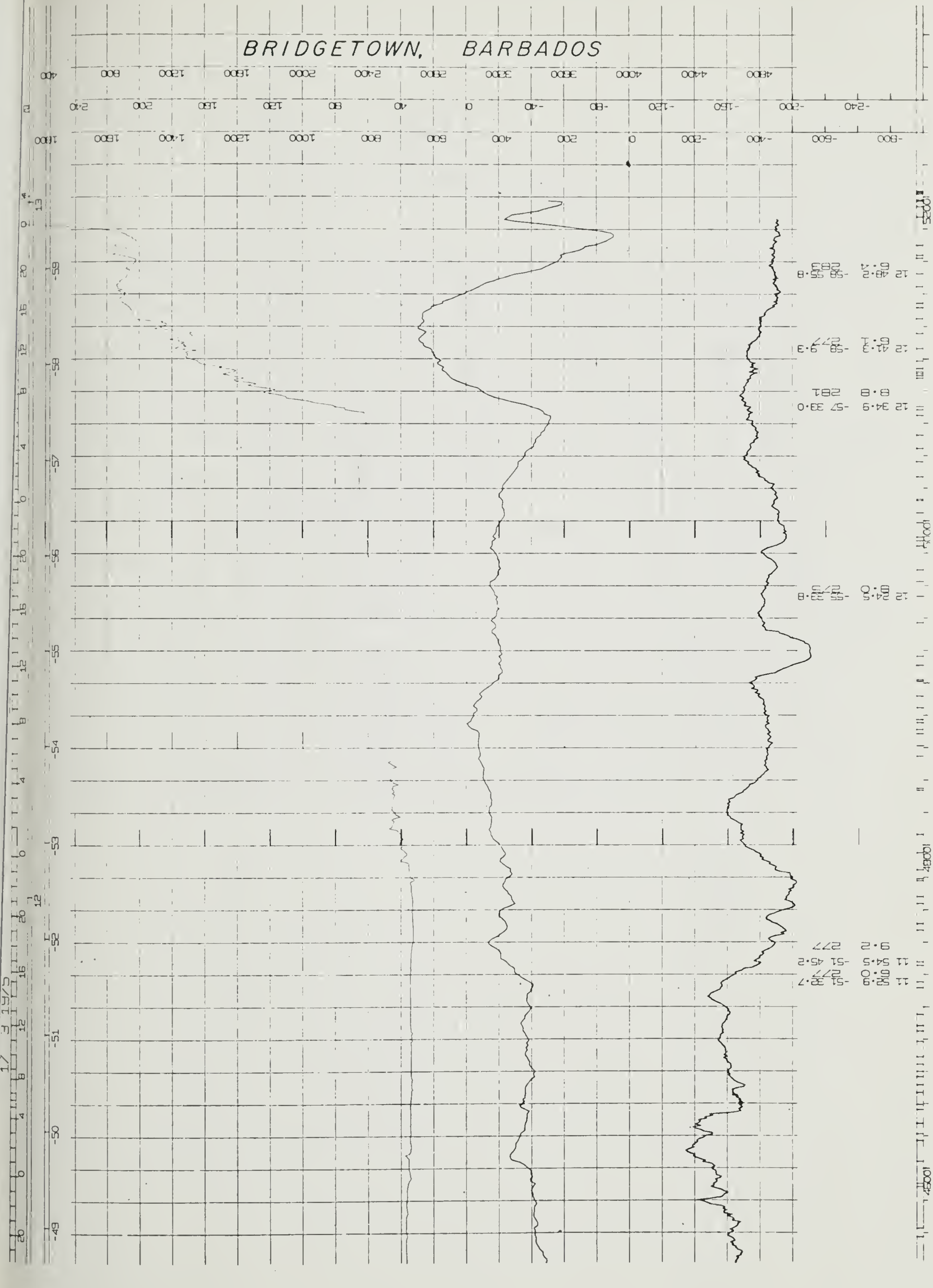
BRIDGETOWN, BARBADOS

PART C

Seismic Reflection Records

Seismic profiler data are presented as reduced copies of the original recordings. The vertical scales on the left side and right side of each page are seconds of two-way reflection time and nominal fathoms. The time of day and ship's heading appear along the bottom of the profiler sections. The courses shown are courses steered as taken from the shipboard logs. These courses generally do not agree precisely with the tabulated navigational data, which are based on the course and speed made good. Hundreds of nautical miles are also annotated on the profiler records. Each fifth profiler sheet number appears at the top of the pages; the intervening sheets are bracketed by two black dots. Major time-breaks in the profiler records are indicated by slanted lines in the lower time scale. The station locations are prefixed by the letter S followed by the station number. Sonobuoy locations are prefixed by the letter R.

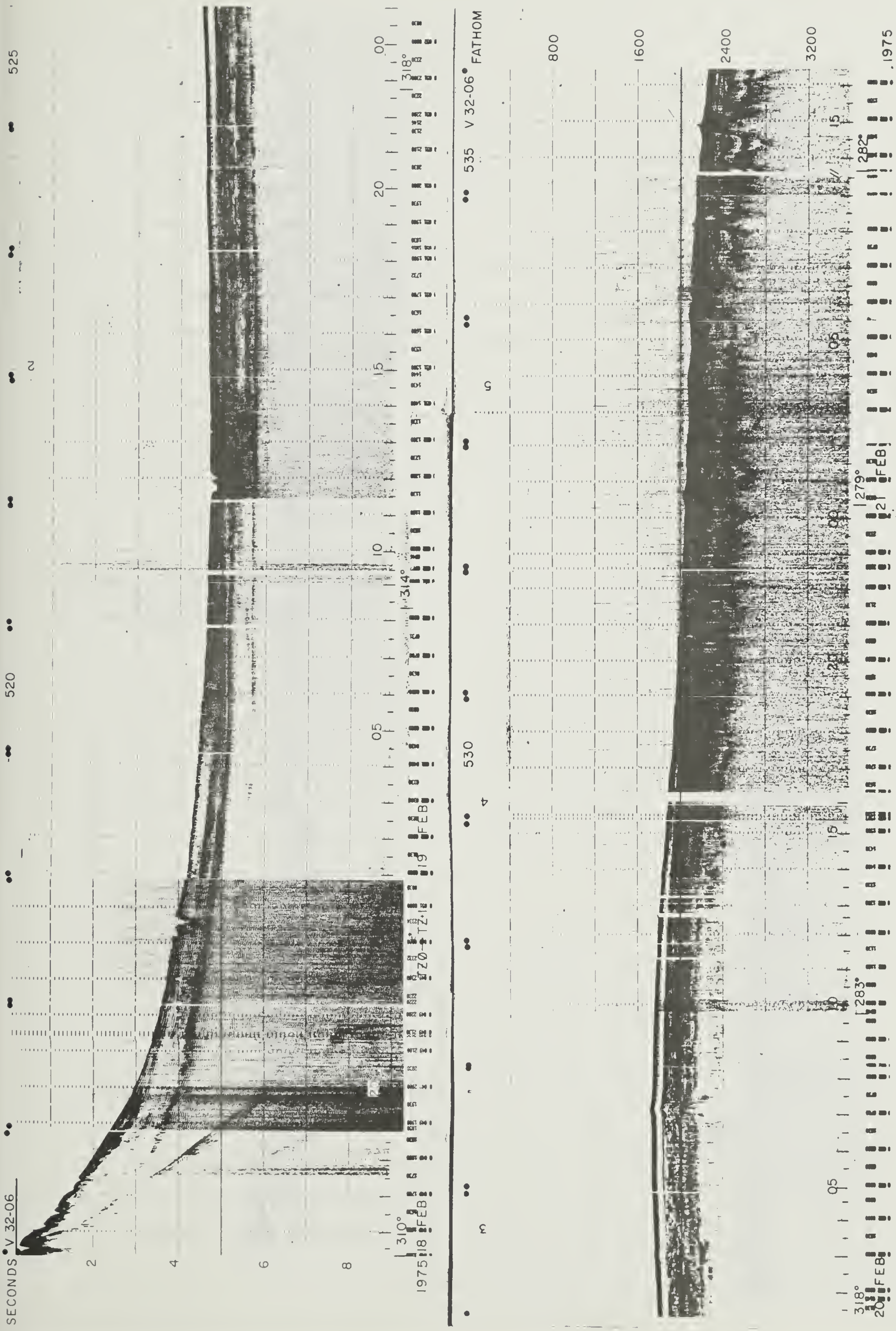
SECONDS
V 32-06
525
520
2
4
6
8
1975 18 FEB
310°
19 FEB
314°
318°
535
530
V 32-06
FATHOM
800
1600
2400
3200
1975
20 FEB
318°
283°
21 FEB
279°
282°

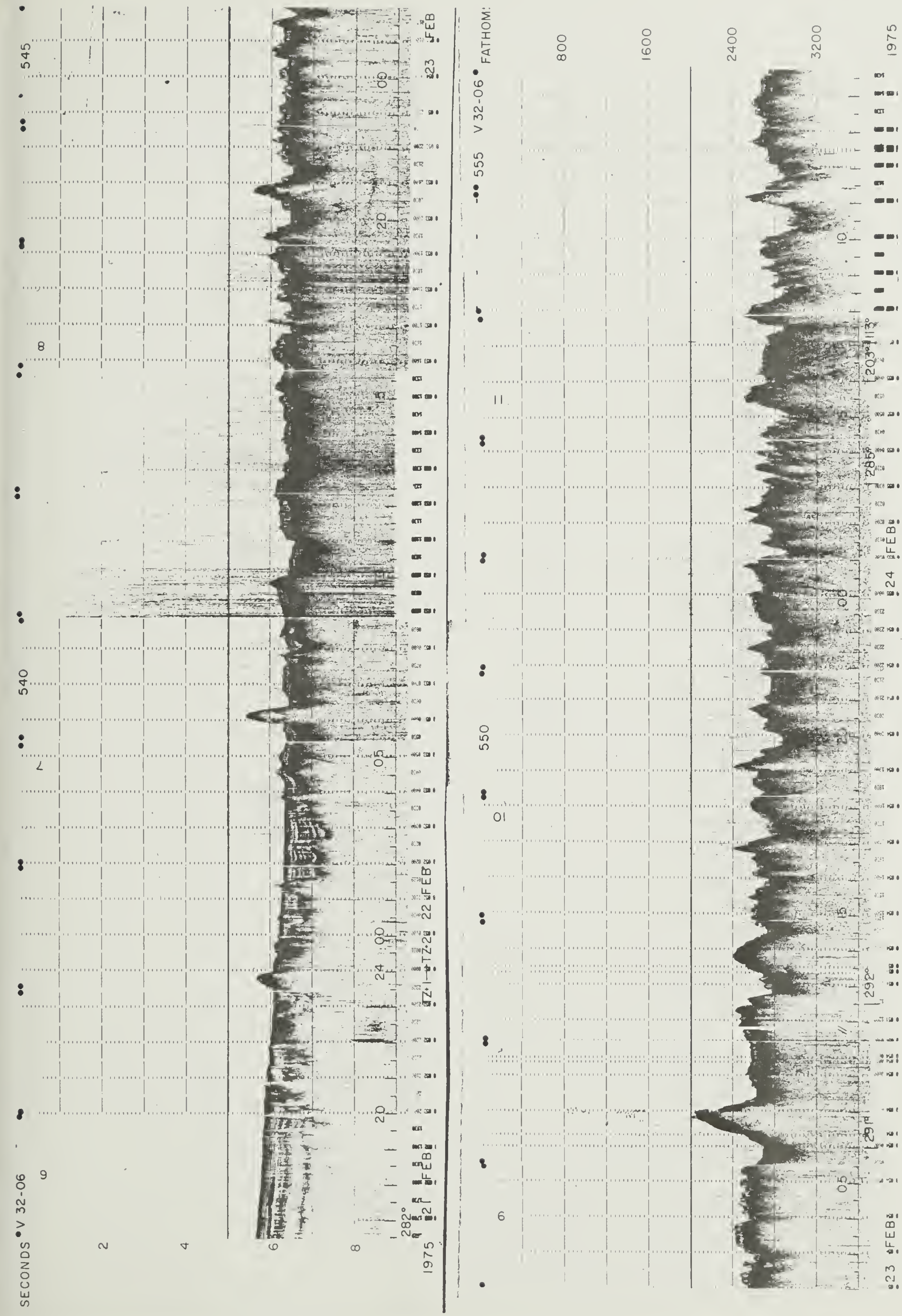
SECONDS • V 32-06
545
540
1975
22 FEB
V 32-06 • FATHOMS
555
550
800
1600
2400
3200
1975
24 FEB
23 FEB

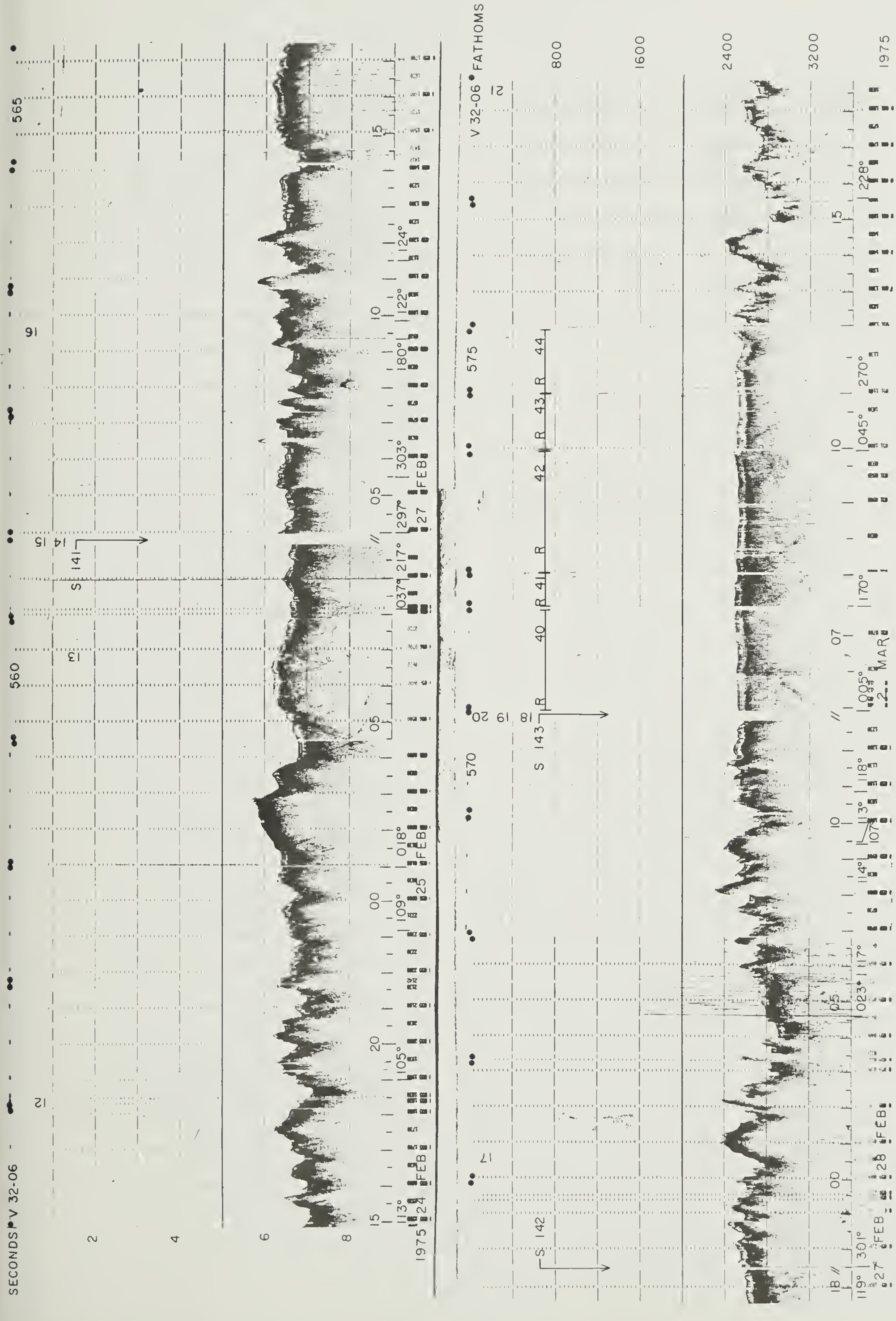
SECONDS V 32-06
V 32-06 FATHOMS
S 141
S 142
S 143
1975

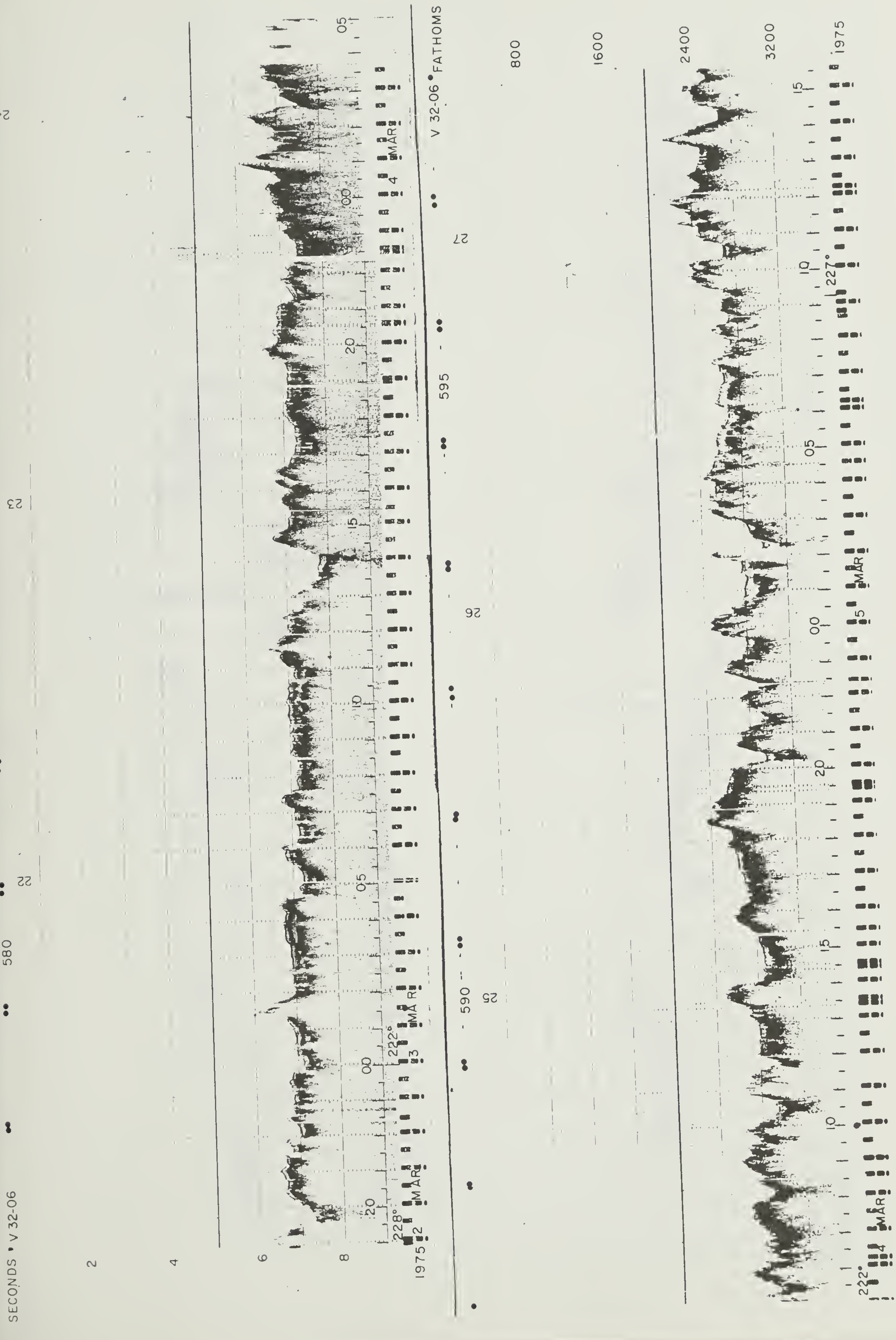
SECONDS • V 32-06
2
4
6
8
1975
228°
222°
MAR
580
585
22
23
24
V 32-06 • FATHOMS
800
1600
2400
3200
590
595
25
26
27
1975
227°
222°
MAR

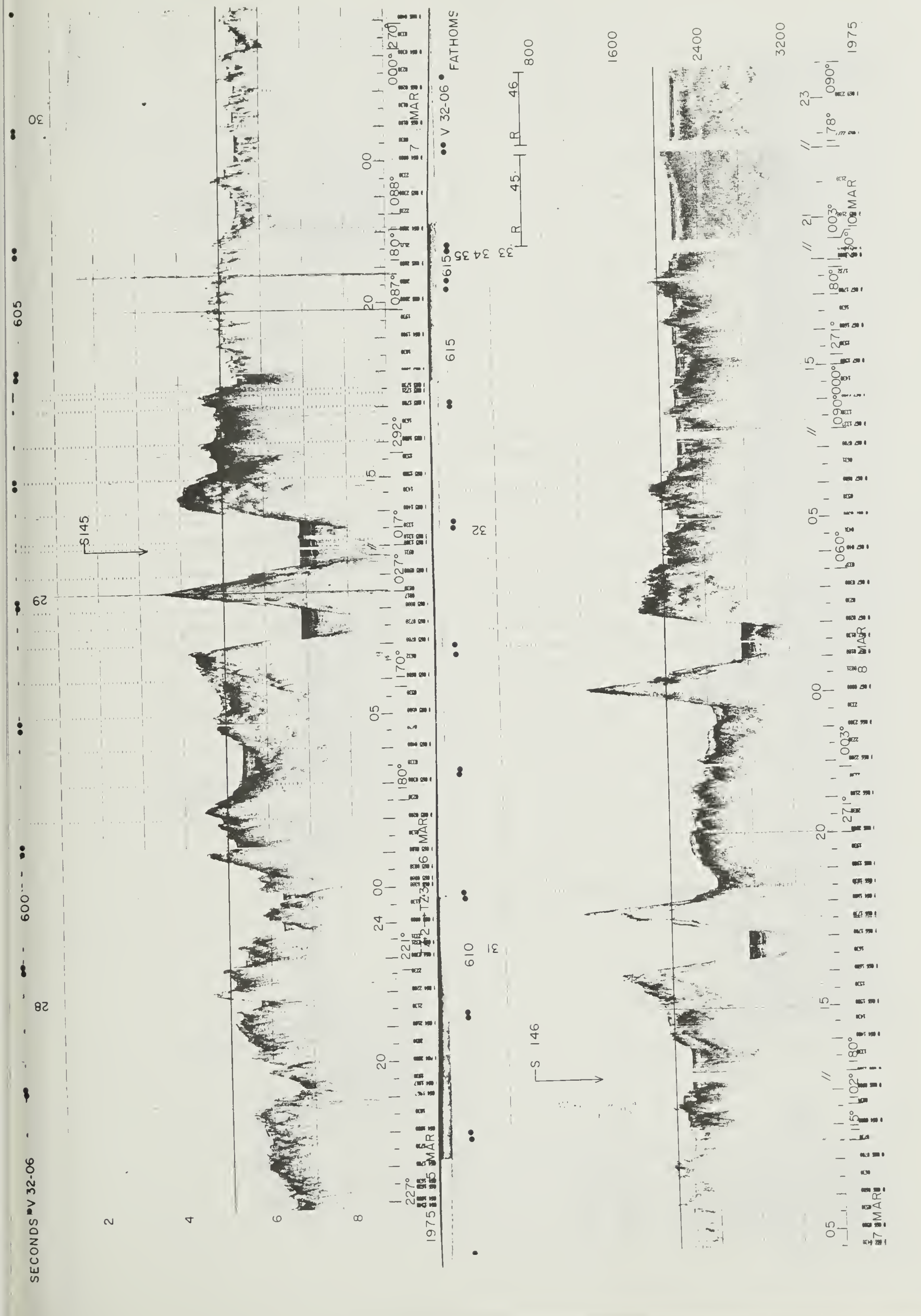
SECONDS V 32-06
2
4
6
8
1975
S145
S 146
V 32-06
FATHOMS
800
1600
2400
3200
1975
605
600
610
615
MAR

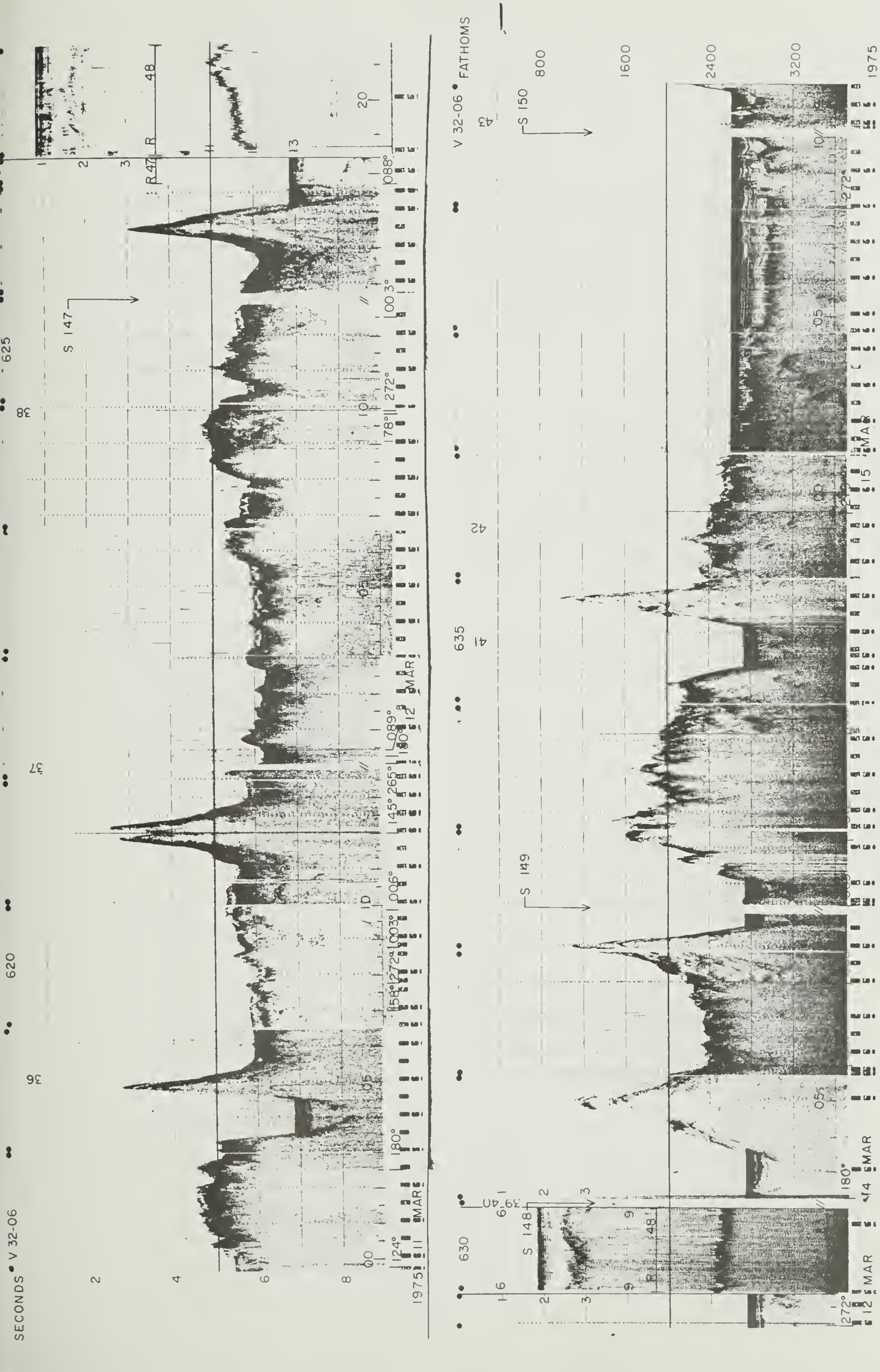
SECONDS V 32-06
V 32-06 FATHOMS
S 147
S 148
S 149
S 150
1975 11 MAR
12 MAR
14 MAR
15 MAR
620
625
630
635
800
1600
2400
3200
1975

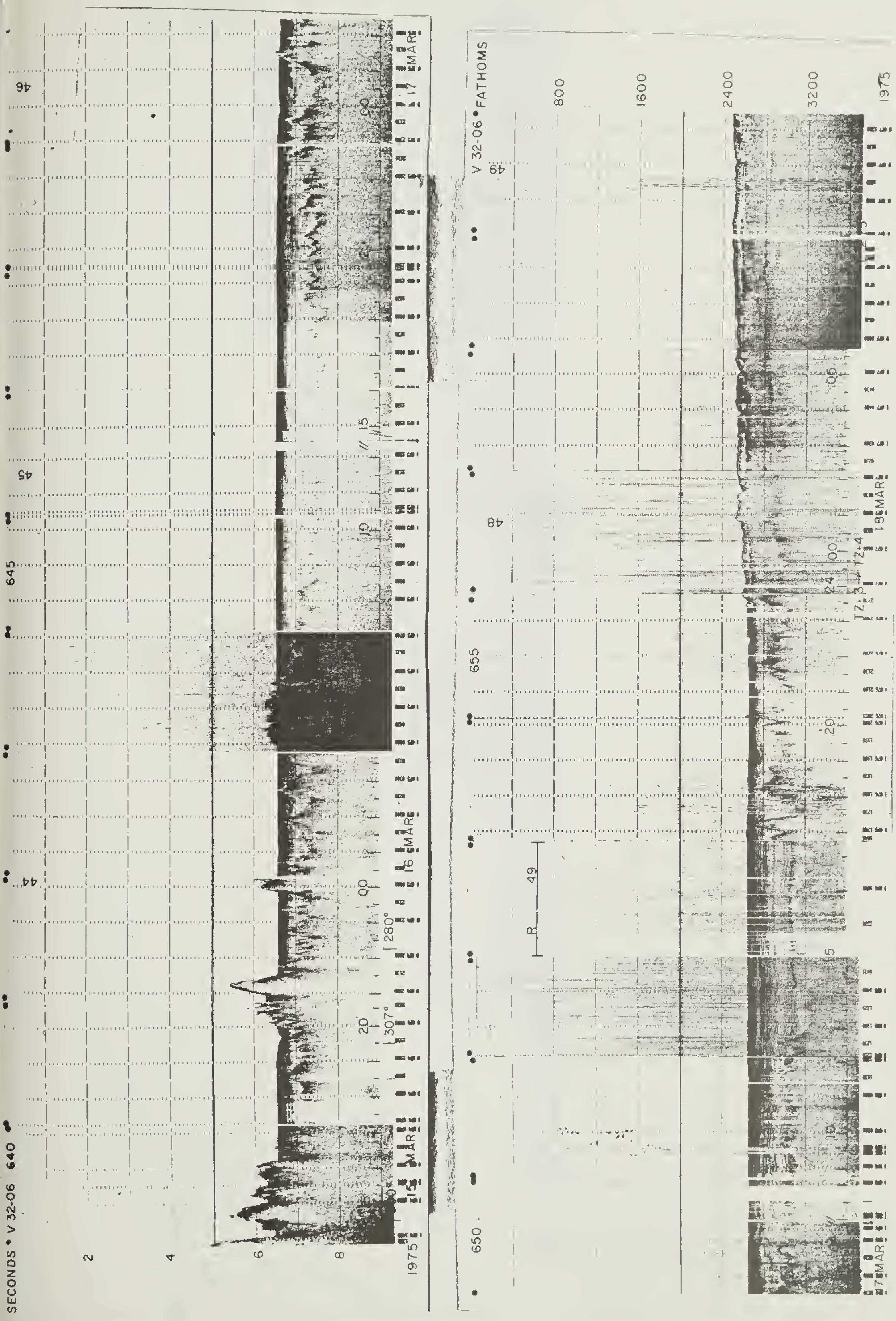
SECONDS • V 32-06 640
645
650
655
V 32-06 • FATHOMS
800
1600
2400
3200
1975
15 MAR
16 MAR
17 MAR
18 MAR
280°
307°
R
49
44
45
46
48
49

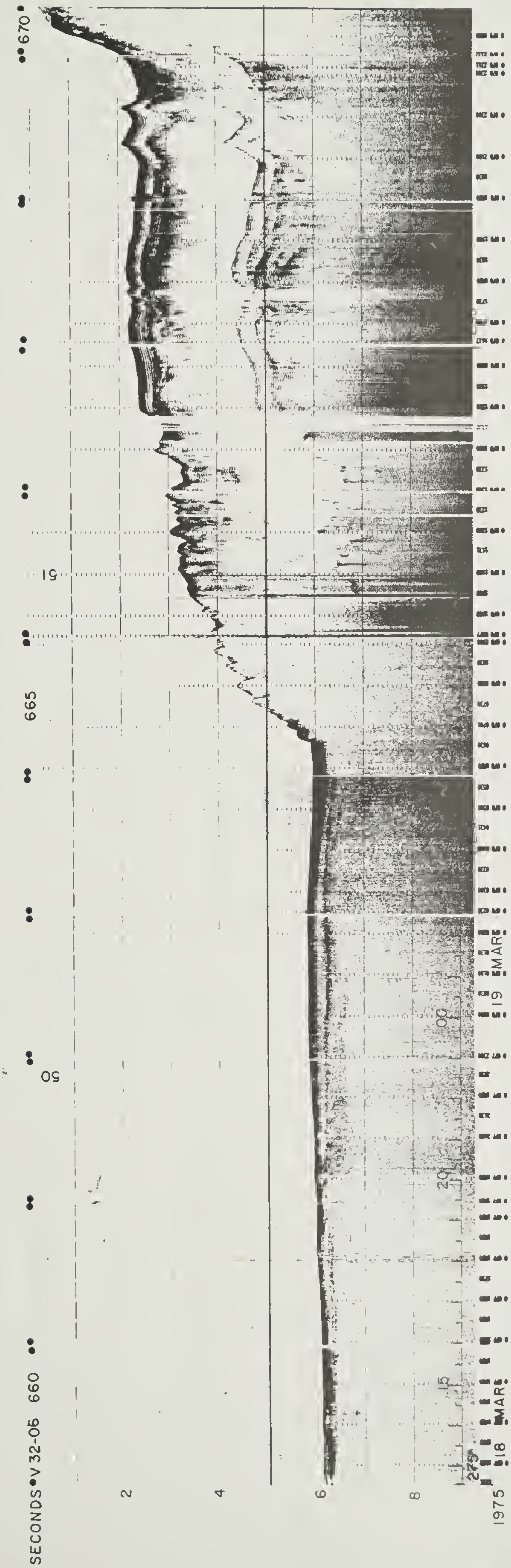

SECONDS•V 32-06 660
665
670
50
51
2
4
6
8
1975
18 MAR
19 MAR

PART D

Sonobuoy Results

RESULTS OF AIRGUN-SONOBUOY STATIONS, V32-06, SURVEY OF IPOD CANDIDATE SITES 7 AND 8

Sonobuoy	Velocity (V) and Standard Deviation (S), km/sec							Water depth	Thicknesses (h), km				Location		Profiler Record
	V_2	S_2	V_3	S_3	V_4	V_5	V_6		h_2	h_3	h_4	h_5	Lat. (N)	Long. (E)	
Site 7															
V32-06 40	1.78*		5.40		6.40			4.76	0.27	1.62			20°49.1'	32°17.9'	571
41	Insufficient data to compute												-	-	572
42	1.83	0.35	4.70		6.10	6.85	7.50?	4.74	0.19	0.65	1.22	1.16	20°53.6'	32°19.6'	573
43	1.78*							4.71	0.23				20°43.9'	32°18.3'	574
44	1.78*		4.80					4.75	0.16				20°46.4'	32°16.3'	575
Site 8															
45	1.89	0.06	3.50		4.50	6.20	7.94?	4.05	0.26	0.25	0.85	1.39	11°18.1'	42°29.2'	616
46	1.78*		3.50		4.85?			4.05	0.22	0.52			11°20.7'	42°28.8'	617
47	Insufficient data to compute												-	-	627
48	1.82	0.09	2.22	0.06	4.50	6.10		5.16	0.29	0.72	0.66		10°47.4'	42°26.4'	628

Notes:

Standard deviations refers to the computed deviation of interval velocity in the preceding column.

Velocities not having a standard deviation are unreversed refraction velocities.

Asterisks denote assumed velocity.

Question marks indicate that the data are poor.

SECTION II

STATION DATA

VEMA 3206 STATION INDEX

Ship		Time		Depth		N	W				
Station	Date	Start	End	Start	End	Latitude	Longitude	Core	TG	K	P
141	25 Feb.	1010	1256	5005	4895	21°09.9'	32°26.7'	63	1		
142	27	1854	2058	4889	4910	20°40.2'	32°13.1'	64	2		1
143	28	1722	1936	4708	4862	20°47.9'	32°17.9'				2
144	2 Mar.	0226	0457	4720	4800	20°48.0'	32°19.4'	65	3	58	3
145	6	1002	1242	5197	5197	10°44.5'	42°26.0'	66	4	59	4
146	7	1040	1248	4035	4064	11°17.5'	42°30.3'	67	5	60	
147	12	1325	1527	4185	4226	10°22.9'	42°25.5'	68	6		
148	13	0849	1050	5206	5204	10°46.7'	42°11.2'	69	7		
149	14	1032	1213	5183	5195	10°46.4'	42°21.5'	70	8		5
150	15	1013	1215	4948	4942	10°27.1'	44°40.2'	71	9		

TG = Thermograd, K = Camera, P = Plankton

PART A

CORE DESCRIPTIONS - VEMA CRUISE 3206

(Preliminary shipboard descriptions by Dave Pratt)

Date: 25 February 1975

Ship Station No.: 141

Core No: 63

Latitude: 21°09.9'N

Longitude: 32°26.7'W

Depth: 4885 m.

Site: 7

Core Length: 927 cm.

0-208 cm

Foraminiferal marl with irregular patches of clay; Moderate yellowish brown (10YR5/4) to dark yellowish brown (10YR4/2). Moist, firm and heavily burrowed. Carbonate content low to moderate. Coarse fraction about 30% consisting mostly of benthonic and planktonic foraminifera. Negligible quartz grains. Basal contact an irregular gradational color change.

208-532 cm

Marl; grayish orange (10YR7/4) to moderate yellowish brown (10YR4/2). Moist, firm and heavily burrowed. Carbonate content moderate. Coarse fraction less than 10% consisting mostly of benthonic and planktonic foraminifera. Basal contact a gradational color change.

532-554 cm

Clay; Dark yellowish brown (10YR4/2) Moist, firm and burrowed. Carbonate content very low. Coarse fraction less than 5% consisting mainly of planktonic foraminifera and quartz.

554-927 cm

Flow in

Date: 27 February 1975

Ship Station No.: 142

Core No: 64

Latitude: 20°40.2'N

Longitude: 32°13.1'W

Depth: 4900 m

Site: 7

Core Length: 571 cm

0-65 cm

Foraminiferal marl ooze; grayish orange (10YR7/2) to moderate yellowish brown (10YR5/4) to dark yellowish brown (10YR4/2). Moist, firm and heavily burrowed. Carbonate content low to moderate. Coarse fraction about 35-40% consisting mostly of benthonic and planktonic foraminifera. Irregular patches of clay are scattered throughout this unit. Basal contact a gradational color change.

65-82 cm

Foraminiferal marl ooze; grayish orange (10YR7/2). Similar to above unit except that it is not burrowed and is homogeneous. No patches of clay are present. Basal contact a gradational color change.

82-480 cm

Interbedded layers of clay and foraminiferal marl ooze similar to above units.

480-571 cm

Flow in.

Date: 2 March 1975

Ship Station No.: 144

Core No: 65

Latitude: 20°48.0'N

Longitude: 32°19.4'W

Depth: 4827 m

Site: 7

Core Length: 414 cm

0-57 cm

Marl; grayish orange (10YR7/4) to dark yellowish brown (10YR4/2). Moist, firm and burrowed. Carbonate content moderate. Coarse fraction less than 5% consisting mainly of planktonic foraminifera. Basal contact an indistinct, irregular color change.

57-72 cm

Foraminiferal marl; moderate to dark yellowish brown (10YR4/2). Moist and firm. Carbonate content low to moderate. Coarse fraction about 10% consisting mainly of benthonic and planktonic foraminifera. Basal contact an irregular, gradational color change.

72-414 cm

Interbedded layers of marl and foraminiferal marl similar to above units.

Date: 6 March 1975

Ship Station No.: 145

Core No: 66

Latitude: 10°44.5'N

Longitude: 42°26.0'W

Depth: 5206 m

Site: 8

Core Length: 565 cm

0-48 cm

Foraminiferal marl; moderate to dark yellowish brown (10YR4/2). Moist and firm. Carbonate content moderate. Coarse fraction 15-20% consisting mostly of benthonic and planktonic foraminifera. Basal contact a sharp textural change.

48-50 cm

Sandy clay; dark yellowish brown (10YR4/2). Moist and firm. Carbonate content very low. Coarse fraction about 20% consisting mostly of a reddish mineral probably limonite. Frequent quartz and mica. Basal contact a sharp color and textural change.

50-480 cm

Clay; olive green (5Y3/2). Moist and firm. Carbonate content very low. Coarse fraction nil. Small stringers of dark minerals are scattered throughout this unit.

480-565 cm

Flow in.

Date: 7 March 1975

Ship Station No.: 146

Core No: 67

Latitude: 11°17.5'N

Longitude: 42°30.3'W

Depth: 4091 m

Site: 8

Core Length: 565 cm

0-165 cm

Foraminiferal chalk ooze, moderate yellowish brown (10YR5/4). Moist, firm and burrowed. Carbonate content high. Coarse fraction 60-70% consisting mostly of benthonic and planktonic foraminifera. Basal contact a gradational color and textural change.

165-167 cm

Foraminiferal ooze; Moderate orange pink (5YR8/4). Moist and semi consolidated. Carbonate content very high. Coarse fraction about 90%; similar in composition to above unit. Basal contact a gradational color and textural change.

167-565 cm

Foraminiferal chalk ooze; Moderate orange pink (5YR8/4) to light brown (5YR6/4) to moderate yellowish brown (10YR5/4). Carbonate content high. Moist and very soupy in places, but mostly firm. Similar in composition to above units.

Date: 12 March 1975

Ship Station No.: 147

Core No: 68

Latitude: 10°22.9'N

Longitude: 42°25.5'W

Depth: 4231 m

Site: 8

Core Length: 441 cm

0-55 cm

Foraminiferal ooze; pale yellowish brown (10YR6/2). Moist and firm. Carbonate content high. Coarse fraction about 80% consisting mostly of benthonic and planktonic foraminifera. Occasional radiolaria. Basal contact a gradational color change.

55-70 cm

Sandy clay; moderate to dark yellowish brown (10YR4/2). Moist, firm and burrowed. Carbonate content low. Coarse fraction about 25% consisting of abundant planktonic foraminifera and radiolaria. Frequest dark minerals. Occasional diatoms and quartz. Basal contact a gradational color change.

70-441 cm

Foraminiferal chalk ooze; Grayish orange (10YR7/4) to moderate to dark yellowish brown (10YR4/2). Moist, firm and burrowed. Carbonate content high. Similar in composition to unit between 0-55 cm. Small irregular patches of sandy clay similar to unit between 55-70 cm are scattered throughout this unit.

Date: 13 March 1975

Ship Station No.: 148

Core No: 69

Latitude: 10°46.7'N

Longitude: 42°11.2'W

Depth: 5212 m

Site: 8

Core Length: 424 cm

0-52 cm

Foraminiferal marl; moderate yellowish brown (10YR5/4). Moist, firm and burrowed. Carbonate content moderate. Coarse fraction about 15% consisting mostly of benthonic and planktonic foraminifera. Basal contact a gradational color change.

52-61 cm

Clay; dark yellowish brown (10YR4/2). Moist and firm. Carbonate content low. Coarse fraction less than 5% consisting mostly of planktonic foraminifera. A small patch of manganese crust is present at about 57 cm. Basal contact a sharp color change.

61-424 cm

Clay; olive black (5Y2/1). Moist and very firm. Carbonate content low. Coarse fraction nil. Small stringers of silty sand are scattered throughout this layer. The silty sand is composed of quartz, mica and dark minerals.

Date: 14 March 1975

Ship Station No.: 149

Core No: 70

Latitude: 10°46.4'N

Longitude: 42°21.5'W

Depth: 5188 m

Site: 8

Core Length: 584 cm

0-8 cm

Foraminiferal marl; moderate yellowish brown (10YR5/4). Moist, firm and burrowed. Carbonate content moderate. Coarse fraction about 10% consisting mostly of benthonic and planktonic foraminifera. Basal contact a gradational color change.

8-11 cm

Sandy clay; moderate brown to dark yellowish brown (10YR4/2). Moist, firm and burrowed. Carbonate content low. Coarse fraction about 30% consisting of mica, quartz and planktonic foraminifera. Small pieces of manganese crust are also found in this layer. Basal contact a sharp color change.

11-290 cm

Clay; olive black (5Y2/1). Moist and very firm. Carbonate content low. Coarse fraction nil. Small stringers of silty sand composed of quartz, mica and dark minerals are found scattered throughout this layer.

290-584 cm

Flow in.

Date: 15 March 1975

Ship Station No.: 150

Core No: 71

Latitude: 10°27.1'N

Longitude: 44°40.2'W

Depth: 4954 m

Site: 8

Core Length: 584 cm

0-3 cm

Marl; moderate yellowish brown (10YR5/4). Moist and firm. Carbonate content moderate. Coarse fraction less than 5% consisting mostly of planktonic foraminifera. Basal contact a gradational color and textural change.

3-6 cm

Clay; moderate to dark yellowish brown (10YR4/2). Moist and firm. Carbonate content low. Coarse fraction less than 5% consisting of manganese micronodules, sub angular quartz grains, sapropel and planktonic foraminifera. Basal contact a sharp color change.

6-194 cm

Clay; black (N-1) to olive black (5Y2/1). Moist, firm and laminated. Carbonate content very low. Coarse fraction less than 5% consisting mainly of sapropel. Frequent mica and planktonic foraminifera. Basal contact a sharp textural change.

194-242 cm

Sand; olive black (5Y2/1). Moist, semi consolidated and graded. Carbonate content very low. Coarse fraction about 80% consisting mostly of sub angular quartz and sapropel. Frequent mica. Basal contact a sharp color change.

242-330 cm

Marl; similar to unit between 0-3 cm. Basal contact a sharp color and textural change.

330-332 cm

Foraminiferal ooze; grayish orange (10YR7/4). Moist and semi consolidated. Carbonate content very high. Coarse fraction about 95% consisting entirely of benthonic and planktonic foraminifera. Basal contact a sharp color and textural change.

332-584 cm

Interbedded layers of marl and clay similar to above units.

PART B

Heat Flow Measurements

Compiled by: Lois K. Ongley and Marcus G. Langseth

The following pages show the geothermal data, for each heat flow station, taken during R/V VEMA cruise 32, leg 6. The data are presented both graphically and in tabular form.

The graphs show Temperature Difference ($T_{sed} - T_{H_2O}$) versus Depth of Penetration in the sediment.

There are two tables for each station. The first shows the depth of penetration, temperature difference and the standard error associated with this temperature difference for each probe. The calculated bottom water temperature is given.

The second table is a gradient and standard error matrix. The values are arranged as follows:

	PROBE 1	PROBE 2	PROBE 3	PROBE 4
1	*************	gradient (2-1)	gradient (3-1)	gradient (4-1)
	************	stand. err. (2-1)	stand. err. (3-1)	stand. err. (4-1)
2	*************	***************	gradient (3-2)	gradient (4-2)
	************	**************	stand. err. (3-2)	stand. err. (4-2)
3	*************	***************	***************	gradient (4-3)
	************	**************	**************	stand. err. (4-3)

The gradient chosen for heat flow calculations is underlined or noted separately. Where the temperature differences were not calculated by computer (stations V32-004 and V32-009) there are no standard error calculations.

TGRAD STATION V32-001 25FEB 75

+=9538 x=1069 ▷=1150 ▽=1160

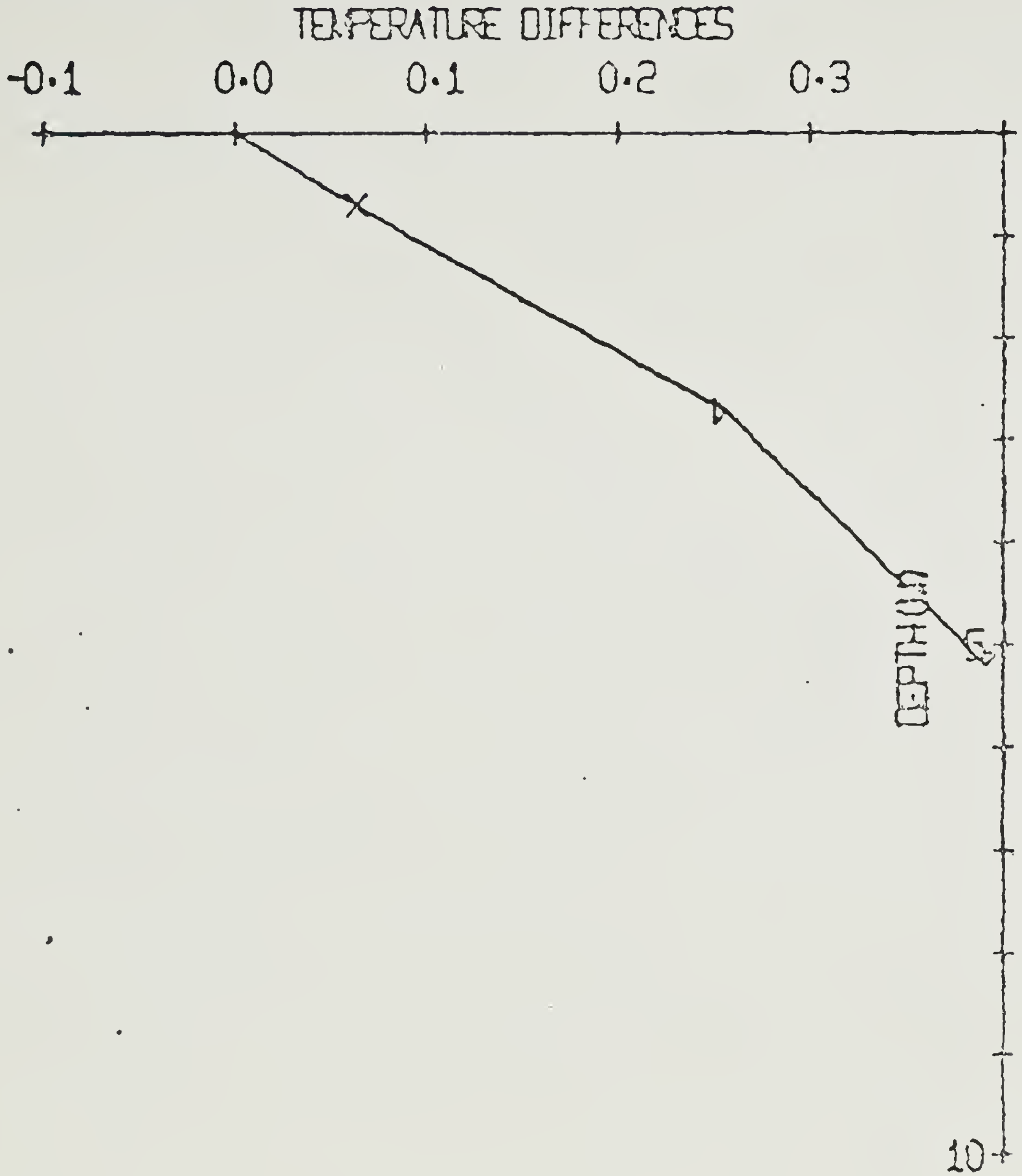

EQUILIBRIUM TEMPERATURE DIFFERENTIAL ESTIMATES

PROBE NO.	DEPTH(M)	DELT(C)	STAN. ERR.
9538	0.00	0.000	0.003
1069	0.70	0.063	0.003
1150	2.72	0.257	0.004
1160	5.20	0.391	0.004

BOTTOM WATER TEMPERATURE 2.37

GRADIENTS AND STANDARD ERRORS (°C/M)

	1	2	3	4
1	******	0.0901	0.0945	0.0752
	*****	0.0063	0.0020	0.0010
2	******	*******	0.0960	0.0729
	*****	******	0.0028	0.0012
3	******	*******	*******	0.0541
	*****	******	******	0.0025

TGRAD STATION V32-002 27FEB 75

+=9538 x=1147 ▷=1157 ▽=1151 ◁=1111 △=1069

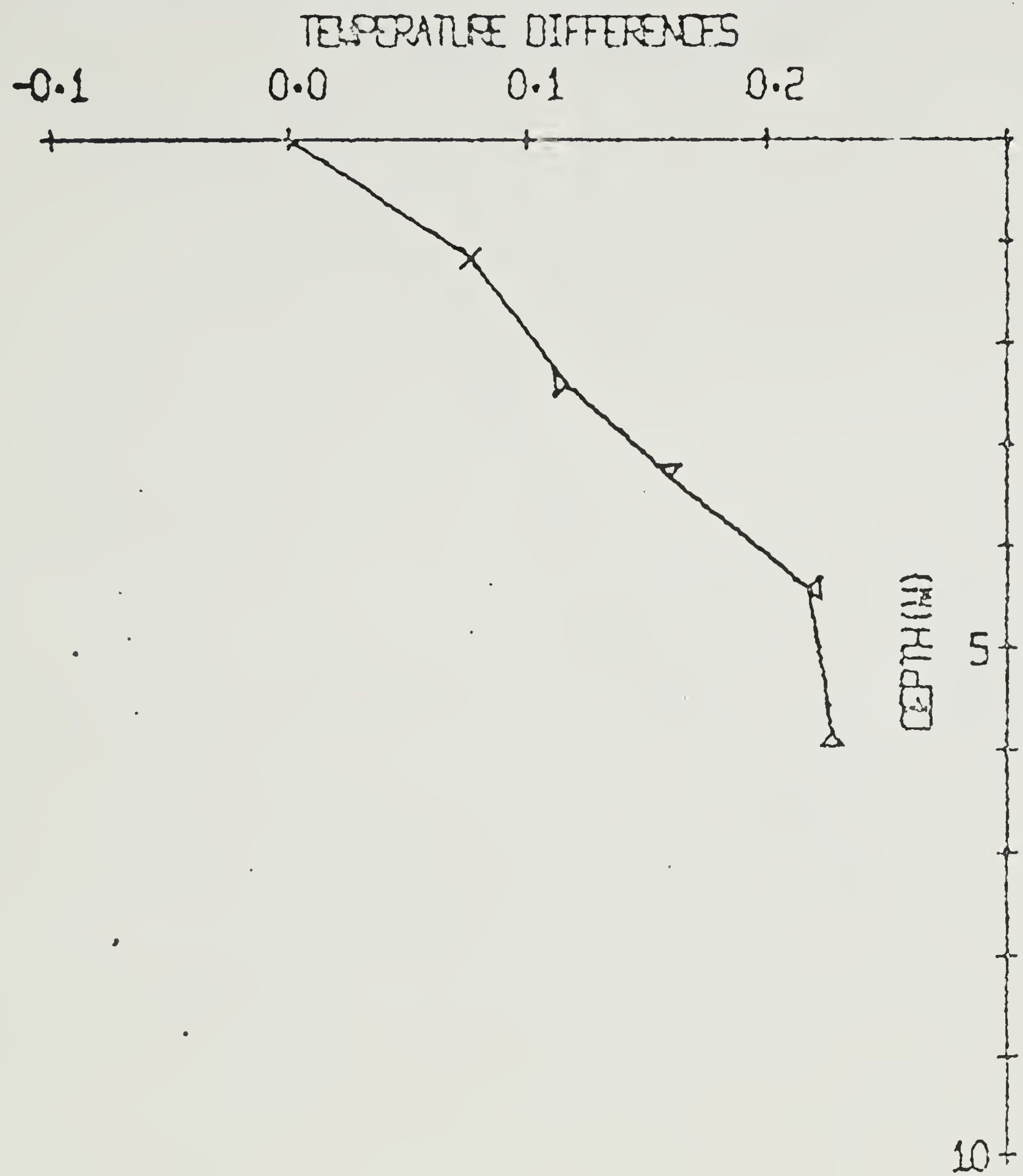

EQUILIBRIUM TEMPERATURE DIFFERENTIAL ESTIMATES

PROBE NO.	DEPTH(M)	DELT(C)	STAN. ERR.
9538	0.00	0.000	0.002
1147	1.17	0.075	0.002
1157	2.41	0.116	0.003
1151	3.33	0.159	0.002
1111	4.43	0.217	0.003
1069	5.85	0.227	0.003

BOTTOM WATER TEMPERATURE 2.33

GRADIENTS AND STANDARD ERRORS (°C/M)

	1	2	3	4	5	6
1	******	0.0646	0.0483	0.0477	0.0490	0.0388
	*****	0.0032	0.0017	0.0010	0.0010	0.0007
2	******	*******	0.0330	0.0336	0.0435	0.0323
	*****	******	0.0034	0.0017	0.0014	0.0010
3	******	*******	*******	0.0462	0.0499	0.0321
	*****	******	******	0.0044	0.0024	0.0014
4	******	*******	*******	*******	0.0530	0.0269
	*****	******	******	******	0.0040	0.0018
5	******	*******	*******	*******	*******	0.0067
	*****	******	******	******	******	0.0037

TGRAD STATION V32-003 02MAR 75

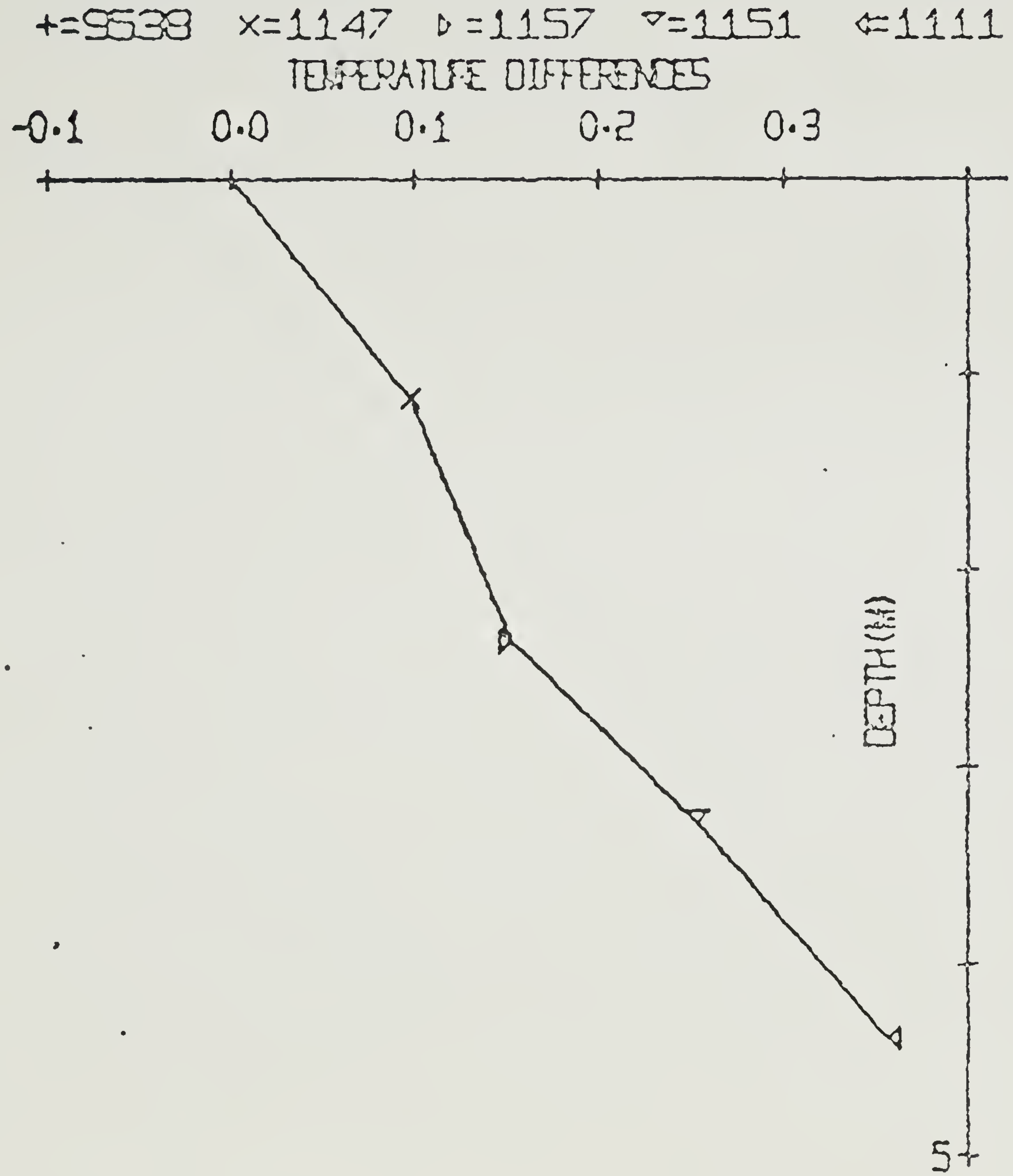

EQUILIBRIUM TEMPERATURE DIFFERENTIAL ESTIMATES

PROBE NO.	DEPTH(M)	DELT(C)	STAN. ERR.
9538	0.00	0.000	0.011
1147	1.12	0.097	0.013
1157	2.36	0.151	0.017
1151	3.28	0.253	0.020
1111	4.38	0.356	0.027

BOTTOM WATER TEMPERATURE 2.30

GRADIENTS AND STANDARD ERRORS (°C/M)

	1	2	3	4	5
1	******	0.0871	0.0643	0.0772	0.0814
	*****	0.0159	0.0088	0.0071	0.0063
2	******	*******	0.0437	0.0721	0.0794
	*****	******	0.0180	0.0113	0.0095
3	******	*******	*******	0.1104	0.1014
	*****	******	******	0.0292	0.0162
4	******	*******	*******	*******	0.0939
	*****	******	******	******	0.0313

TGRAD STATION V32-004 06MAR 75

+=9538 x=1150 ▷=1160

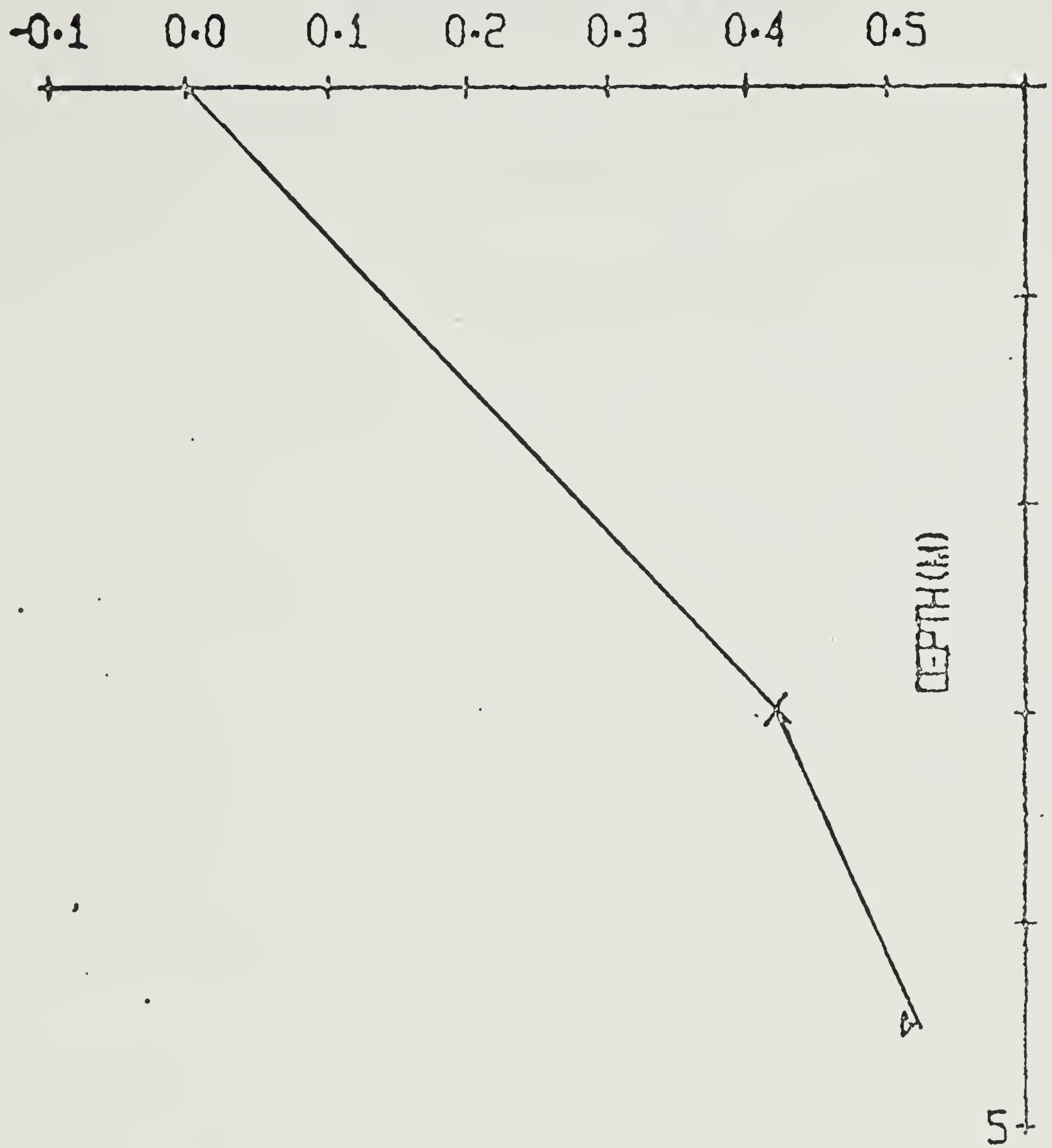

EQUILIBRIUM TEMPARATURE DIFFERENTIAL ESTIMATES

PROBE NO.	DEPTH(M)	DELT(C)	STAN. ERR.
9538	0.00	0.000	~0.015
1150	2.98	0.405	~0.012
1160	4.50	0.52	~0.032

BOTTOM WATER TEMPERATURE 1.73

GRADIENTS AND STANDARD ERRORS (°C/M)

	1	2	3	
1	****** *****	0.1359	0.1156	average 0.126
2	****** *****	******* ******	0.0756	

TGRAD STATION V32-005 07MAR 75

+=9538 x=1147 ▷=1111 ▽=1069

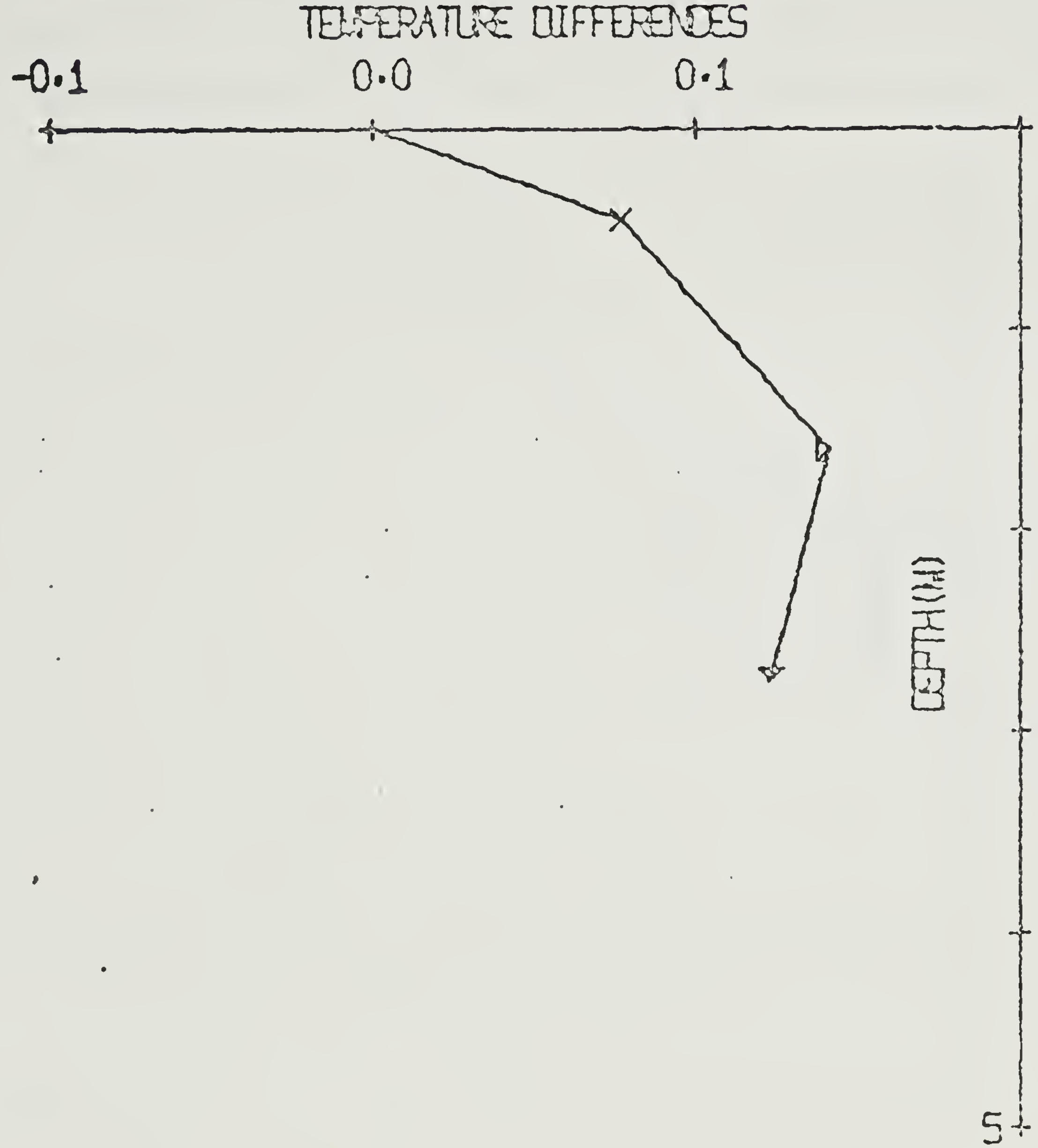

EQUILIBRIUM TEMPERATURE DIFFERENTIAL ESTIMATES

PROBE NO.	DEPTH(M)	DELT(C)	STAN.ERR.
9538	0.00	0.000	0.006
1147	0.45	0.077	0.003
1111	1.60	0.141	0.004
1069	2.75	0.123	0.004

BOTTOM WATER TEMPERATURE 2.38

GRADIENTS AND STANDARD ERRORS (°C/)

	1	2	3	4
1	******	0.1713	0.0883	0.0447
	*****	0.0163	0.0046	0.0028
2	******	*******	0.0558	0.0200
	*****	******	0.0048	0.0027
3	******	*******	*******	-0.0157
	*****	******	******	0.0055

TGRAD STATION V32-006 12MAR 75

+=9538 x=1147 ▷=1151 ▽=1111 ⇐1145 △=1069

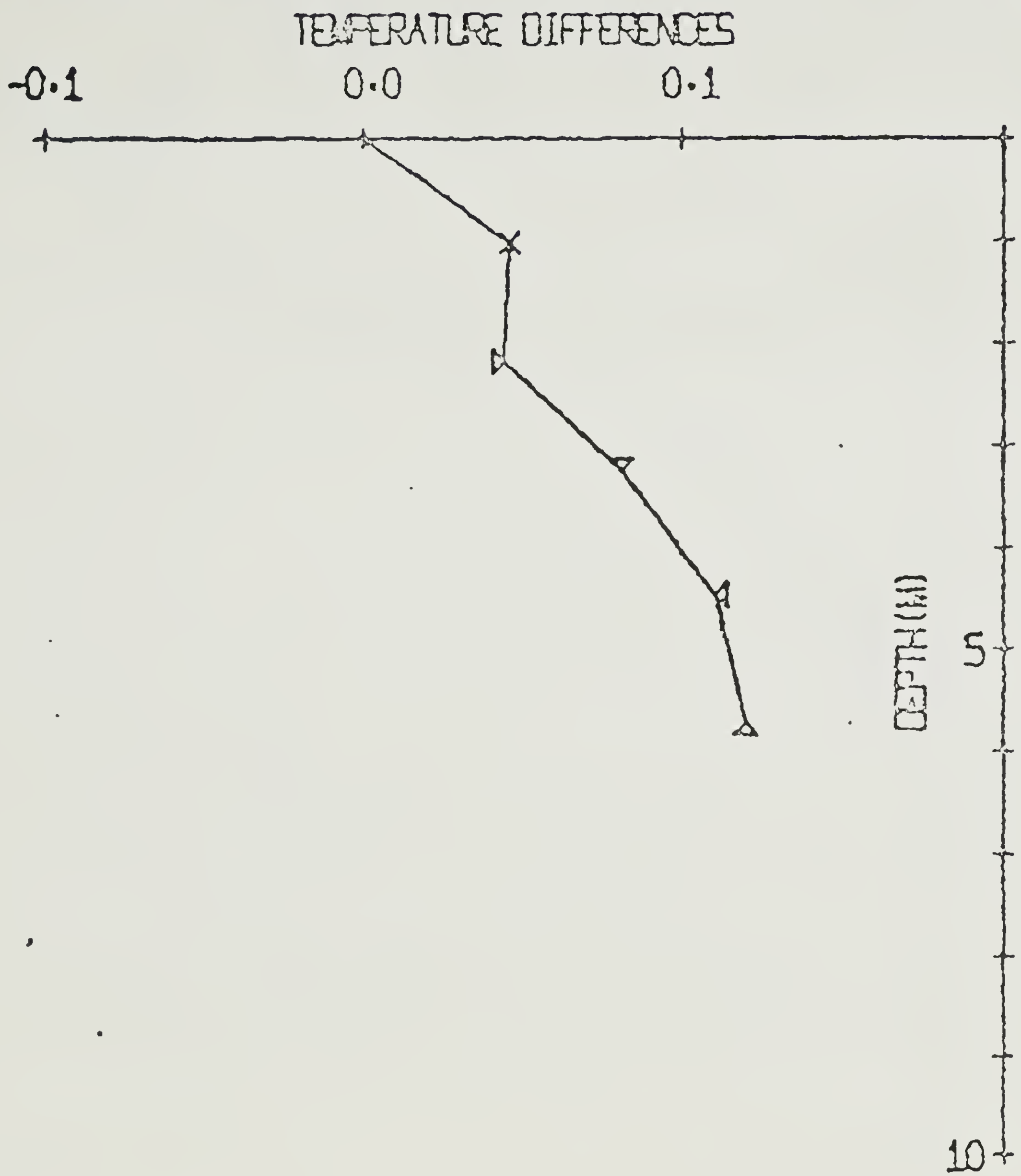

EQUILIBRIUM TEMPERATURE DIFFERENTIAL ESTIMATES

PROBE NO.	DEPTH(M)	DELT(C)	STAN. ERR.
9538	0.00	0.000	0.004
1147	1.03	0.045	0.008
1151	2.18	0.044	0.006
1111	3.27	0.080	0.007
1145	4.48	0.110	0.012
1069	5.73	0.119	0.009

BOTTOM WATER TEMPERATURE 1.86

GRADIENTS AND STANDARD ERRORS (°C/)

	1	2	3	4	5	6
1	******	0.0445	0.0202	0.0247	0.0246	0.0203
	*****	0.0093	0.0036	0.0027	0.0029	0.0018
2	******	*******	-0.0015	0.0156	0.0186	0.0156
	*****	******	0.0090	0.0049	0.0043	0.0026
3	******	*******	*******	0.0337	0.0287	0.0212
	*****	******	******	0.0038	0.0060	0.0032
4	******	*******	*******	*******	0.0242	0.0157
	*****	******	******	******	0.0119	0.0049
5	******	*******	*******	*******	*******	0.0074
	*****	******	******	******	******	0.0125

TGRAD STATION V32-007 13MAR 75

+=9538 x=1147 ▷=1151 ▽=1111 ⇐1145 △=1149

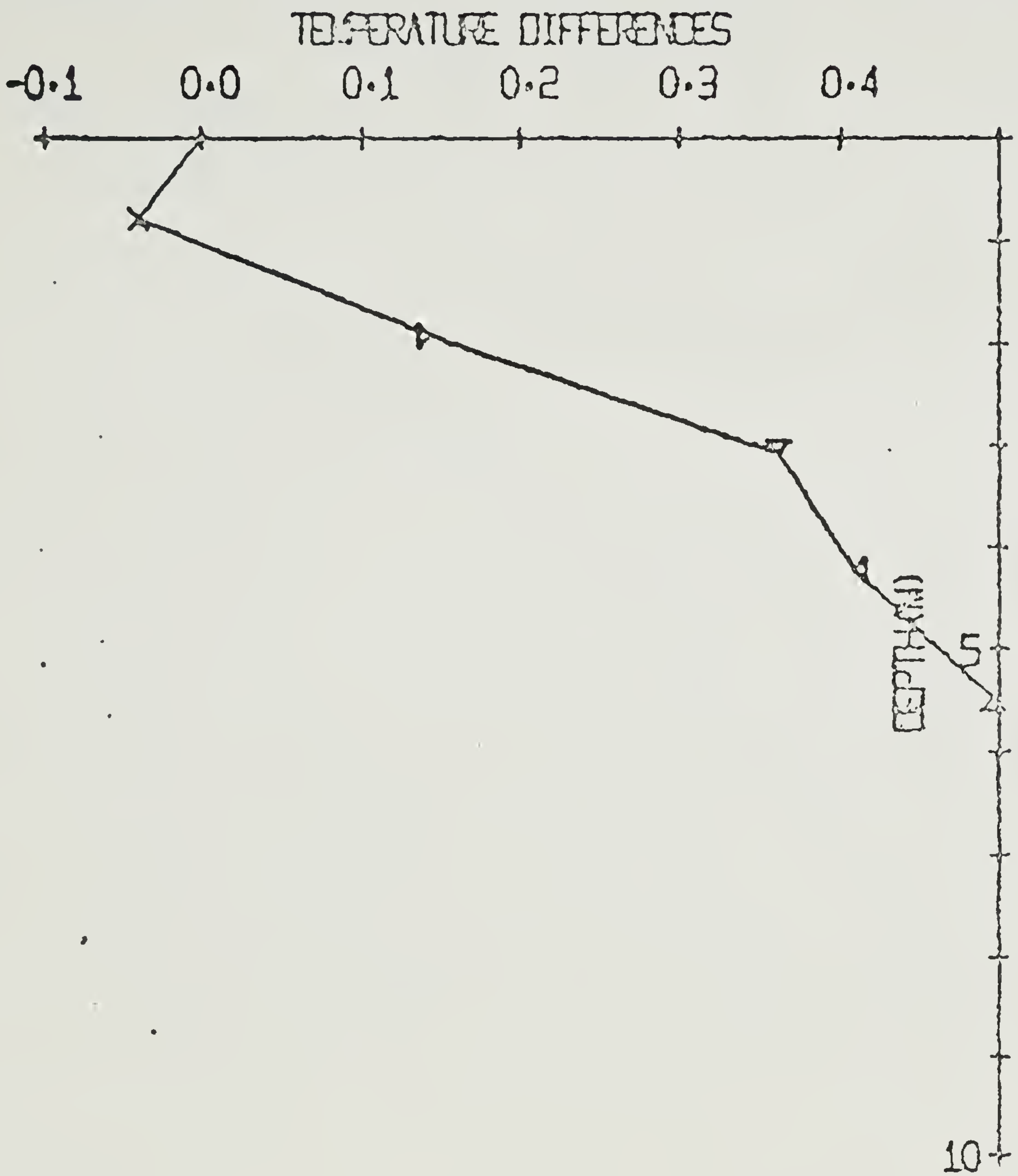

EQUILIBRIUM TEMPERATURE DIFFERENTIAL ESTIMATES

PROBE NO.	DEPTH(M)	DELT(C)	STAN. ERR.
9538	0.00	0.000	0.008
1147	0.78	-0.040	0.013
1151	1.93	0.143	0.012
1111	3.08	0.361	0.011
1145	4.23	0.403	0.012
1149	5.48	0.496	0.032

BOTTOM WATER TEMPERATURE 1.71

GRADIENTS AND STANDARD ERRORS (°C/)

	1	1	3	4	5	6
1	******	-0.0515	0.0746	0.1174	0.0965	0.0905
	*****	0.0200	0.0076	0.0046	0.0034	0.0060
2	******	*******	0.1601	0.1747	0.1301	0.1141
	*****	******	0.0156	0.0077	0.0052	0.0074
3	******	*******	*******	0.1393	0.1150	0.0992
	*****	*******	******	0.0147	0.0074	0.0097
4	******	*******	*******	*******	0.0407	0.0560
	*****	******	******	******	0.0146	0.0143
5	******	*******	*******	*******	*******	0.0700
	*****	******	*******	******	******	0.0275

TGRAD STATION V32-008 14MAR 75

+=9538 x=1147 ▷=1151 ▽=1111 ⊲=1145

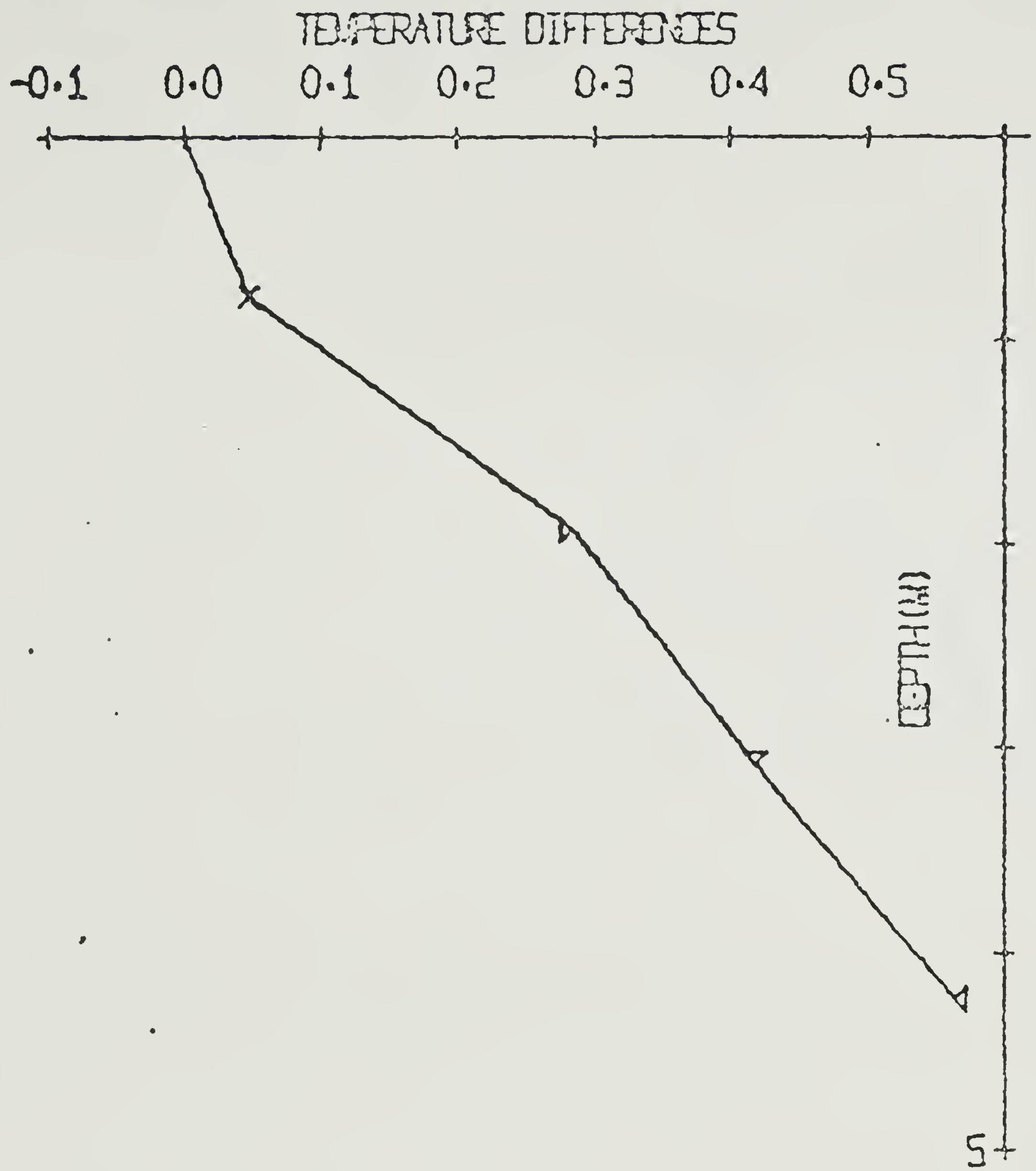

EQUILIBRIUM TEMPERATURE DIFFERENTIAL ESTIMATES

PROBE NO.	DEPTH(M)	DELT(C)	STAN. ERR.
9538	0.00	0.000	0.012
1147	0.78	0.047	0.010
1151	1.93	0.283	0.011
1111	3.08	0.417	0.009
1145	4.23	0.564	0.006

BOTTOM WATER TEMPERATURE 1.71

GRADIENTS AND STANDARD ERRORS (°C/M)

	1	2	3	4	5
1	******	0.0607	0.1466	0.1356	0.1333
	*****	0.0211	0.0087	0.0050	0.0032
2	******	*******	0.2049	0.1610	0.1497
	*****	******	0.0137	0.0062	0.0036
3	******	*******	*******	0.1171	0.1221
	*****	******	******	0.0130	0.0057
4	******	*******	*******	*******	0.1272
	*****	******	******	******	0.0099

TGRAD STATION V32-009 15MAR 75

+=9538 x=1147 ▷=1151 ▽=1111 ⇐1145 △=1158

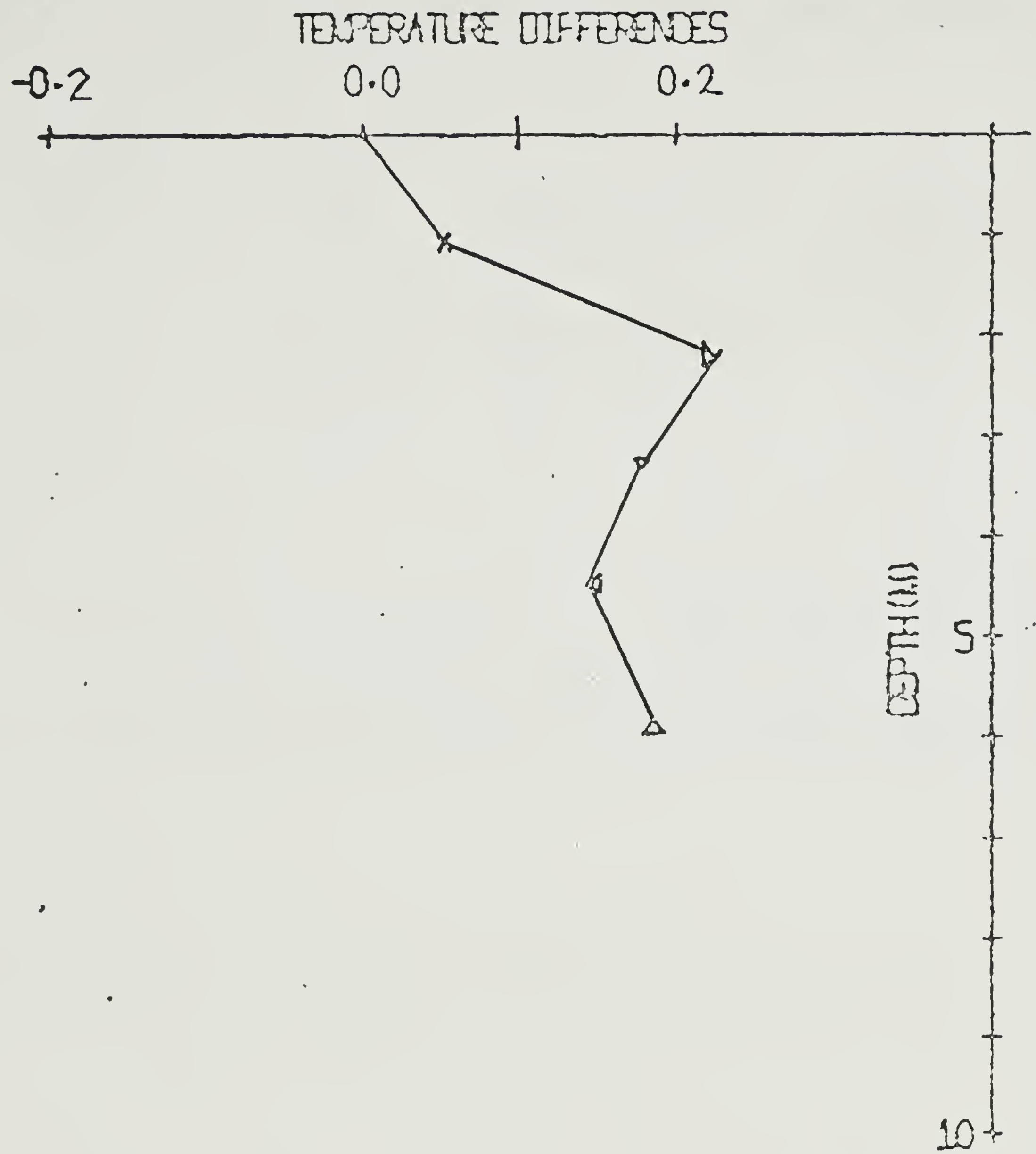

EQUILIBRIUM TEMPERATURE DIFFERENTIAL ESTIMATES

PROBE NO.	DEPTH(M)	DELT(C)
9538	0.00	0.000
1147	1.08	0.053
1151	2.23	0.218
1111	3.38	0.174
1145	4.53	0.142
1158	5.78	0.181

BOTTOM WATER TEMPERATURE 1.65

GRADIENTS AND STANDARD ERRORS (°C/M)

	1	2	3	4	5	6
1	****** *****	0.0491	0.0978	0.0515	0.0313	0.0313
2	****** *****	******* ******	0.1435	0.0526	0.0258	0.0272
3	****** *****	******* ******	******* ******	-0.0333	-0.0330	-0.0104
4	****** *****	******* ******	******* ******	******* ******	-0.0278	0.0029
5	****** *****	******* ******	******* ******	******* ******	******* ******	0.0312

TABLE 1: R/V VEMA cruise 32 Heat Flow Values at IPOD Site # 7

Latitude (N)	Longitude (W)	Depth (corr m)	P (cm)	N	Gradient (°C/10m)	Heat Flow (HFU)	Evaluation	Station	Location
21° 9.9'	32° 26.7'	4885	520	3	0.729*	1.74**	7	1	Center of OBS #1
20°40.2'	32° 13.1'	4900	585	5	0.490	1.17**	9	2	SE corner of OBS #2
20°48.0'	32° 19.4'	4827	438	4	0.794	1.90**	6	3	Center of OBS # 2

P = penetration into sediment   N = number of probes in mud.

* The gradient between the uppermost and lowermost probes. The gradient between the two bottom probes is 0.54 which corresponds to a heat flow of 1.29.

** The thermal conductivity is assumed from nearby stations to be 2.39 mcal/°C sec cm.

TABLE 2: R/V VEMA Cruise 32 Heat Flow Values at IPOD Site #8

Latitude (N)	Longitude (W)	Depth (corr m)	P (cm)	N	Gradient (°C/10m)	Conductivity	Heat Flow (HFU)	Evaluat.	Station
10°44.5'	42°26.0'	5206	450	2	1.26	2.45A	3.09	4	4
11°17.5'	42°30.3'	4091	275	3	N. L.	-	-	5	5
10°22.9'	42°25.5'	4231	573	5	0.208	2.30A	0.48	5	6
10°46.7'	42°11.2'	5212	548	5	1.14	2.45A	2.79	6	7
10°46.4'	42°21.5'	5188	423	4	1.50	2.45A	3.68	8	8
10°27.1'	44°40.2'	4954	578	5	N. L.	-	-	5	9

P = penetration into sediment
N = number of probes in mud

N. L. = Non linear
A = Assumed conductivity

PART C

Deep-Sea Photography

One representative photograph is shown for each camera station obtained. The field of view for each frame is approximately 4.5 x 4.0 meters.

02 March 1975

K #58, 4827 m

Lat: 20°48.0'N

Long: 32°19.4'W

Frame 7 of 8

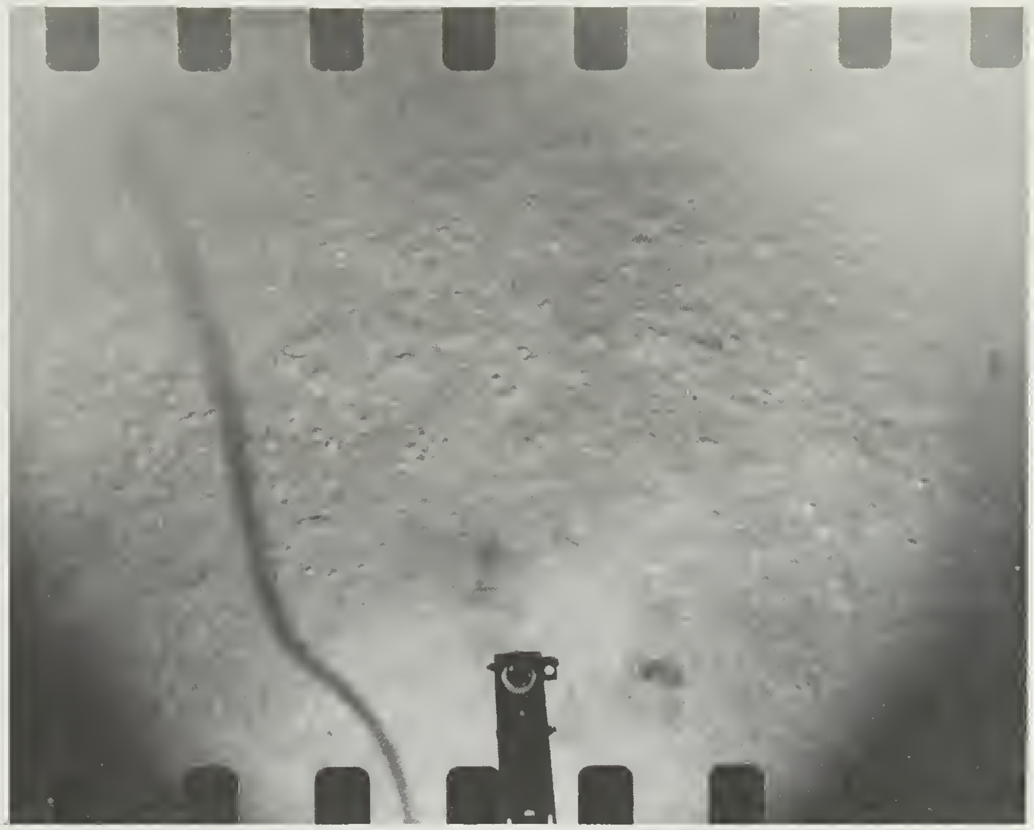

06 March 1975

K #59, 5206 m

Lat: 10°44.5N

Long: 42°26.0W

Frame 14 of 21

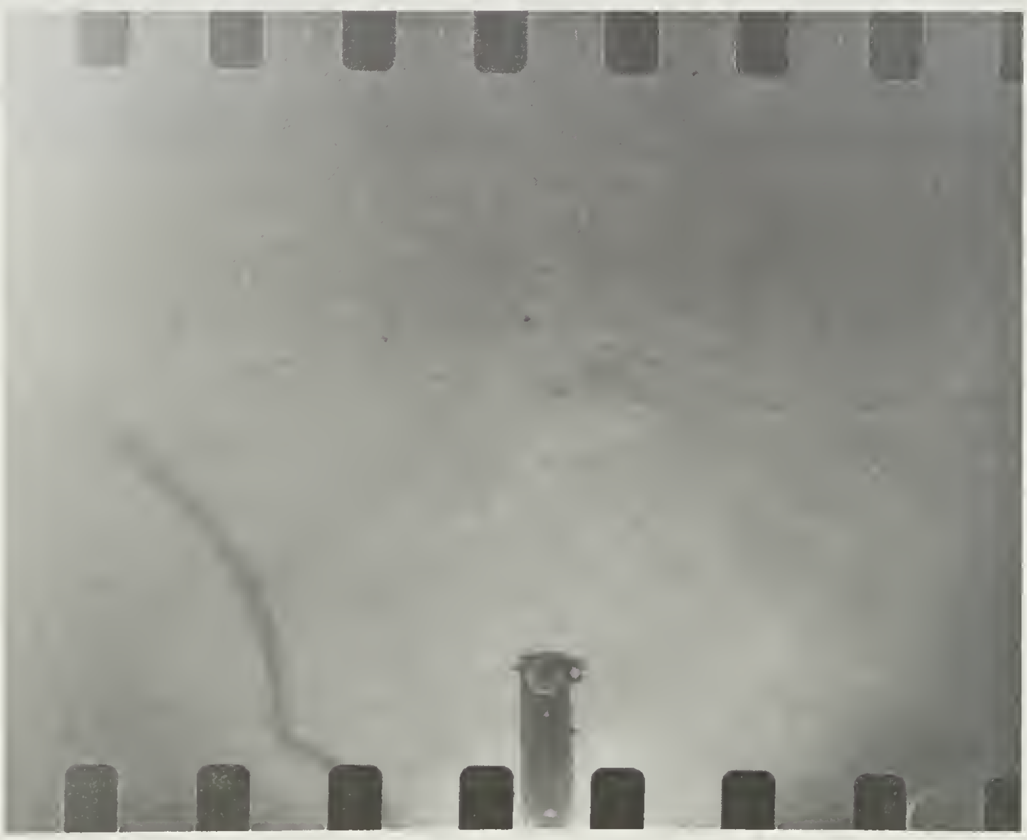

07 March 1975

K #60, 4091 m

Lat: 11°17.5N

Long: 42°30.3W

Frame 6 of 8

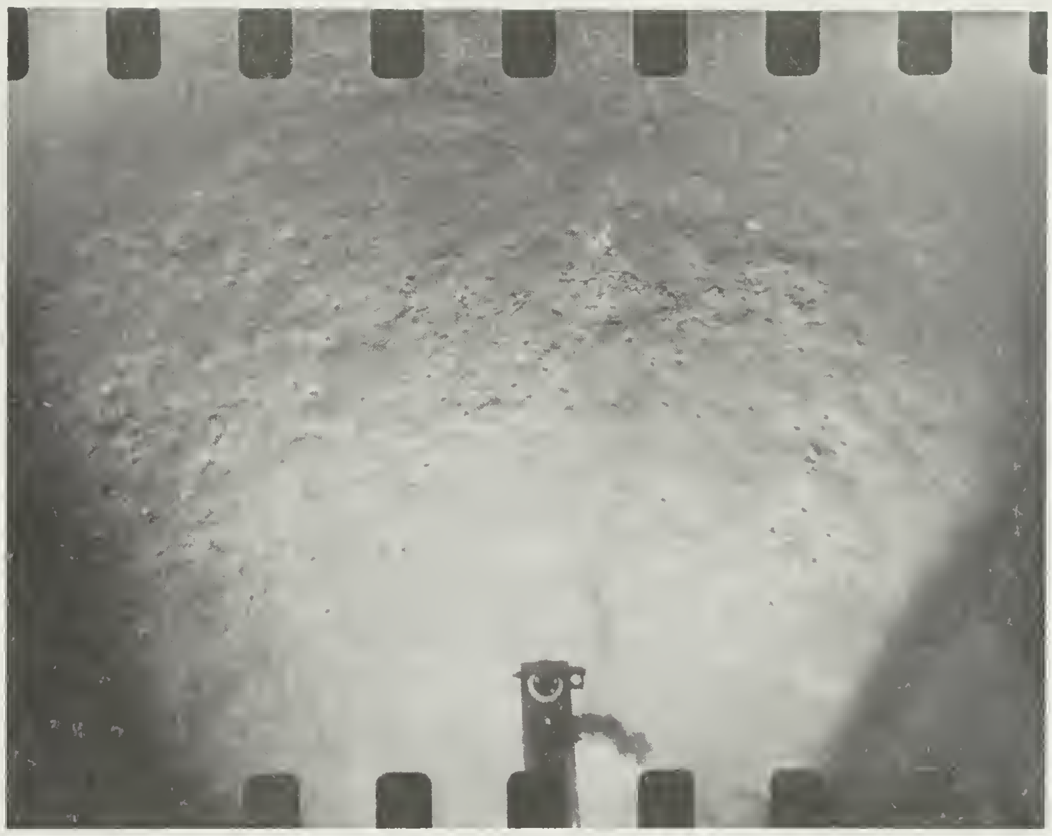

REFERENCES

Bullard, E.C. and R.G. Mason, The magnetic field over the ocean; In The Sea, Vol. III, Ed., M.N. Hill, Interscience, New York, 1963, 963 p.

Cain, J.C., S. Hendricks, W.E. Daniels, and D.C. Jensen, Computation of the main geomagnetic field from spherical harmonic expansions; Goddard Space Flight Center Publ., X-611-64-316, 1964, 47 p.

Ewing, J.I. and G.B. Tirey, Seismic Profiler, J. Geophys. Res., Vol. 67, p. 2509-2527, 1961.

Ewing, J.I. and R. Zaunere, Seismic profiling with a pneumatic sound source, J. Geophys. Res., Vol. 69, No. 22, p. 4913-4915, 1964.

Gerard, R., M. Langseth and M. Ewing, Thermal gradient measurements in the water and bottom sediment of the western Atlantic, J. Geophys. Res., Vol. 67, p. 785-803, 1960.

Guier, W.H., Satellite navigation using integral Doppler data, the AN/SRN-9 equipment; J. Geophys. Res., Vol. 71, No. 24, p. 5903, 1966.

Heirtzler, J.R., VEMA cruise no. 16, geomagnetic measurements; Technical Report No. 2, CU-3-61-Nonr-Geology, Lamont Geological Observatory, Palisades, N. Y., 1961.

Langseth, M., Techniques of measuring heat flow through the ocean floor; A.G.U. Geophys. Monograph No. 8, 1965.

Talwani, M., A computer system for the reduction, storage and display of underway data acquired at sea; Technical Report No. 1, CU-1-69, N00014-67-A-0108-0004, August 1969, 348 p.

Talwani, M., Gravity, Vol. IV, Part I, The Sea, A. Maxwell, Ed., J. Wiley and Sons, Interscience, New York, Ch. 8, 1970, p. 251-297.

Talwani, M., W.P. Early and D.E. Hayes, Continuous analog computation and recording of cross-coupling and off-leveling errors; J. Geophys. Res., Vol. 71, No. 8, p. 2079-2090, 1966.

Thorndike, E.M., Deep sea cameras of the Lamont Observatory; Deep-Sea Research, Vol. 5, p. 234-237, 1959.

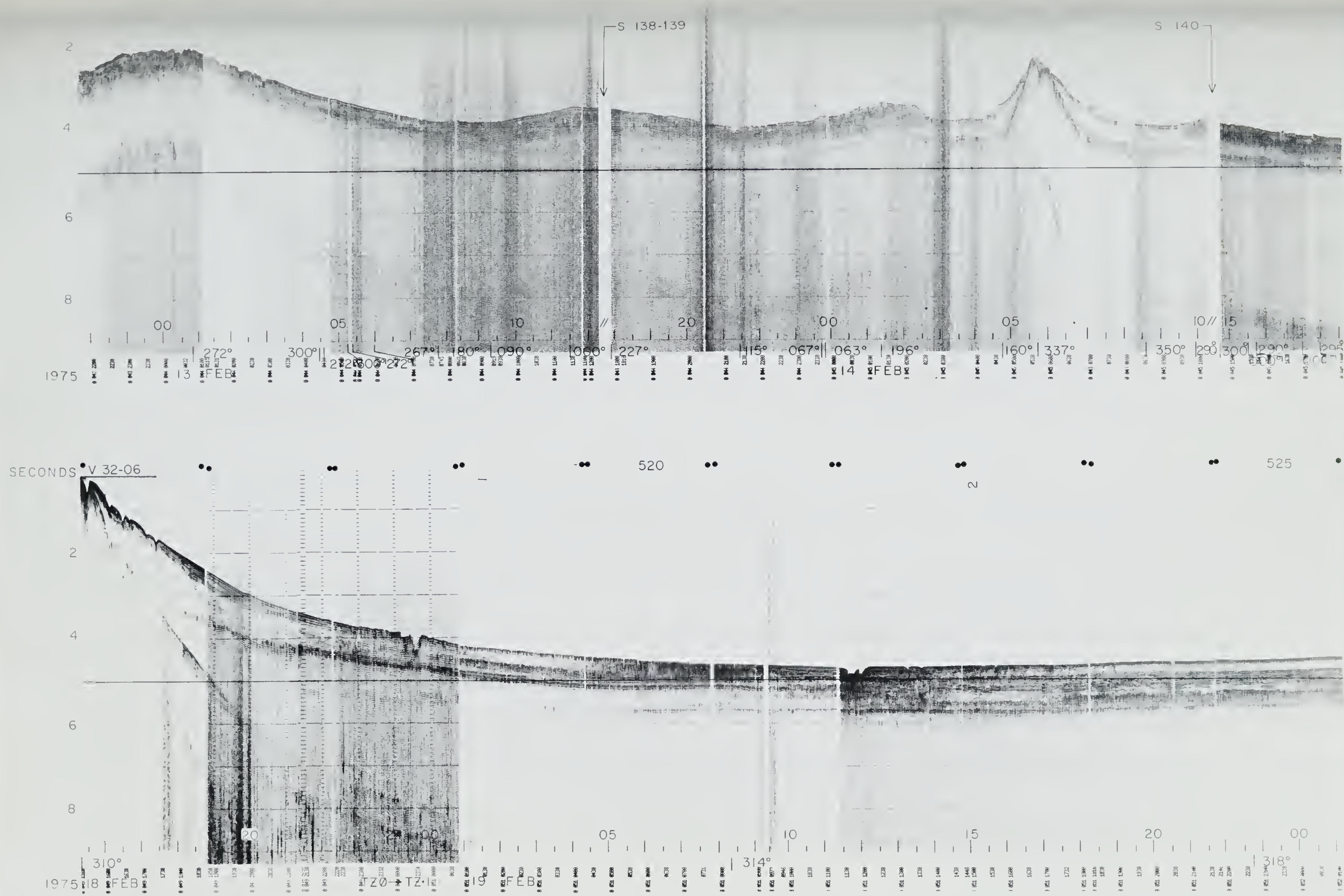
S 138-139
S 140
1975
13 FEB
14 FEB
SECONDS
V 32-06
520
525
1975
18 FEB
19 FEB
TZØ→TZ1

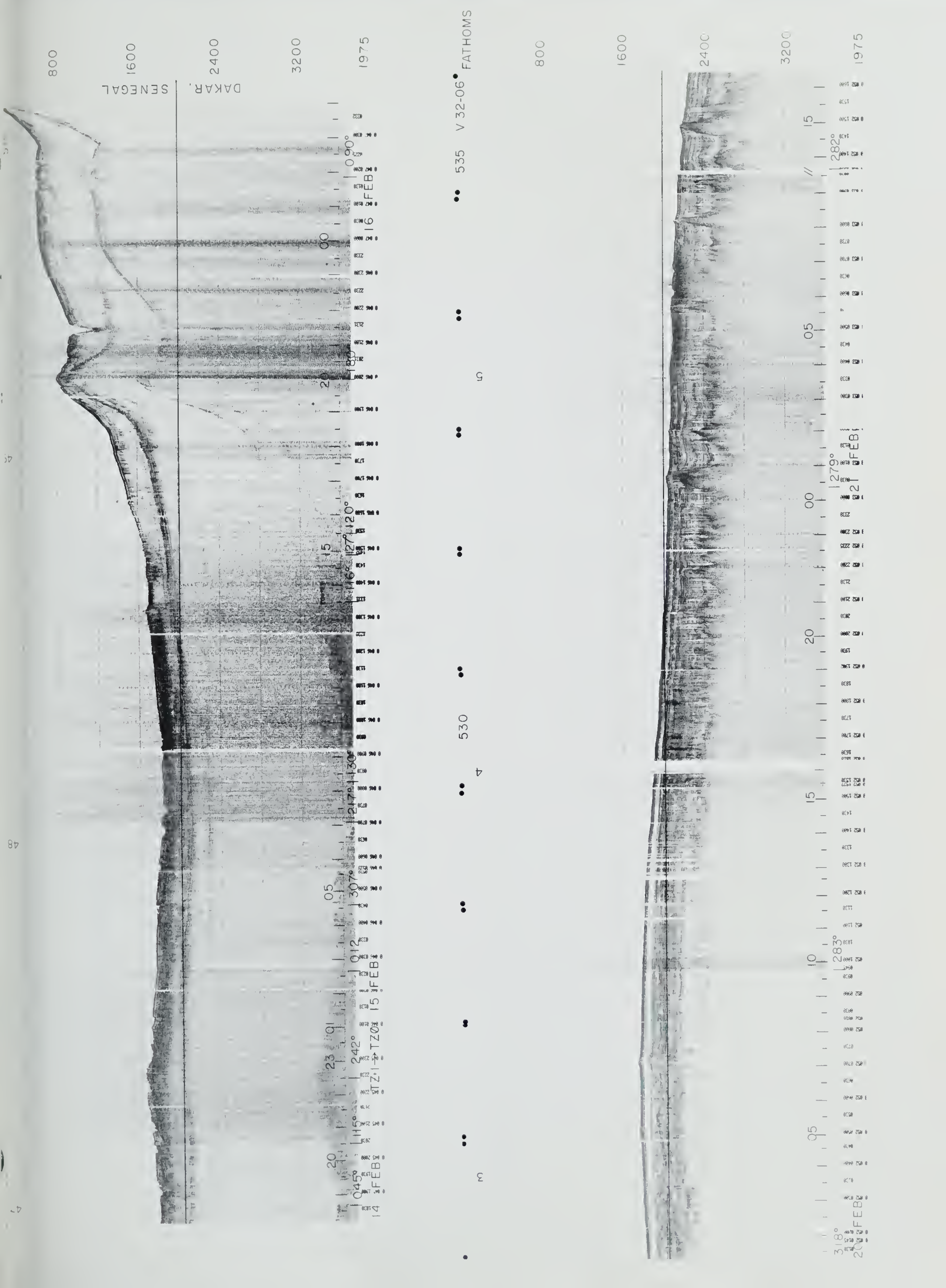

DAKAR, SENEGAL
V 32-06
FATHOMS
535
530
800
1600
2400
3200
1975
14 FEB
15 FEB
16 FEB
21 FEB
20 FEB
TZ+1→TZ0

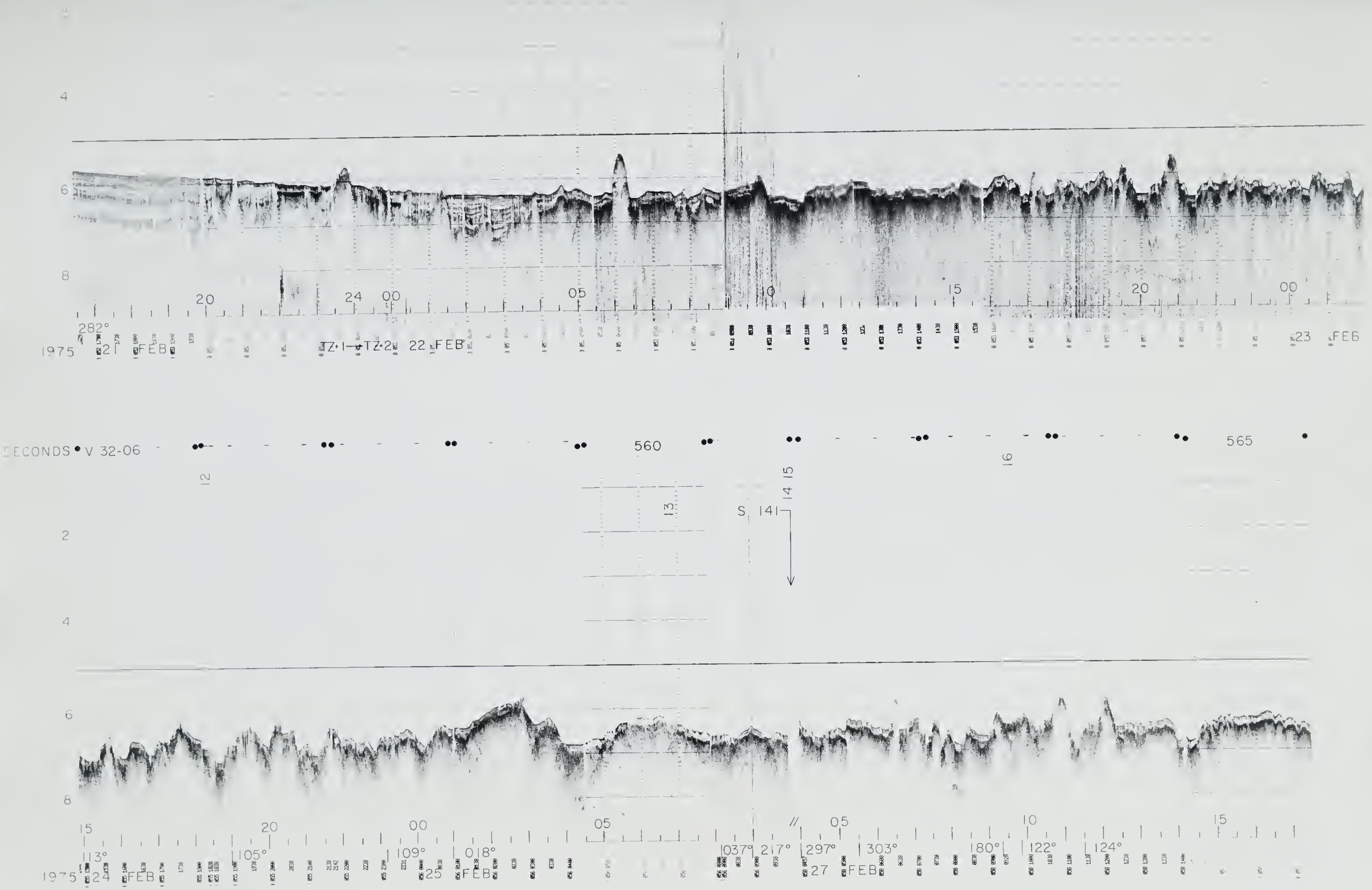

1975 21 FEB
22 FEB
23 FEB
SECONDS • V 32-06
560
565
1975 24 FEB
25 FEB
27 FEB

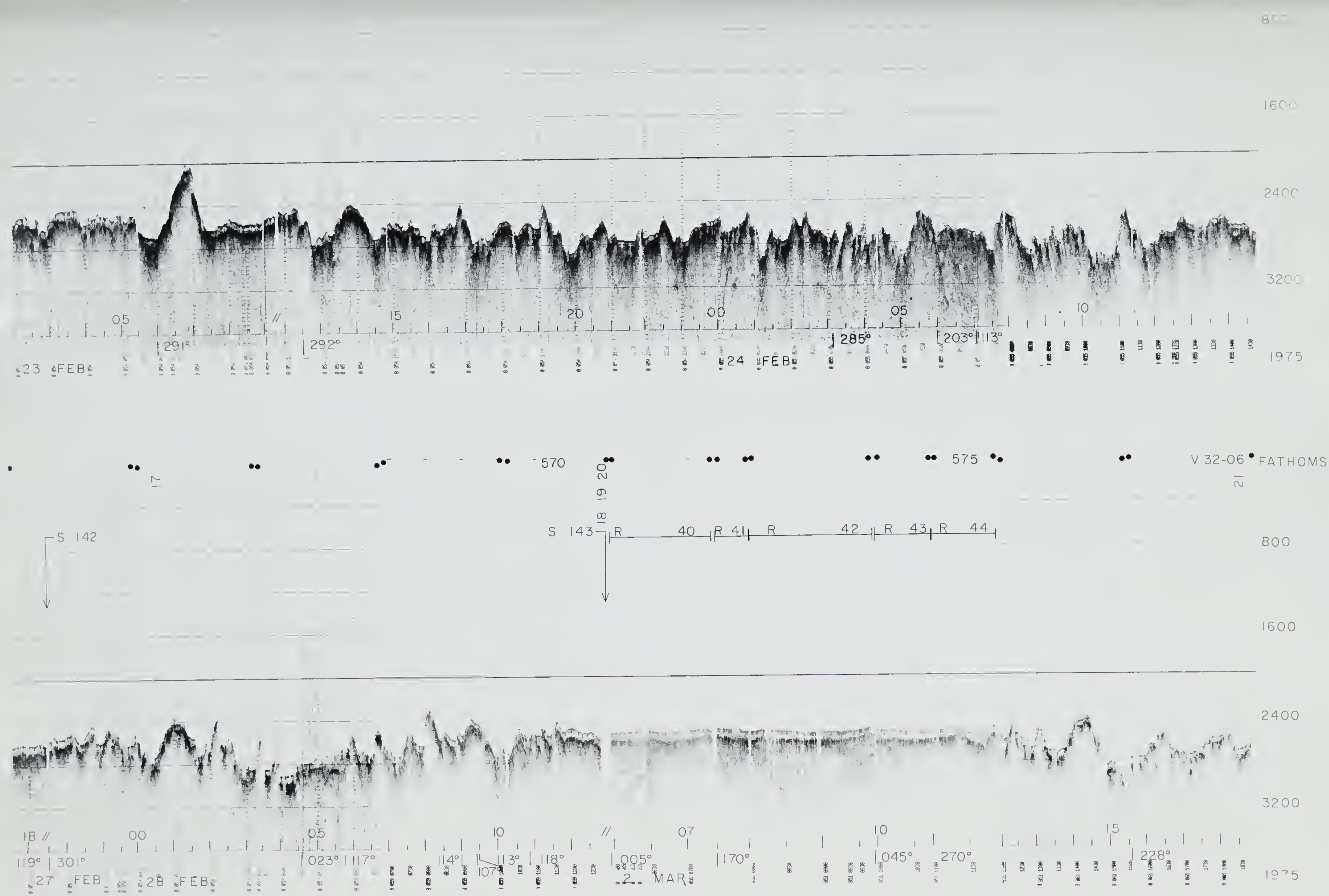

V 32-06
FATHOMS
1975
800
1600
2400
3200
23 FEB
24 FEB
27 FEB
28 FEB
2 MAR
291°
292°
285°
203°
113°
570
575
S 142
S 143
R 40 R 41 R 42 R 43 R 44
119°
301°
023°
117°
114°
107°
118°
005°
170°
045°
270°
228°

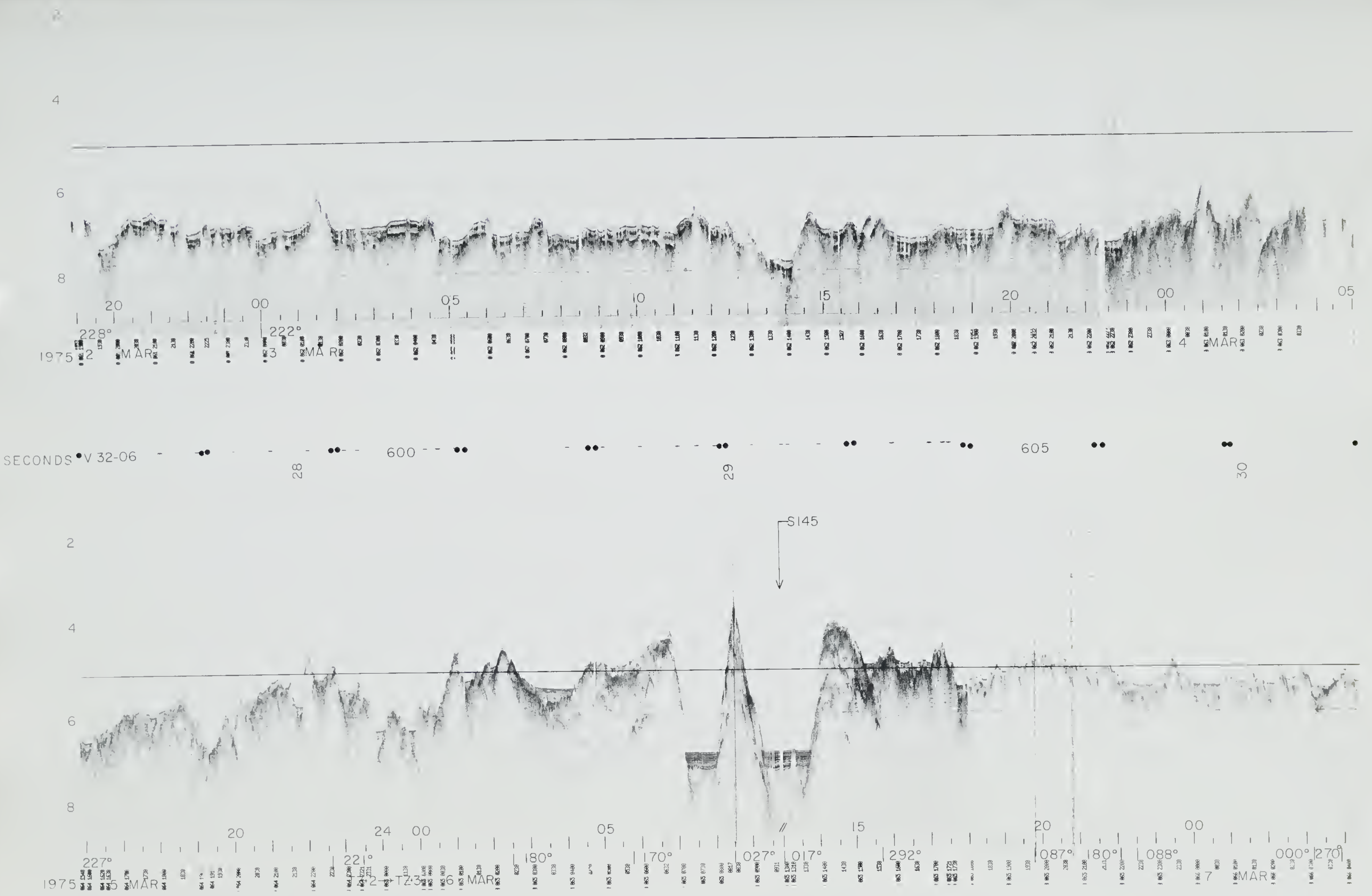

SECONDS
V 32-06
600
605
28
29
30
S145
1975 2 MAR
3 MAR
4 MAR
1975 5 MAR
6 MAR
7 MAR
228°
222°
227°
221°
180°
170°
027°
017°
292°
087°
180°
088°
000°
270°

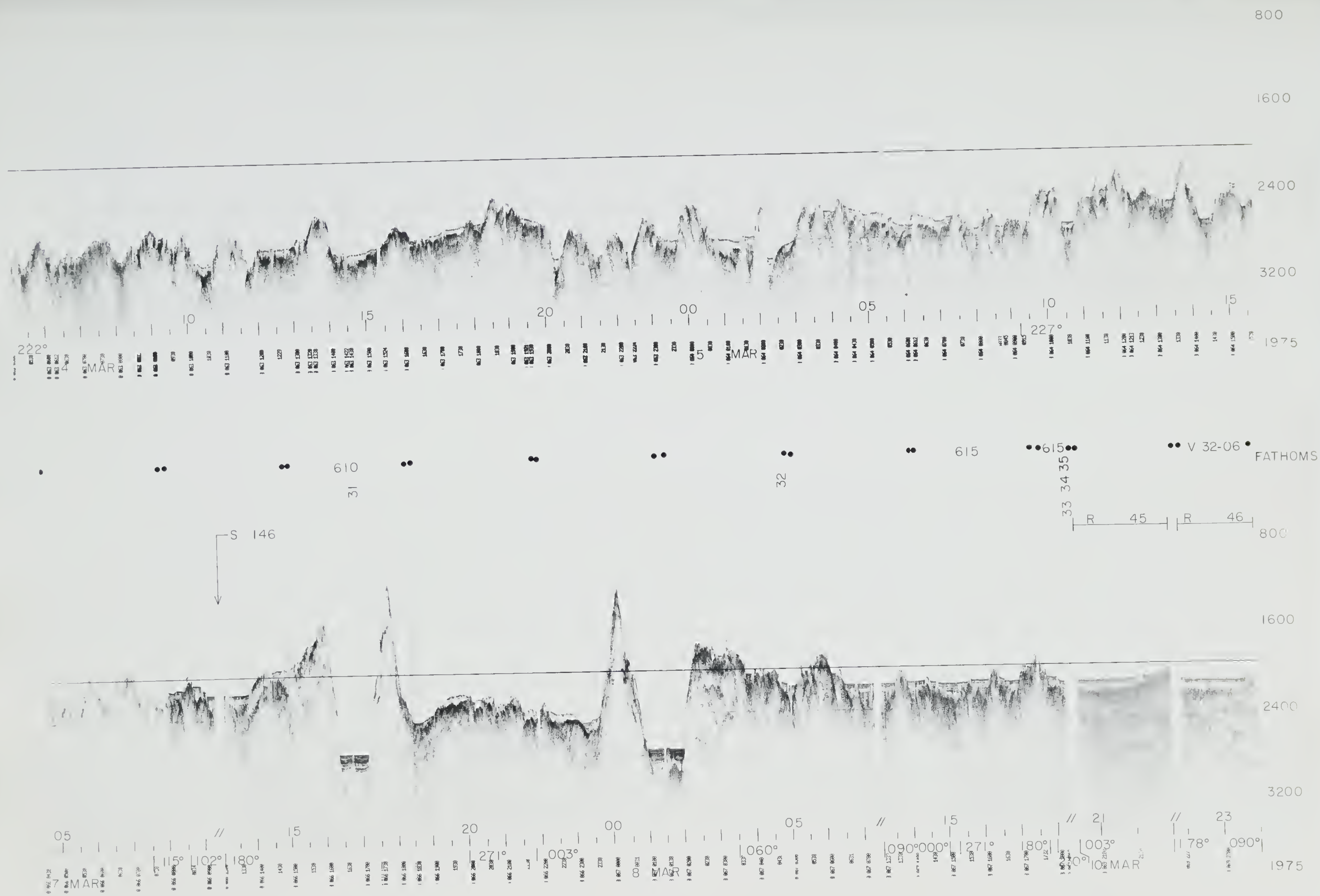

800
1600
2400
3200
1975
FATHOMS
V 32-06
615
610
31
32
33
34
35
R 45
R 46
S 146
4 MAR
5 MAR
7 MAR
8 MAR
10 MAR
222°
227°
115°
102°
180°
271°
003°
060°
090°
000°
178°

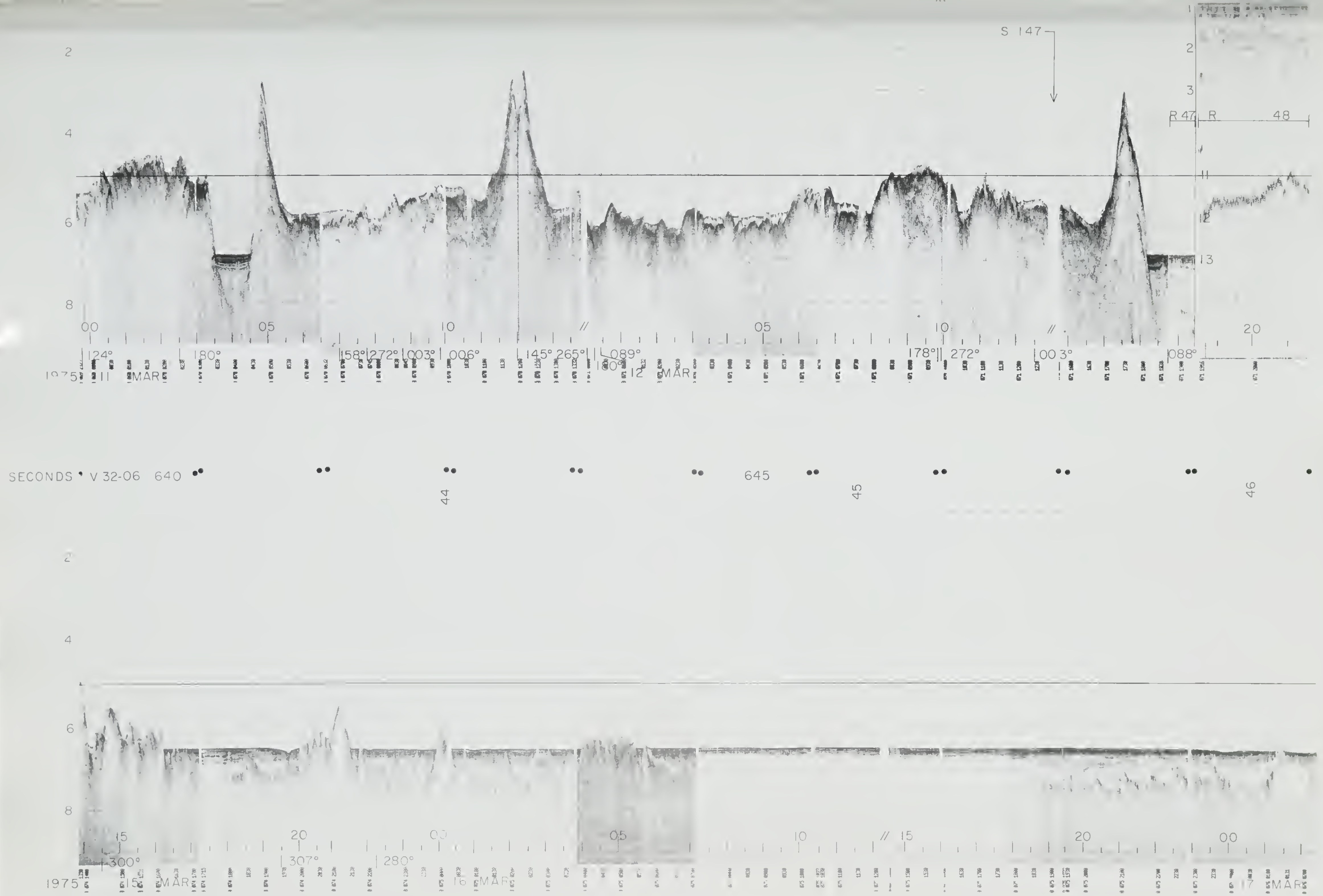

S 147
R 47
R
48
SECONDS
V 32-06
640
645
44
45
46
1975
11 MAR
12 MAR
15 MAR
16 MAR
17 MAR
124°
180°
158°
272°
003°
006°
145°
265°
089°
100°
178°
272°
003°
088°
300°
307°
280°

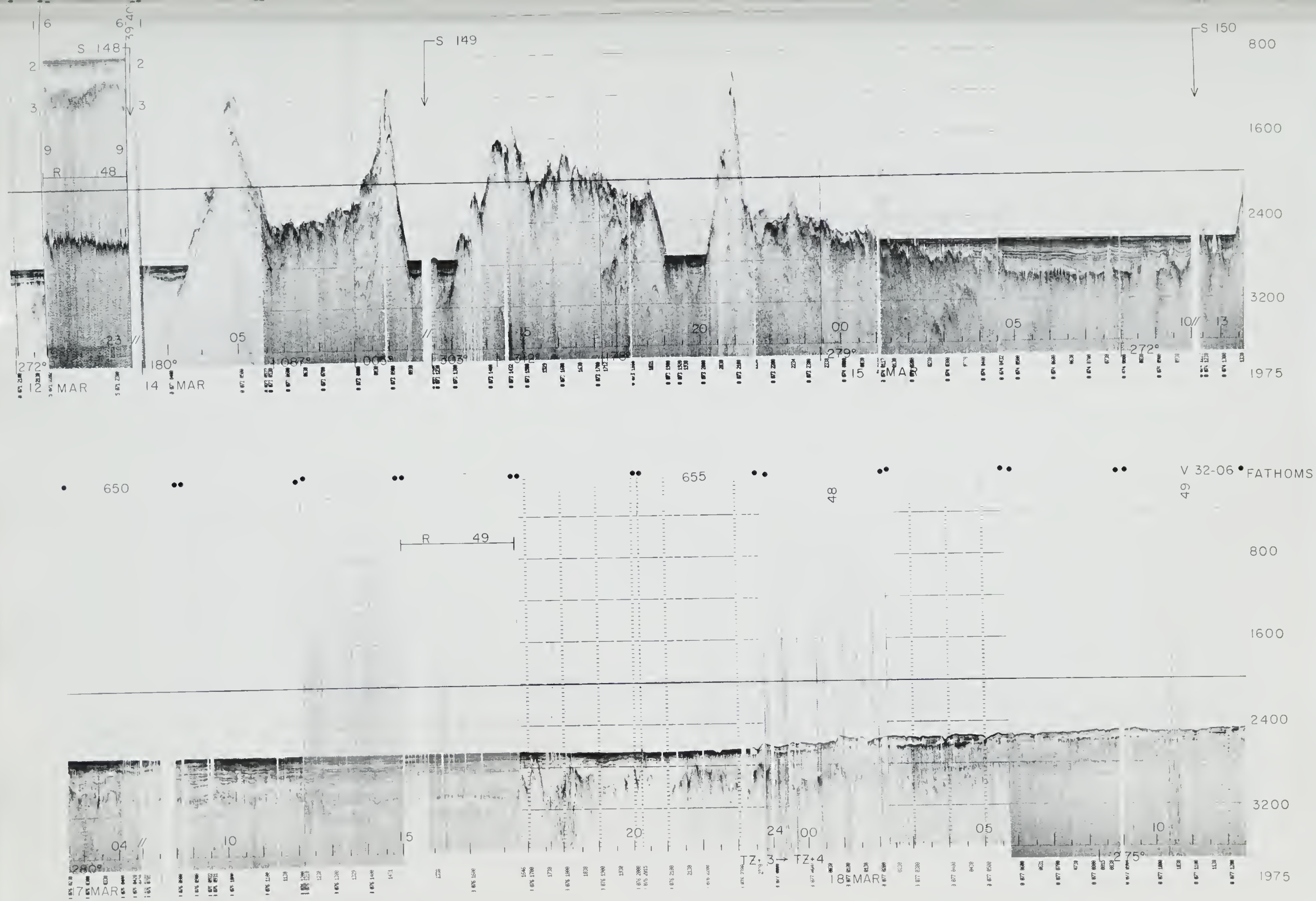

S 148
S 149
S 150
R 48
R 49
12 MAR
14 MAR
15 MAR
17 MAR
18 MAR
272°
180°
087°
005°
303°
312°
178°
279°
275°
280°
TZ+3 → TZ+4
650
655
48
49
V 32-06
FATHOMS
800
1600
2400
3200
1975

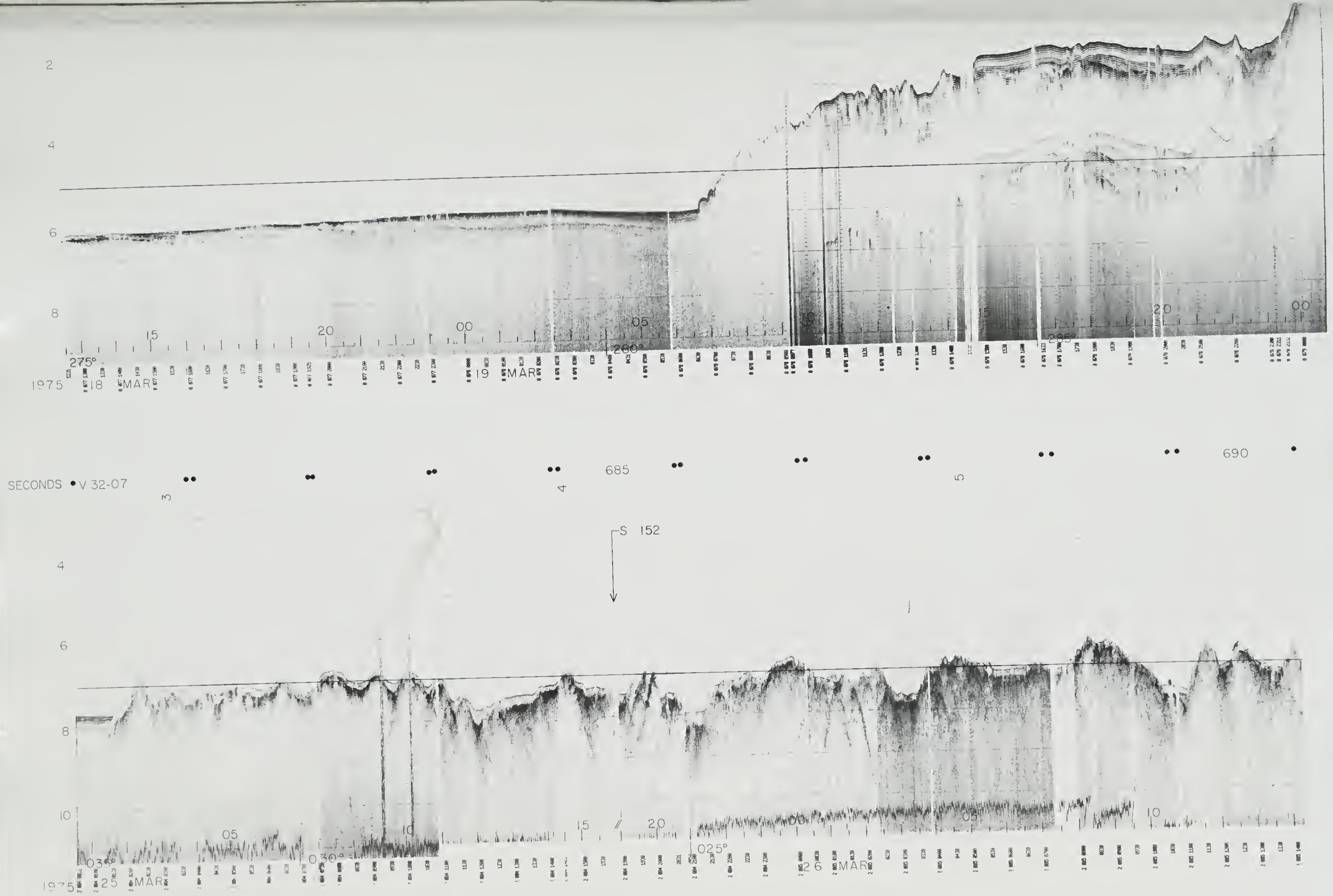
SECONDS • V 32-07
2
4
6
8
15
20
00
05
00
20
275°
280°
285°
1975 18 MAR
19 MAR
3
4
5
685
690
S 152
4
6
8
10
05
10
15
20
00
05
10
035°
030°
025°
1975 25 MAR
26 MAR

Columbia University in the City of New York

LAMONT GEOLOGICAL OBSERVATORY

PALISADES, NEW YORK

Results of IPOD Site Survey Aboard RV VEMA Cruise 32-06

PART B. CANDIDATE SITE 7

William J. Ludwig and Philip D. Rabinowitz

Technical Report No. CU-5-75

International Phase of Ocean Drilling
U.S. National Science Foundation
Subcontract UC NSF C-482-2

TABLE OF CONTENTS

ILLUSTRATIONS

*The originals of these maps have been deposited with the IPOD Site Survey Data Bank at L-DGO.

INTRODUCTION

IPOD candidate site ATL 7 lies along an east-west "flow line" determined from magnetic anomalies and azimuths of fracture zones (Figure 1). Sites 3 and 7 are in the areas of the oldest magnetic anomalies seaward of the Cretaceous quiet zones (anomalies 31 to 34; approximately 75 to approximately 81 m.y.-old crust). Drilling at these sites is intended to test for symmetry (or nonsymmetry) in properties of oceanic crust generated on opposite sides of a spreading center.

The site ATL 7 area was surveyed with R.V. VEMA of Lamont-Doherty Geological Observatory during a one-week period of February 1975 (Figure 2). Our objectives were: (1) to find and map the oldest recognizable magnetic anomaly and make seismic refractions measurements about it in a locality where there is sufficient sediment for spudding in the drill stems, (2) to map, in as much detail as time would permit, the bathymetry, sediment distribution, and variations in gravity field strength, and (3) to obtain sediment cores, photographs of the sea floor, and heat flow measurements at prime drilling sites. The drilling sites chosen were to be further surveyed by R.V. VALDIVIA (Germany).

The data collected during VEMA cruise 32-06 in the survey area is presented by Ludwig and Rabinowitz (1975). In this report, we portray the results in maps and diagrams to help guide the selection of the prime drilling site and to allow interpretation of the drilling results in terms of the local and regional structure. Prior to the survey, very little was known of the site ATL 7 area except that it should, through extrapolation of isochrons, be an area of ~75 to 80-m.y.-old crust. The only pre-survey geophysical data available to us was from three cruises of R.V. VEMA that passed through the area with all instruments recording.

The western extension of the Kane fracture zone runs through IPOD candidate site 3. Rabinowitz and Ludwig (1975) were able to trace the fracture

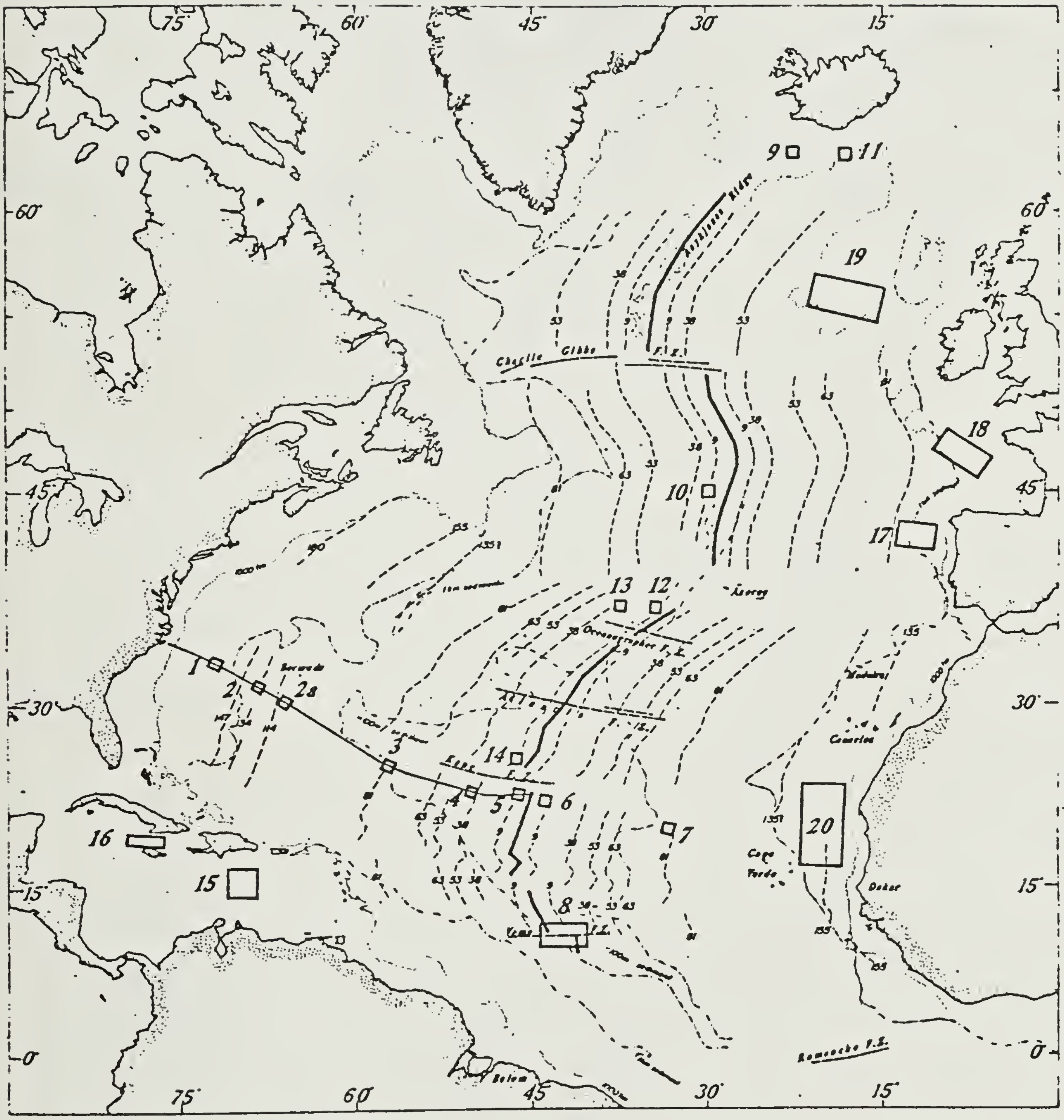

igure 1. Proposed Atlantic drilling sites for International Phase of Ocean Drilling. Sites 3, 4, 7 and 8 were surveyed by R/V VEMA in February and March, 1975.

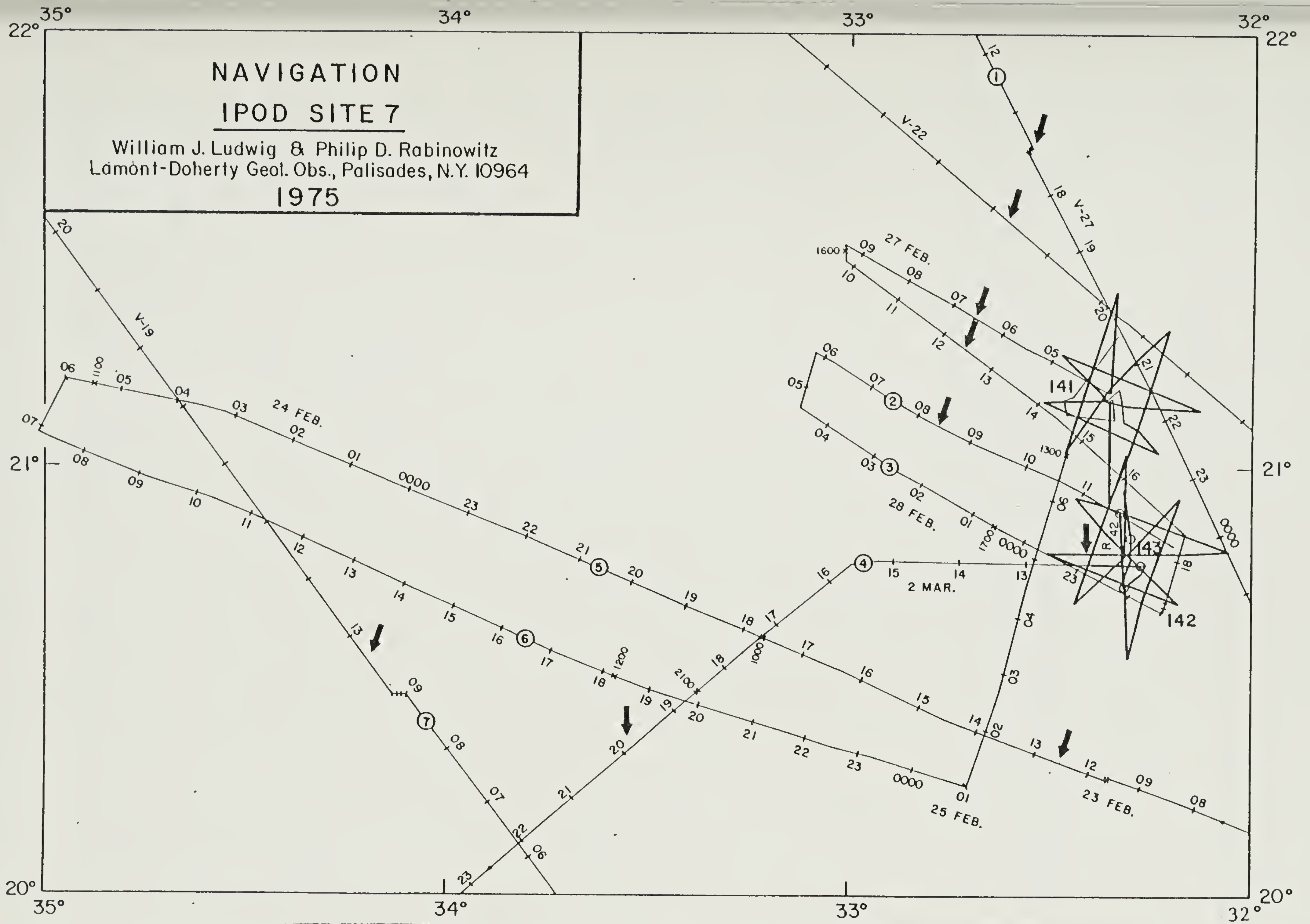

Fig. 2. Ship's navigation. Date and time of day are indicated. Numbers 141-143 are ship's stations. Arrows denote boundary between smooth and rough basement (topography). Small circles are sonobuoy stations. Circled numbers 1-7 designate the seismic reflection profiles shown in Figure 3.

3

to 62^{o}W, a distance of about 1700 km westward from the axis of the mid-Atlantic ridge. Site 7 should lie near the approximate conjugate portion near the eastern extension of the Kane fracture zone.

SITE 7 DATA

Figures 3a and 3b show a number of west-east seismic reflection profiles along the traverses shown in Figure 2. The outstanding feature of the profiles is the change from fairly smooth to rough basement accompanied by a decrease in elevation of the sea floor and an abrupt thinning of the sediments. In places, this change is quite abrupt, as in profiles 1 and 5, and is easily recognized; elsewhere, the change seems to be more gradual (profiles 2 and 4). The rough-to-smooth basement boundary is marked by arrows on Figure 3.

Contours of the bathymetry observed along the track lines in Figure 2 and along additional track made by R.V. VALDIVIA indicate an alternating series of ridges and troughs that trend north-south (Figure 4). Although drawn as continuous features, it is possible that they are offset left-laterally in the vicinity of latitude 21°05'N, which corresponds in position with an abrupt offset in position of the contact between the rough and smooth basement (Figure 2). An important problem that remains to be explained is why the sea floor <u>declines</u> in elevation towards the flank of the mid-Atlantic ridge.

The site 7 survey area is characterized by generally positive free-air gravity anomalies up to 25 mgals (Figure 5) which parallel the bathymetry. The larger anomalies (>10 mgal) are generally associated with the higher elevation (smooth basement) sea floor.

Magnetic anomalies are shown as profiles along the ship's track in Figure 6. A prominent linear negative anomaly is identified as anomaly 34 (approximately 81 m.y.B.P.). This anomaly is offset right laterally near $\sim 20^{o}.3$'N.

The results of four airgun-sonobuoy profiles made in the immediate

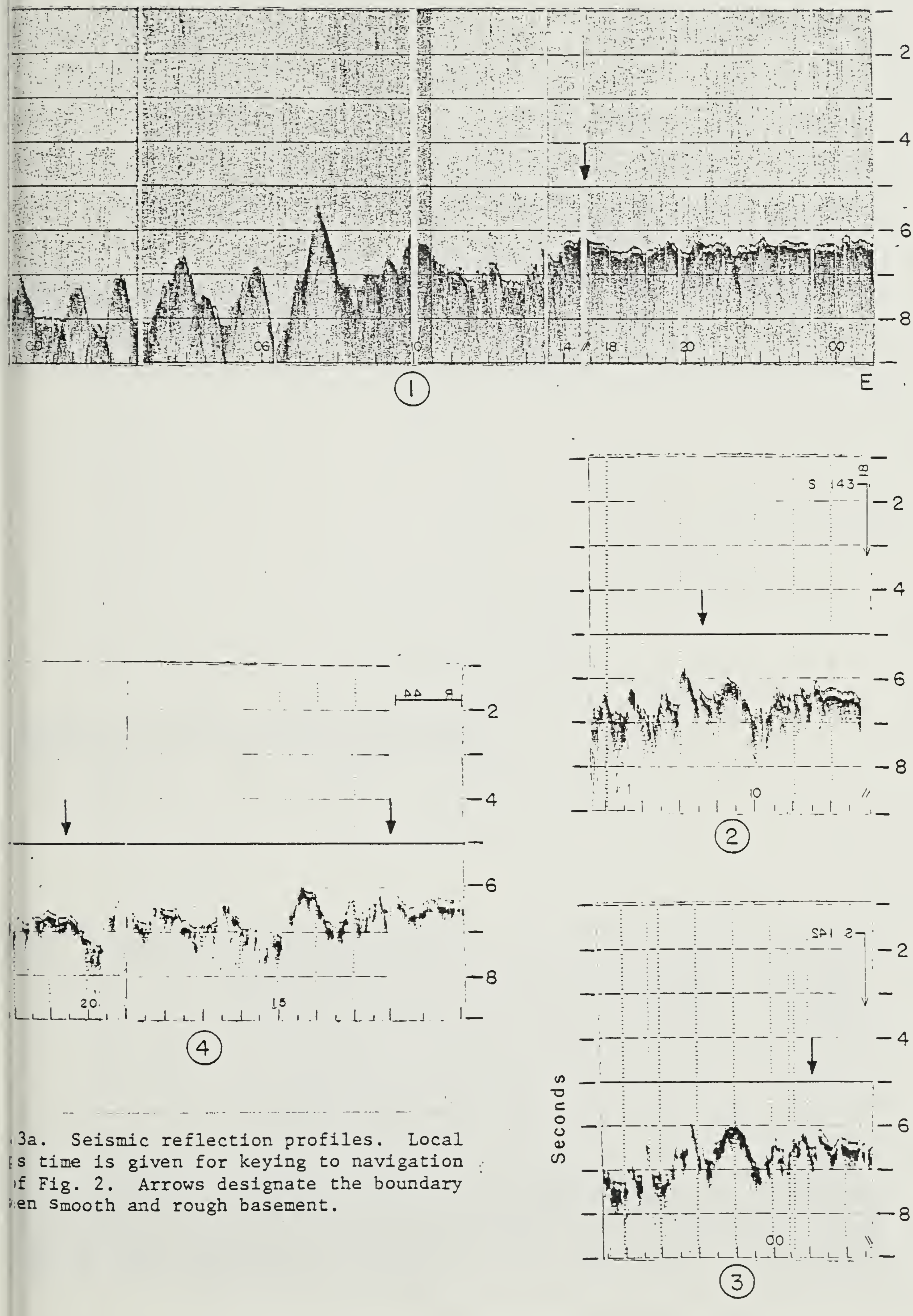

3a. Seismic reflection profiles. Local
s time is given for keying to navigation
f Fig. 2. Arrows designate the boundary
en smooth and rough basement.

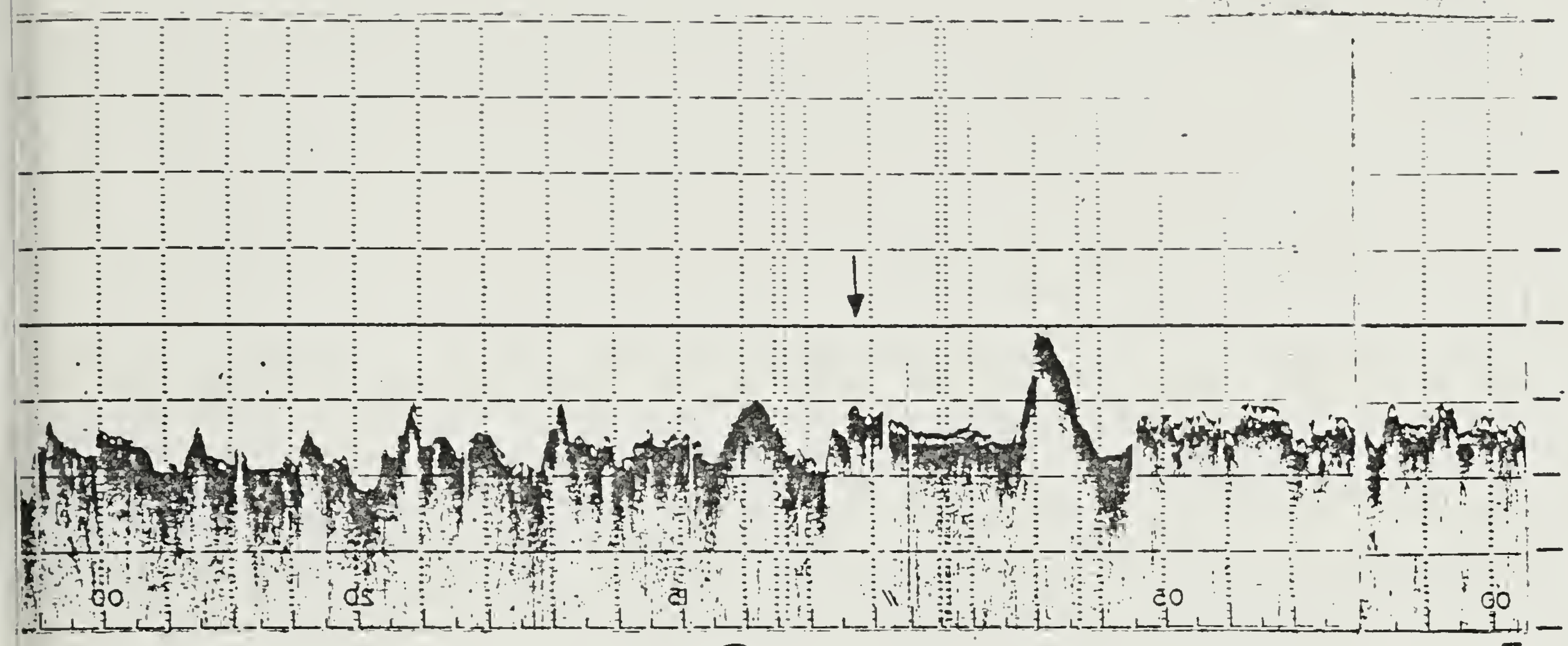

5

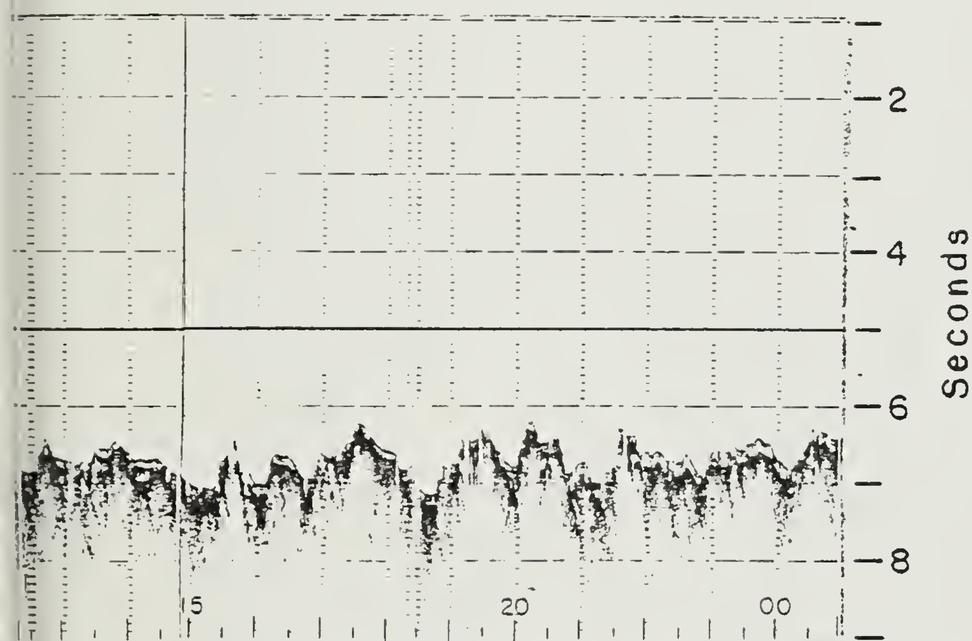

6

Fig. 3b. Explanation same as for Fig. 3a.

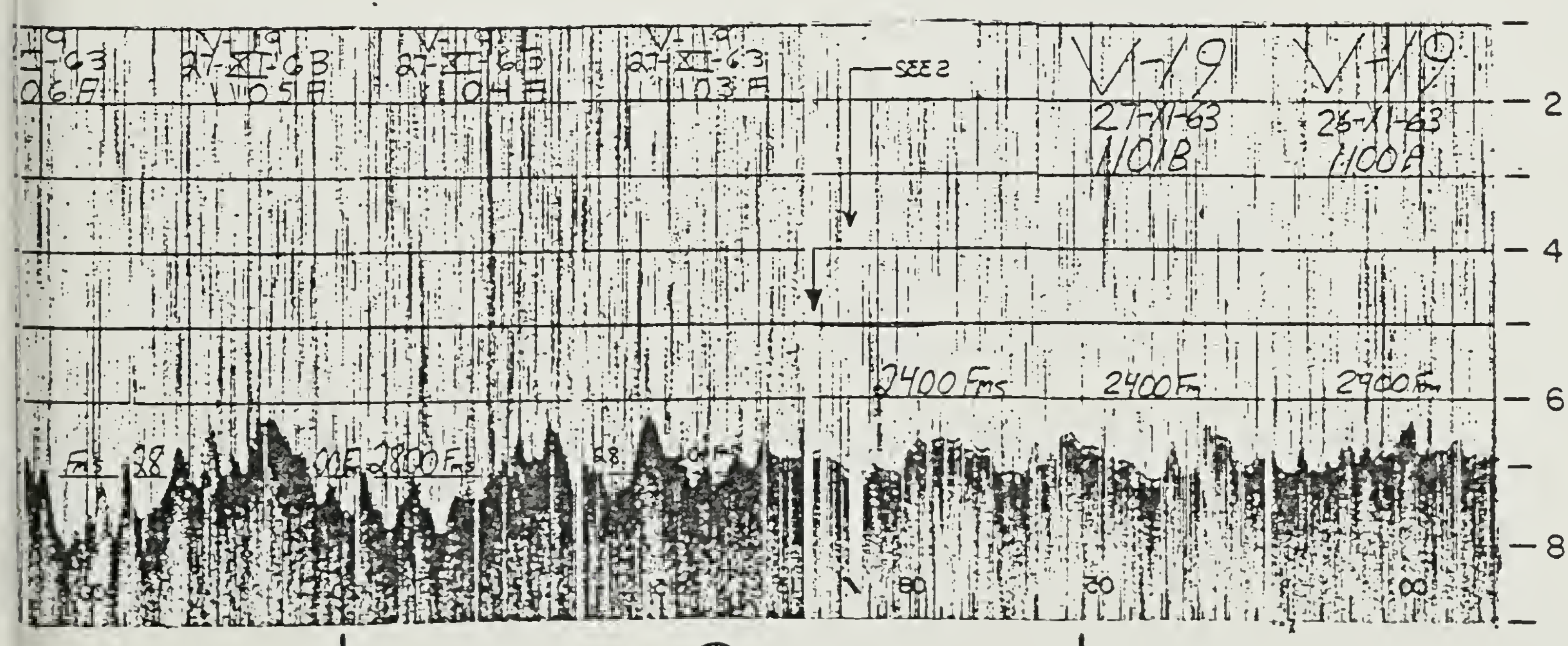

7

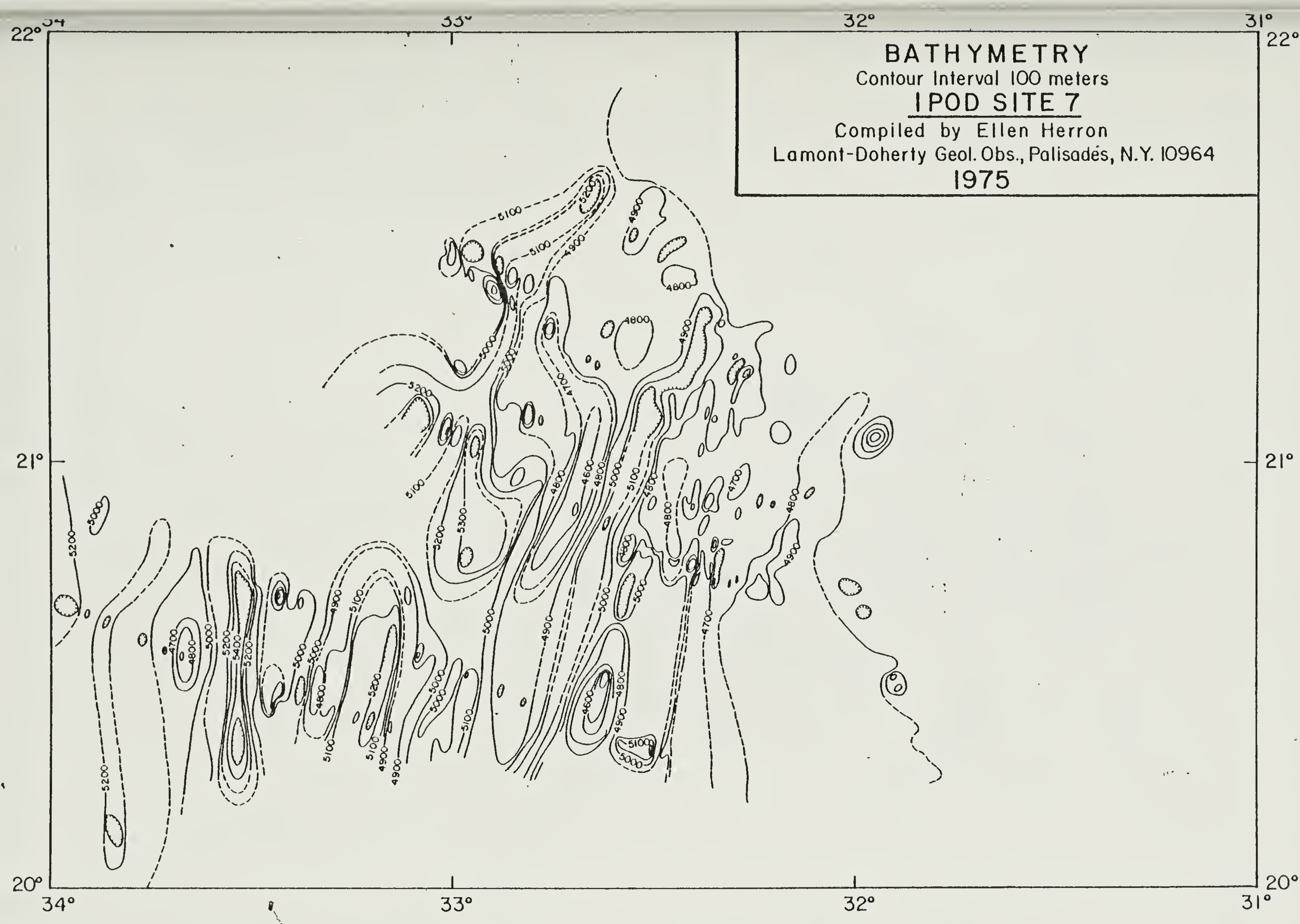

Fig. 4. Bathymetry map. Contour interval 100 meters (corrected).

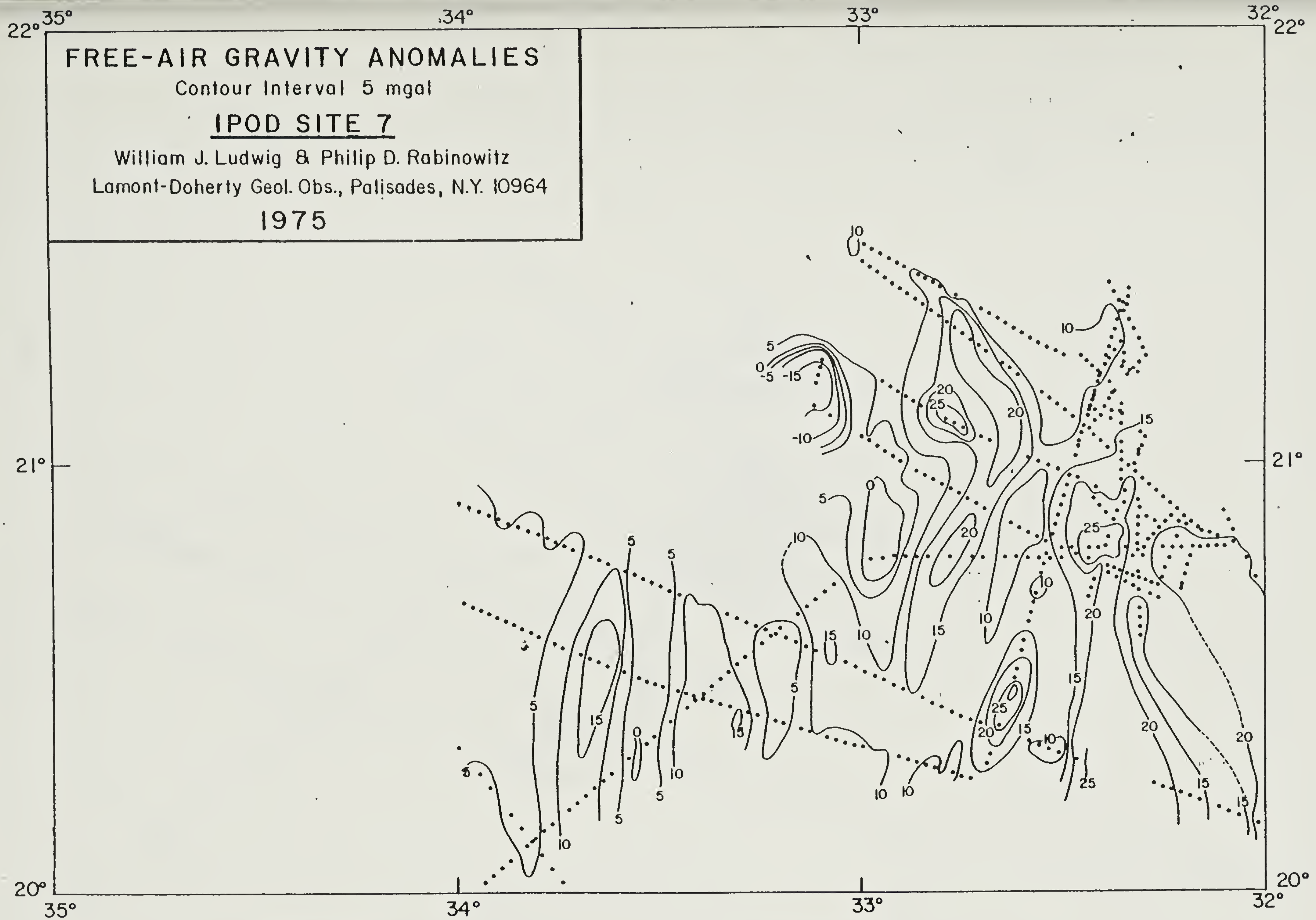

Fig. 5. Free-air gravity map. Contour interval 5 mgal. Control for the map is indicated by dotted lines.

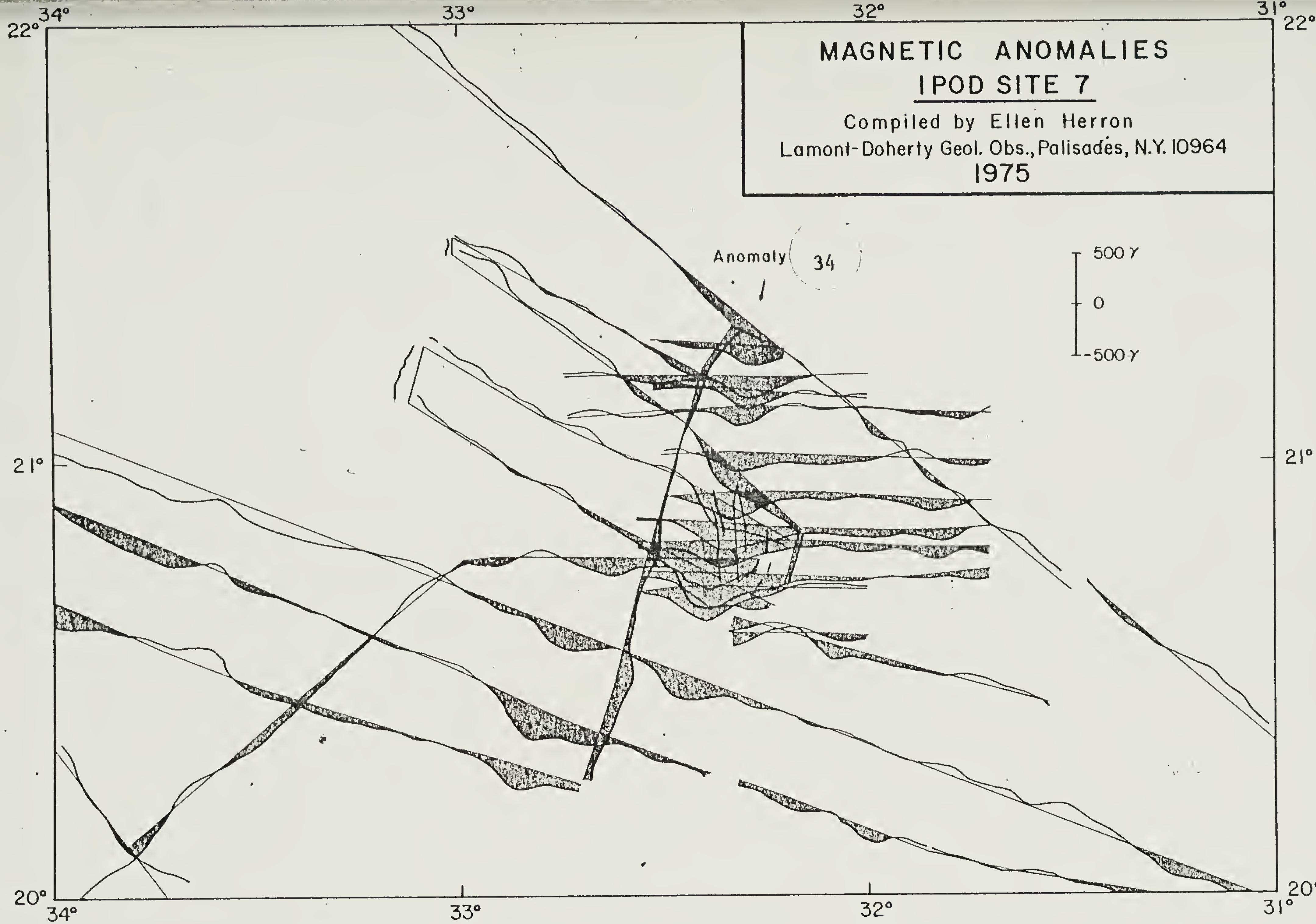

Fig. 6. Magnetic anomalies. West-East lines were made by R/V VALDIVIA; all others by R/V VEMA.

vicinity of OBS drop 2 (Figure 2) are tabulated by Ludwig and Rabinowitz (1975) and are shown as seismic structure sections in Figure 7. Profiles 40 and 42 were recorded in opposite directions. The thin cover of sediments resulted in unreliable measurements of velocity, even though the computations were carried out by use of the regular T^2/X^2 program as well as a special program for thin layers. Therefore, a velocity of 1.78 km/sec was used as sediment velocity whenever a value was assumed for refraction calculations.

Sonobuoy profile 42 measured two velocity layers, 4.7 and 6.1 km/sec in layer 2, whereas the velocity solutions of profile 40 gave a single 5.4 km/sec basement layer. The two-component layer 2 solution of profile 42 yields a combined layer thickness that is 0.25 km greater than the single layer solution. Through examinations of sonobuoy data, Houtz and Ewing (1976) showed that seismic layer 2 may be a two- or three-component layer, depending on age of the sea floor with distance from the axis of the mid-Atlantic ridge. At the crest of the ridge, layer 2 is a three-component layer with velocities 3.3 km/sec (2A), 5.2 km/sec (2B), and 6.1 km/sec (2C). The velocity of layer 2A increases to that of layer 2B on crust of about 40 m.y. while the thickness of layer 2A decreases to about 100 m. There is no corresponding distal increase of velocity with age in layers 2B and 2C. Accordingly, the 4.7, 6.1, and 6.8 km/sec layers of sonobuoy profile 42 are, respectively, identified as layer 2B, 2C, and layer 3.

Seismic refraction profiles were recorded along eight different azimuths by an ocean bottom seismometer located in a sediment pond in the "smooth" area of ocean crust (Figures 2 and 8). A similar, star-shaped pattern of shots to three OBS located about 20 miles to the north was not successful.

Time-distance graphs for the refraction profiles are presented in Figures 9-12. The data from the eight radial profiles are combined to form four end-to-end (or split) profiles. Because of uncertainties in picking the

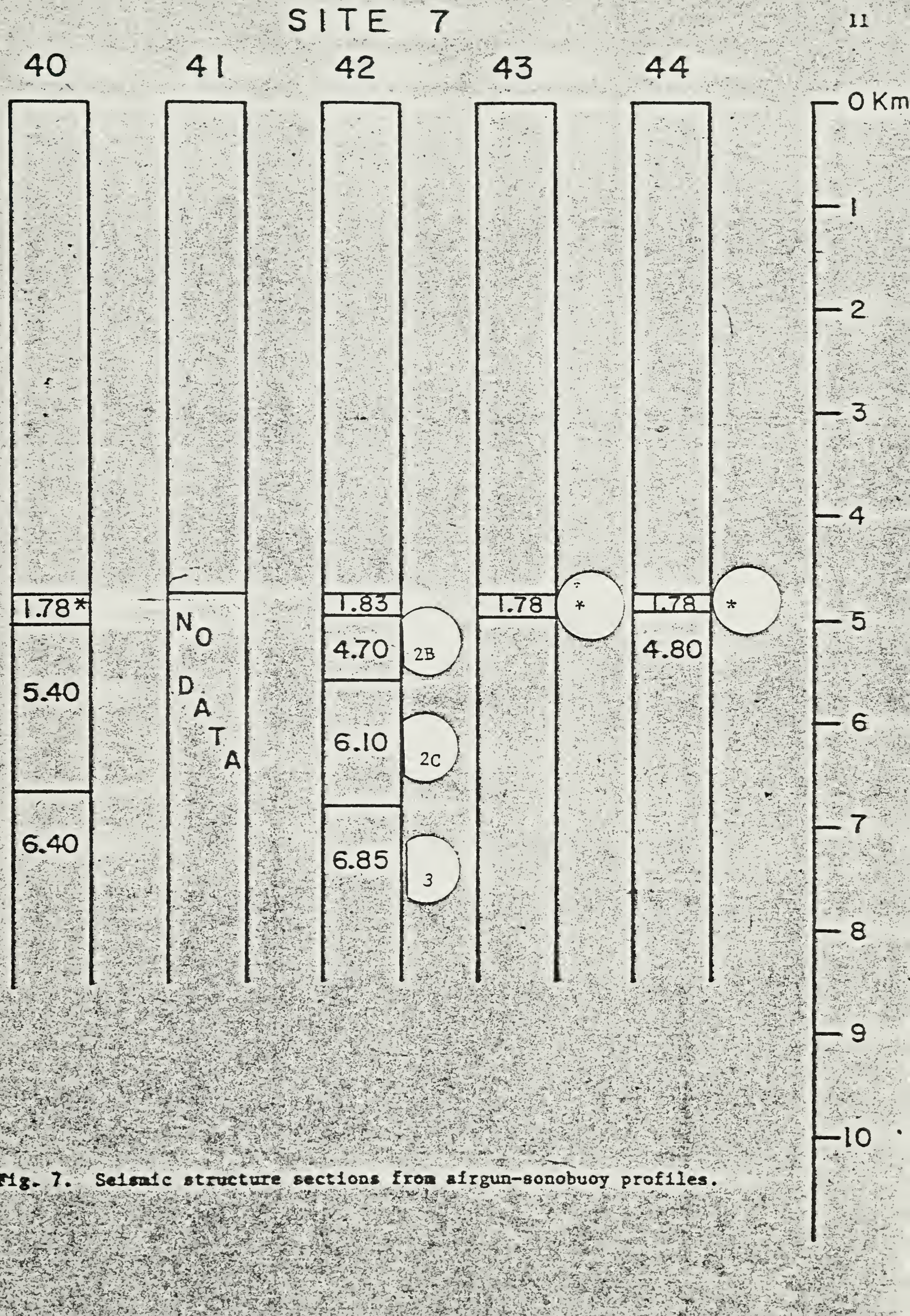

Fig. 7. Seismic structure sections from airgun-sonobuoy profiles.

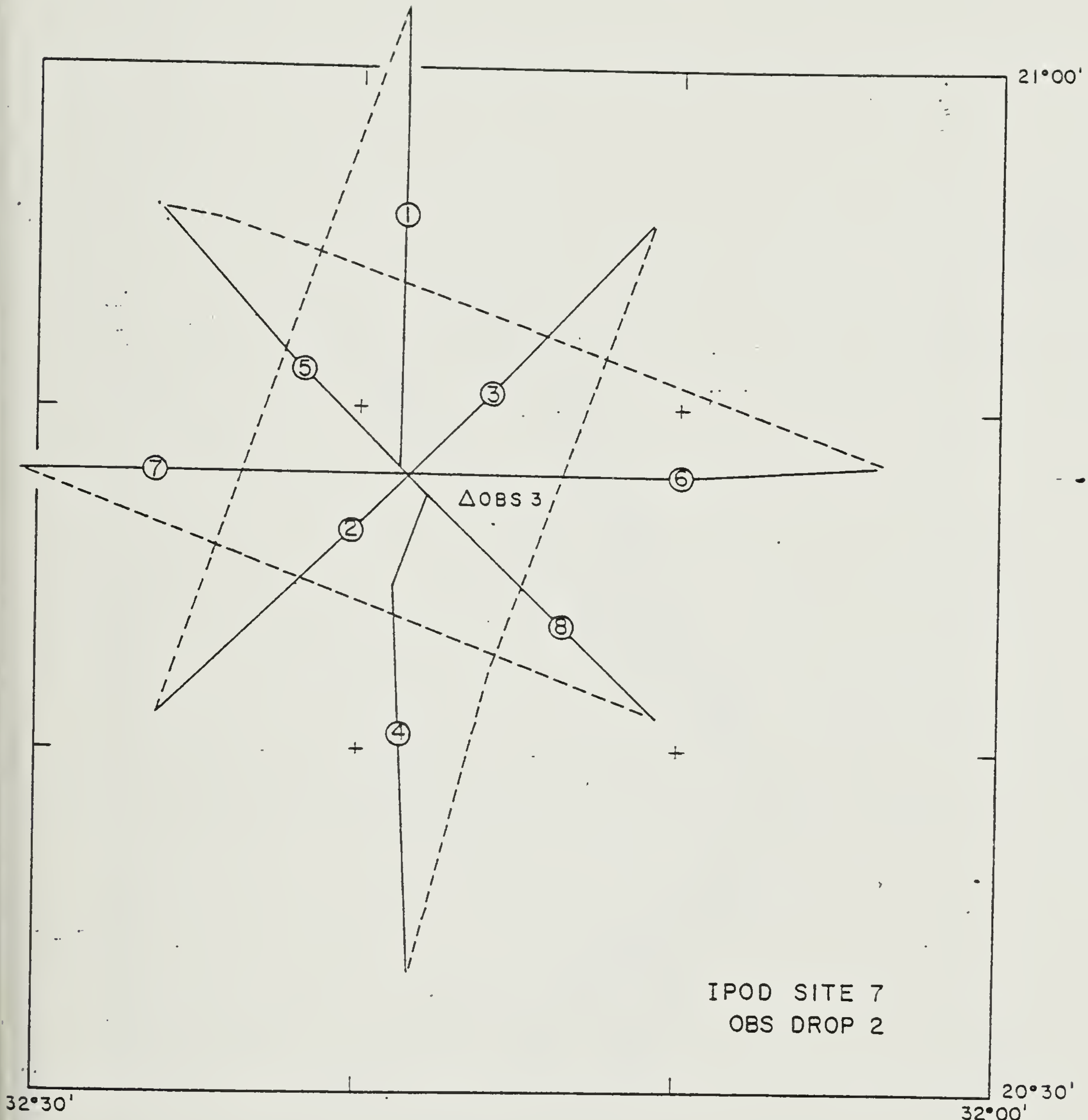

Fig. 8. Location of OBS refraction profiles.

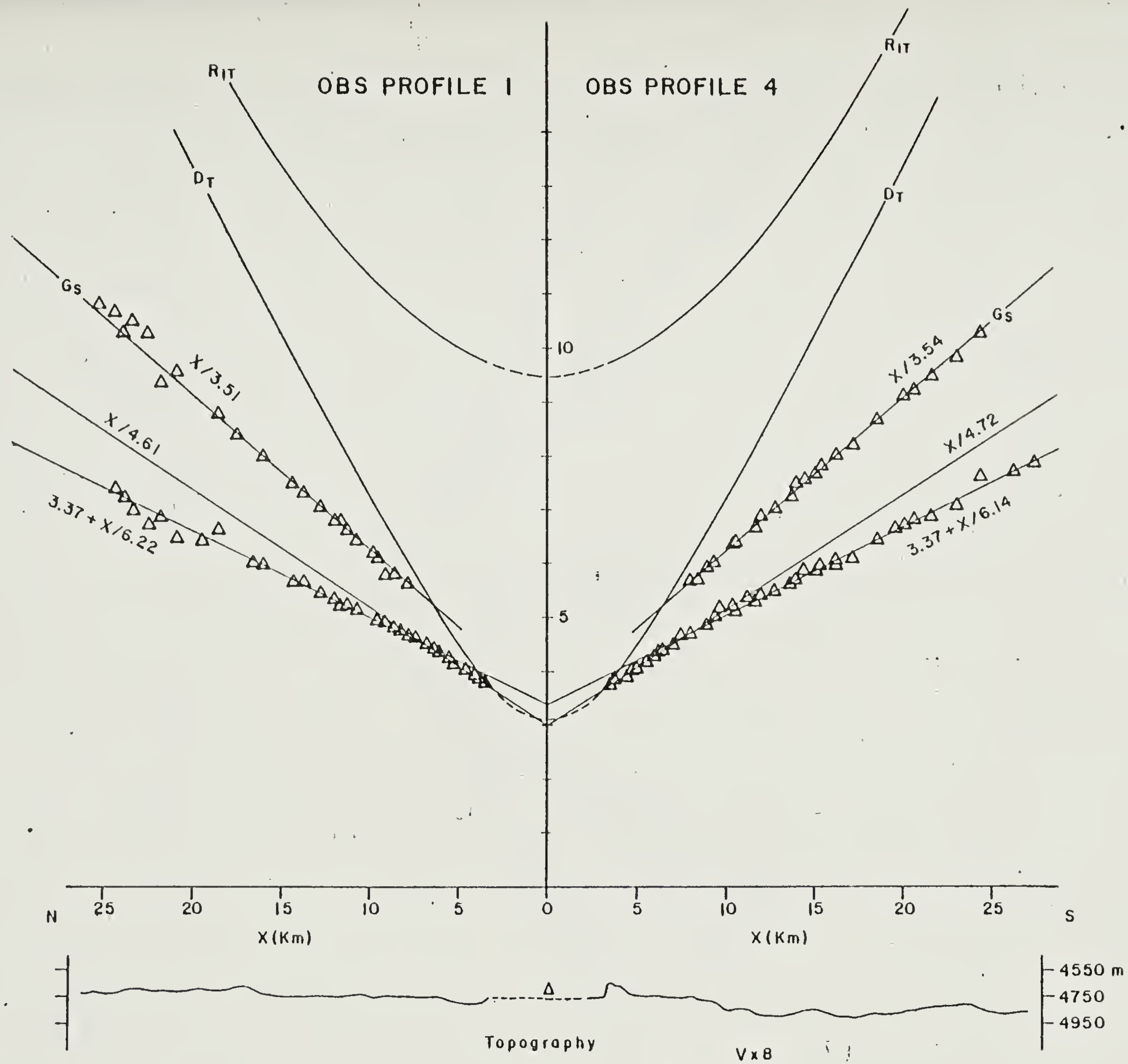

Fig. 9. Time-distance graph, OBS profiles 1 and 4.

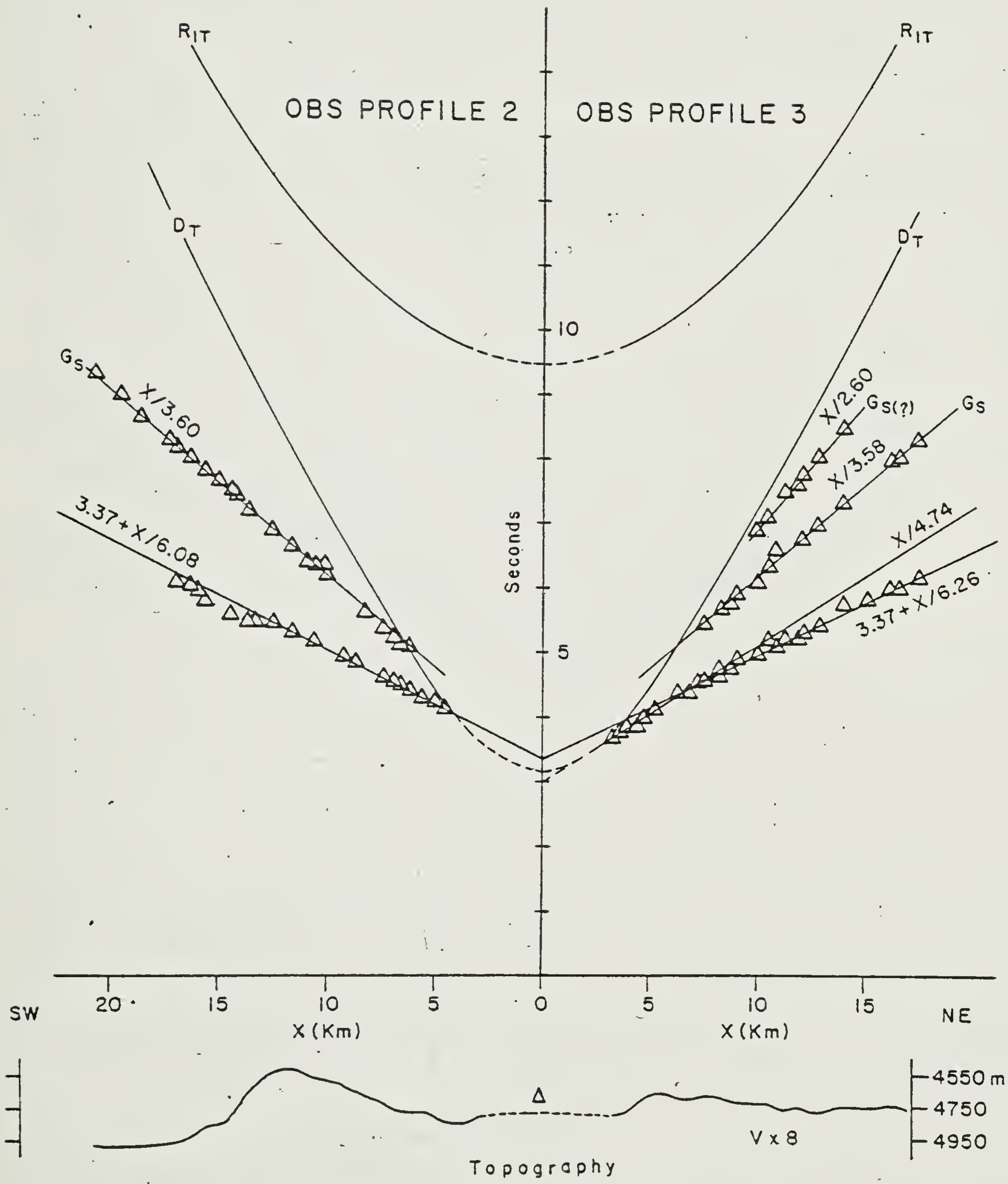

Fig. 10. Time-distance graph, OBS profiles 2 & 3.

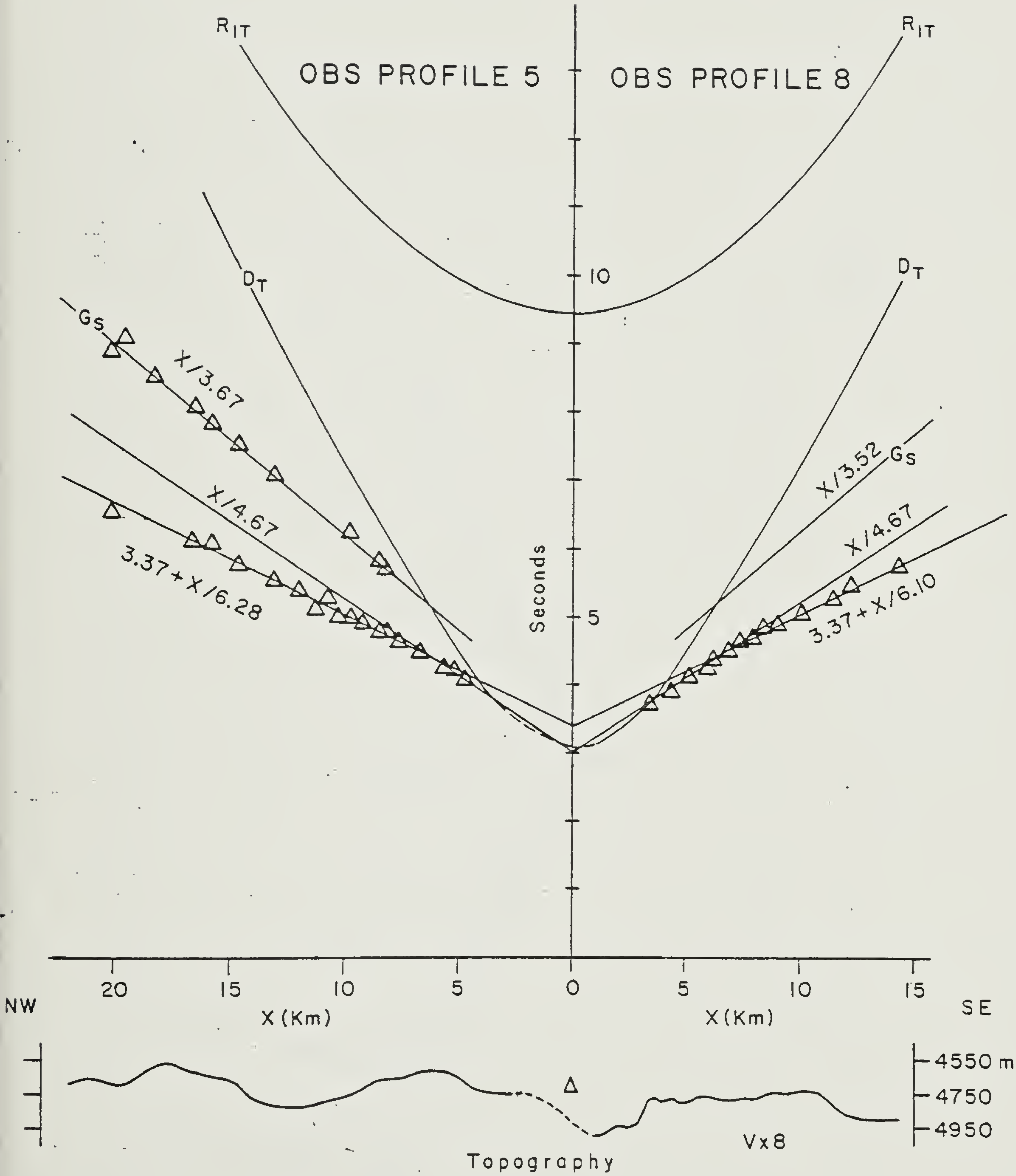

Fig. 11. Time-distance graph, OBS profiles 5 & 8.

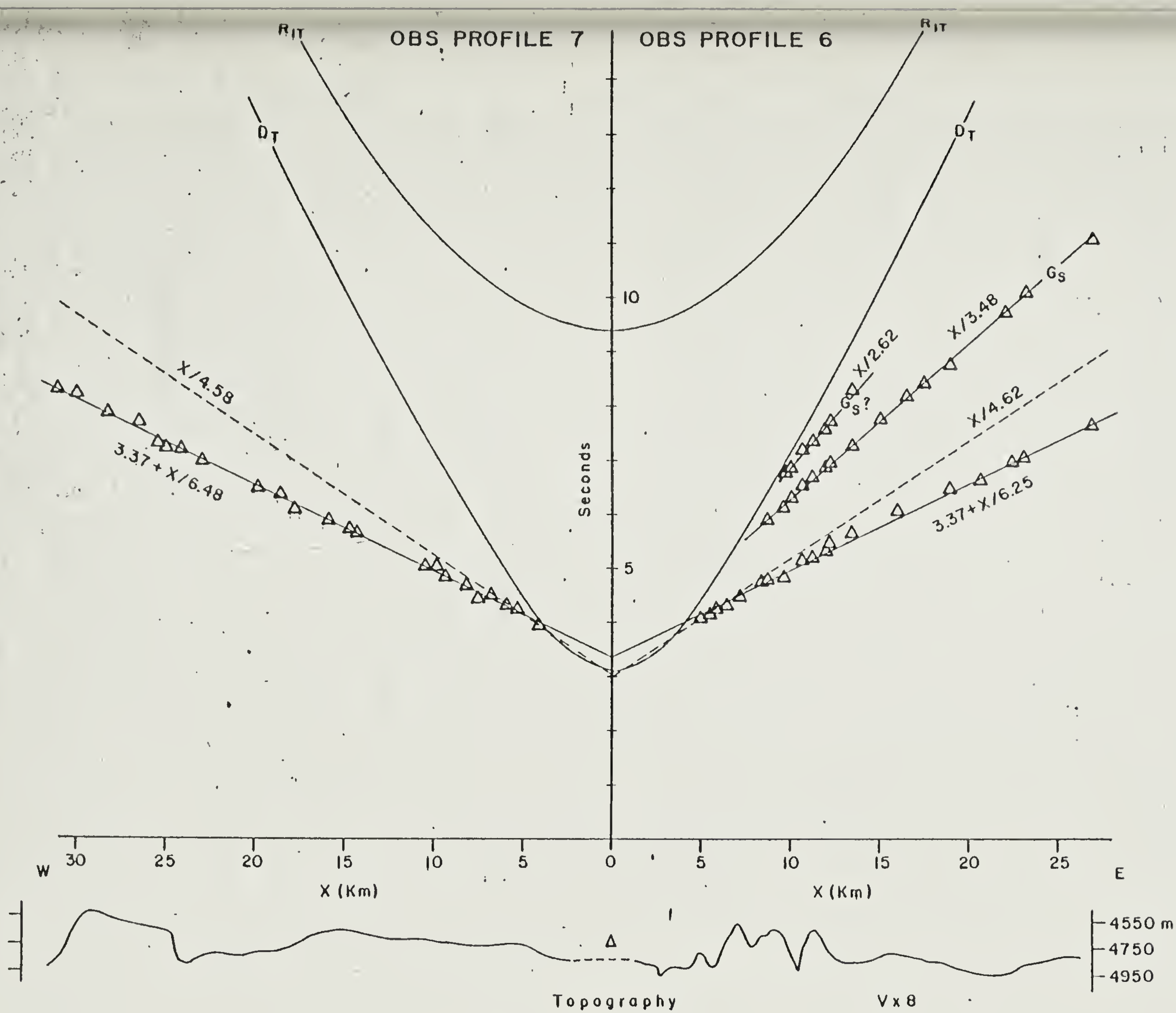

Fig. 12. Time-distance graph, OBS profiles 7 and 6.

beginnings of refracted waves (see Appendix), the profiles were interpreted as a group by fitting the data points by eye to apparent velocity lines having the same time intercept. According to this method of interpretation, two refractors of velocity 4.7 and 6.2 km/sec were identified and classified as layer 2B and 2C. Our identification of the 6.2 km/sec refractor as layer 2C is based on its depths, about 0.30 km below sea floor, which corresponds approximately with the depth to layer 2C as measured by sonobuoy 42.

The azimuthal distribution of velocities in layer 2C has velocities near 6.25 km/sec recorded in the northerly directions and velocities near 6.10 recorded in the southerly directions, indicating that the structure may be approximated by a homogeneous plane-layer dipping gently southward. No seismic anisotropy is observable for the top of layer 2C. Hence, the average of the apparent velocity observed in each direction may be used to closely approximate the true velocity. There seems to be no azimuthal variation of velocity in layer 2B, suggesting that there is some lateral heterogeneity in the uppermost oceanic crust within a short distance from the OBS.

Velocities of 3.48 - 3.54 km/sec are identified as transformed shear waves which have been propagated through layer 2C. The intercept times of shear wave velocity lines (V_{S3}) are consistent with the interpretation of P to S conversion at the sediment-basement interface and shear propagation in the crustal rocks to the OBS. The P- and S-wave data give Poisson's ratios near the predicted value of 0.25 (Table 1). On two profiles (3 and 6), we observed arrivals whose velocity (2.6 km/sec), intercepts, and UP/VS ratios indicate that they may be transformed shear waves from layer 2B.

Three sediment temperature gradient measurements were made at IPOD site ATL 7 (see Table 2). All three stations had relatively uniform sedimentary cover (0.2 seconds). It has been found that, in areas where the sediment is uniform, heat flow is representative of the flux from deep in the lithosphere

(Lister, 1972). Therefore, the heat flow measured at this site gives a reliable estimate of the heat flux from depth. Heat flow measurements taken during other cruises in the area are listed in Table 3. The uniformity in the thermal gradients and heat flow values near site 7 is striking. The mean heat flow is 1.41 HFU. This average is in close agreement with the compilations of Sclater and Francheteau (1970) in the North Pacific and South Atlantic Oceans, which give means of 1.43 and 1.42 respectively.

The two relatively high thermal gradients measured in the site 7 area may indicate a locally anomalous area. It should be noted that all three of the stations were taken near a "rough-smooth" boundary in the basement topography. The boundary between topographic provinces may be related to this local anomaly. A standard Ewing thermograd with six thermistor sensors (five sediment probes and one water probe) was used to measure the thermal gradients. The instrument is described by Langseth (1965). Thermal conductivities of core samples were not measured. Values used to calculate heat flow were estimated from nearby heat flow stations.

RECOMMENDATIONS FOR DRILLING

In order to take advantage of the best coverage of geophysical data, the drill site should be located in the immediate vicinity of the OBS site (20°47'N, 32°17'W). Here approximately 200 m of pelagic sediment overlie a 4.7 km/sec layer 2B, 300 meters thick. The thickness of layer 2, as determined by sonobuoy profiles 40 and 42 is about 1700 m.

However, the final selection of the drill site should not be made until all other survey data are integrated with this present survey. Also, the problems relating to the change from rough to smooth basement should be first discussed with the Ocean Crust Panel before final site selection.

ACKNOWLEDGMENTS

This study was supported by the IPOD Site Survey Management under subcontract with the Deep Sea Drilling Project (UC NSF C-482-2).

We thank the officers, crew, and scientific staff of R.V. VEMA 3206 for their assistance in gathering the data. Special appreciation is expressed to A.C. Hubbard and G. Carpenter for their diligent efforts with the OBS at sea. VEMA 3206 was led by W.J. Ludwig. The section on heat flow measurements was taken in part from a report, "Geothermal Measurements at Sites 7 and 8," by L. Ongley and M. Langseth. R.E. Houtz assisted with the analysis of the sonobuoy and OBS data.

APPENDIX

Seismic Refraction Measurements

For the survey work in the site 7 area VEMA was equipped with three ocean bottom seismographs, furnished by L-DGO through IPOD Site Survey Management. The OBS employed is a 3-unit (vertical and horizontal seismometers and hydrophone) self-recording pop-up system that is contained in a buoyant sphere with a time-release mechanism (Carmichael et al., 1973). The experimental procedure of making seismic refraction measurements with an OBS and method of data reductions are described by Ewing and Ewing (1961) and Davis et al. (1976), among others. Explosives used as the sound source was an untried two-component explosive purchased from EXCOA, called SAF-T-PAK. One component of the explosive is a 5-lb package of pellets in a plastic bag (cartridge) sealed at each end with a metal clip; the other is a bottle of activator fluid. The cartridges were packed five to a cardboard carton in vermiculite packing material for shipment by air cargo to VEMA at Dakar.

Our experiment with the OBS called for shooting an 8-arm star-shaped pattern of shots to three OBS in a triangular array in order to measure apparent velocities and apparent azimuths of the signals from the shots. Unfortunately, the ship's pit log was not operating and we did not have a shipboard OBS playback system. Furthermore, satellite fixes at this latitude were infrequent and the OBS prototype models did not have a pinger or transponder to allow fixing its location (when on bottom) during the experiment.

Aboard VEMA, we made two 3-instrument drops in the survey area (Figure 2). 5-to 15-lb charges of the SAF-T- PAK were fired every 2-5 minutes over a 24-hour period in each experiment. Here, and at Site 8, the clips used to

seal the cartridges did not provide a watertight seal. After activation, we had to seal both ends by twisting and tie-wrapping the plastic closed. In reclosing, we could not always let out the same amount of air; hence, the sinking rate varied considerably. Most important, initiation of the SAF-T-PAK with a No. 9 engineer's special blasting cap was not reliable. We experienced considerable DUDS and partial explosions of the SAF-T-PAK charge.

Because of various problems, only OBS #3, Drop #2, recorded sufficient information to allow construction of travel time graphs. However, signal-to-noise levels were generally poor, which often made picking the beginning of the refracted arrivals difficult. The horizontal distances between shot-points and OBS were calculated from direct water waves. Hence, the scatter of arrivals (data points) in Figures 9-12 are caused, in part, by observational errors. We believe that the shot size (acoustic energy) was not sufficient to obtain refractions from layer 3. Interpretation of the data in terms of refracted P and S-waves from layer 2C, rather than from layer 3, gives the least amount of scatter of the data points from the velocity lines. Needless-to-say, the results of the OBS experiment should be accepted with caution.

Profiles	Velocity, km/sec						Thickness, Km			OBS Locations	
	V_1	V_2 [1]	V_3	V_4	V_{4S} [2]	PR [3]	Water [4]	h_2 [5]	h_3	Latitude	Longitude
1/4	1.51	1.8	4.67	6.18	3.54	0.26	4.75	0.20	0.31	20°47.3'N	32°16.6'W
2/3		1.8	4.72	6.17	3.59	0.24	4.75	0.20	0.31		
5/8		1.8	4.67	6.19	3.60	0.25	4.75	0.20	0.30		
7/6		1.8	4.60	6.36	3.48	0.29	4.75	0.20	0.27		

Notes:

Profiles are end-to-end unreversed (split) profiles. They are computed by using the average velocity of the apparent velocities observed in each direction as the true velocity and assuming horizontal layers.

1 The velocity 1.8 km/sec is the average velocity in the sediments determined from airgun sonobuoy measurements (Ludwig and Rabinowitz, 1975).

2 V_{4S} is the S-wave velocity propagated through the 6.2 km/sec layer.

3 PR denotes Poisson's ratio of the P-wave velocity and S-wave velocity. Its average value for elastic solids is 0.25.

4 Water thickness refers to the water depth at the time the OBS was launched.

5 The thickness of the sediments is observed to be about 0.20 km from seismic reflection measurements (Figure 3) and airgun-sonobuoy measurements (Figure 7). Velocity-intercept data for the basement layer result in near-zero thickness for the sediments.

TABLE 1

TABLE 2: R/V VEMA cruise 32 Heat Flow Values at IPOD Site # 7

Latitude (N)	Longitude (W)	Depth (corr m)	P (cm)	N	Gradient (°C/10m)	Heat Flow (HFU)	Evaluation	Station	Location
21° 9.9'	32° 26.7'	4885	520	3	0.729*	1.74**	7	1	Center of OBS #1
20°40.2'	32° 13.1'	4900	585	5	0.490	1.17**	9	2	SE corner of OBS #2
20°48.0'	32° 19.4'	4827	438	4	0.794	1.90**	6	3	Center of OBS # 2

P = penetration into sediment N = number of probes in mud.

* The gradient between the uppermost and lowermost probes. The gradient between the two bottom probes is 0.54 which corresponds to a heat flow of 1.29.

** The thermal conductivity is assumed from nearby stations to be 2.39 mcal/°C sec cm.

	Latitude (N)	Longitude (W)	Depth (corr m)	P (cm)	N	Gradient (°C/10 m)	Conductivity (mcal/°Cseccm)	Heat Flow (HFU)	Evaluation	Station
VEMA 19[1]										
	15°32'	30°02'	5396	1330	3	0.63	2.12	1.34	10	176
	20°28'	34°07'	5115	631	2	0.59	2.33	1.38	5	178
VEMA 22*										
	17°37'	27°02'	4359	658	3	0.89N.L.	2.39A	2.13	-	38
	19°01'	29°09'	4736	1108	3	0.67	2.39A	1.60	8	39
	19°40'	30°07'	4711	671	3	0.58	2.39A	1.39	8	40
	20°42'	31°27'	4404	1278	4	0.57	2.39A	1.36	8	41
VEMA 23*										
	18°33'	28°09'	4649	1205	3	0.63	2.87	1.81	7	62
	17°42'	29°52'	4645	1001	3	0.45	2.69	1.21	8	63
	17°13'	32°21'	4955	1297	3	0.56	2.61	1.46	9	64
VEMA 26*										
	16°38'	31°06'	4894	1126	3	0.46	2.13	0.98	8	9
	16°33'	31°34'	5053	373	1	0.29	1.92	0.56	3	10
	19°40'	26°07'	4550	1142	3	0.41	2.30	0.94	10	11
	19°17'	26°07'	4387	992	3	0.62	2.27	1.41	7	12
	19°17'	26°07'	4387	-	-	-	2.22	-	-	13
VEMA 27*										
	22°36'	28°00'	5546	911	2	0.52	2.04	1.05	8	95
ATLANTIS II 42[2]										
	19°45'	29°01'	4695	930	3	0.48	2.57	1.23	-	4
	19°52'	31°54'	4940	890	3	0.50	2.56	1.28	-	6
	19°39'	34°25'	5165	750	5	0.53	2.54	1.36	-	7

TABLE 3 (Continued)

Latitude (N)	Longitude (W)	Depth (corr m)	P (cm)	N	Gradient (°C/10m)	Conductivity (mcal/°Csec cm)	Heat Flow (HFU)	Evaluation	Station
KURCHATOV[3]									
19°15.1'	26°07.9'	4600	150	3	0.36	2.52	0.91	-	434
21°51.3'	29°14.6'	5342	240	3	0.58	2.45	1.42	-	435
23°09.5'	31°48.0'	5760	270	2	0.55	2.50	1.38	-	436

P = penetration into sediment; N = number of probes in mud; N. L. = non-linear; A = assumed conductivity.
* unpublished Lamont-Doherty Geological Observatory data.
1 Langseth et al., 1966.
2 Von Herzen and Simmons, 1972.
3 Hobart et al., in press.

REFERENCES

Carmichael, D., G. Carpenter, A. Hubbard, K. McCamy, and W. McDonald, 1973, A recording ocean bottom seismograph: Jour. Geophys. Res., v. 78, p. 8748-8750.

Davis, E. E., C. R. B. Lister, and B. T. R. Lewis, , Seismic structure of the Juan de Fuca ridge: ocean bottom seismometer results from the median valley: Jour. Geophys. Research, v. 81, p. 354-3555.

Ewing, J., and M. Ewing, 1961, A telemetering ocean bottom seismograph: Jour. Geophys. Research, v. 66, p. 3863-3878.

Hobart, M. A., G. B. Udintsev and A. K. Popova (in press), Heat flow measurements in the East Central Atlantic Ocean and near Atlantis Fracture Zone; in, Vinogradov, A. P., and G. Udintsev (eds.), Issledovaiya po Problema Riftozone Mirskogo Okeana, v. 3, Moscow: Nauk.

Houtz, R., and J. Ewing, 1976, Upper crustal structure as a function of plate age: Jour. Geophys. Research (in press).

Langseth, M. G., Jr., X. Le Pichon, and M. Ewing, 1966, Heat flow through the Atlantic Ocean floor and convection currents, Jour. Geophys. Research, v. 71, p. 5321-5355.

Langseth, M., (1965), Techniques of measuring heat flow through the ocean floor; in, Terrestrial Heat Flow, ed. Wm. H. K. Lee, Monograph 8, Amer. Geophys. Union, p. 58.

Lister, C. R. B. (1972), On the thermal balance of mid-ocean ridge; Geophys. J. R. Astr. Soc. 26, p. 515-535.

Ludwig, W. J., and P. D. Rabinowitz, 1975, Results of IPOD Site Surveys aboard R/V VEMA cruise 32-06; Part A. Data Report, Lamont-Doherty Geological Observatory, Tech. Rept. CU-1-75, 70pp.

Rabinowitz, P. D., and W. J. Ludwig, 1975, Results of IPOD site surveys aboard R/V VEMA cruise 3207: Part C. Candidate site 3, Lamont-Doherty Geological Observatory, Tech. Rept. CU-4-75, 20pp.

Sclater, J. G. and J. Francheteau (1970), The implications of terrestrial heat flow observations in current tectonic and geochemical models of the crust and upper mantle of the Earth; Geophys. J. R. Astr. Soc., 20, p. 509-542.

Von Herzen, R. P., G. Simmons and A. Folinsbee (1970) Heat flow between the Caribbean and Mid-Atlantic Ridge; J. Geophys. Res., 75, p. 1973-1974.

LAMONT-DOHERTY GEOLOGICAL OBSERVATORY

OF COLUMBIA UNIVERSITY

PALISADES, NEW YORK

Results of IPOD Site Surveys Aboard R/V VEMA Cruise 32-06

Part C: CANDIDATE SITE 8

William J. Ludwig and Philip D. Rabinowitz

Technical Report No. CU-6-75

International Phase of Ocean Drilling,

U.S. National Science Foundation,

Subcontract UC-NSF-C842-2

TABLE OF CONTENTS

Illustrations

* The original maps have been deposited with the IPOD Site Survey Management at L-DGO.

INTRODUCTION

IPOD candidate site 8, Vema fracture zone, offsets the mid-Atlantic ridge about 300 km at 11°N (Figure 1). Tentative plans for drilling include a shallow and a deep hole spaced about 10 and 30 km north of the fracture zone, a shallow and a deep hole in the axial trough of the fracture zone, and a shallow hole about 30 km south of the fracture zone.

During a two-week period of March, 1975, the Lamont-Doherty Geological Observatory conducted a geophysical survey of the site 8 region for the purpose of providing the JOIDES/IPOD Advisory Panel on the Ocean Crust with information to help them select the best possible sites for drilling and to facilitate the integration of the regional geological and geophysical framework with the results of the drilling. The survey was limited to the area bounded by 10° and 11°30'N and by 42° and 43°W (Figure 2). Continuously recorded bathymetric, seismic reflection, gravity and magnetic measurements were obtained along the ship's track (Figure 3). Seismic refraction profiles and on-station coring, heat flow, camera, and nephelometer measurements were obtained in select locations. The data collected are given in Part A of this technical report (Ludwig and Rabinowitz, 1975). In this part of the report, the data are presented in the form of maps and diagrams and are discussed in terms of the goals of IPOD drilling.

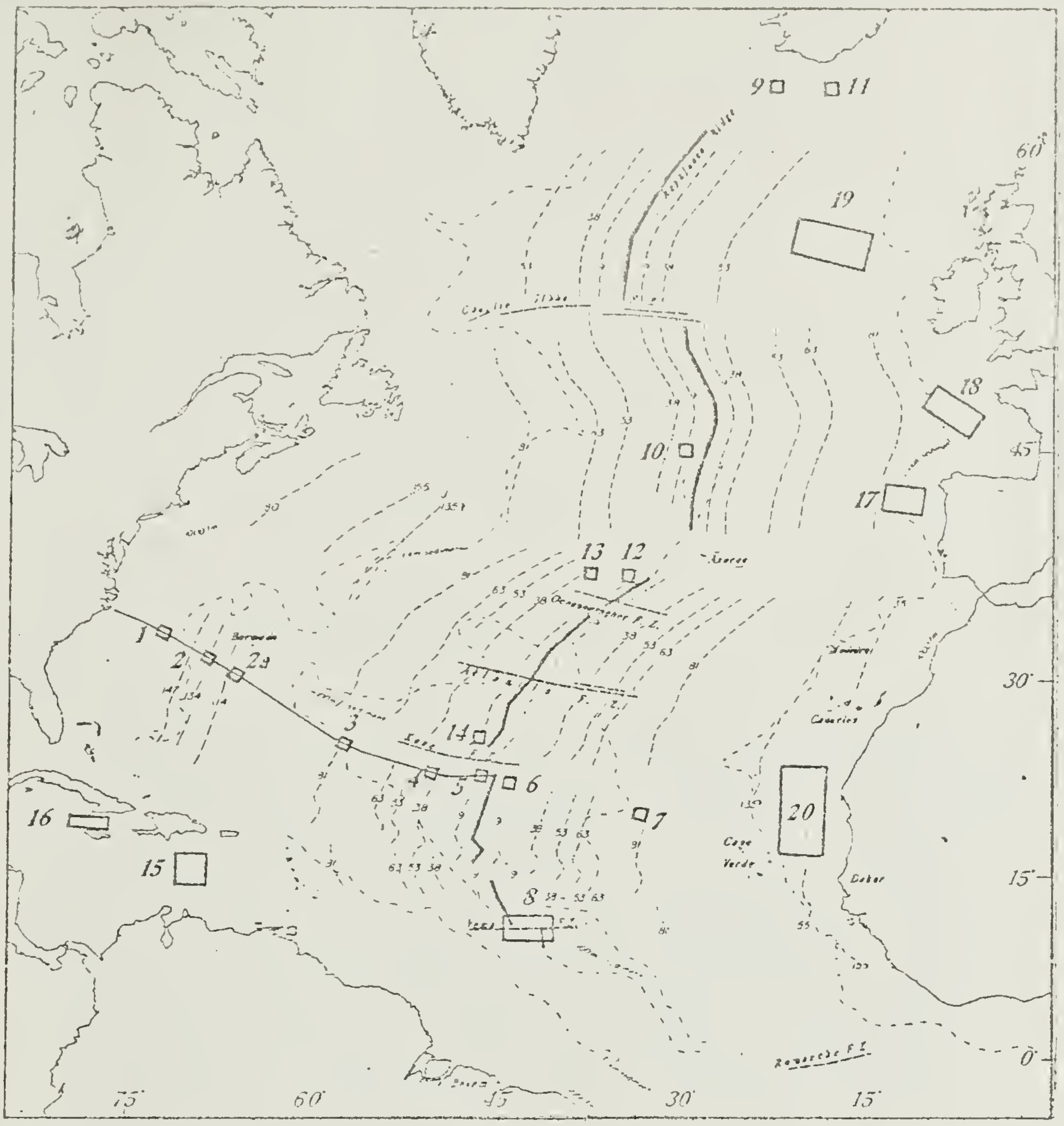

Fig. 1 IPOD candidate sites in the North Atlantic. Site 8, Vema fracture zone, was surveyed by R/V VEMA during March 1975.

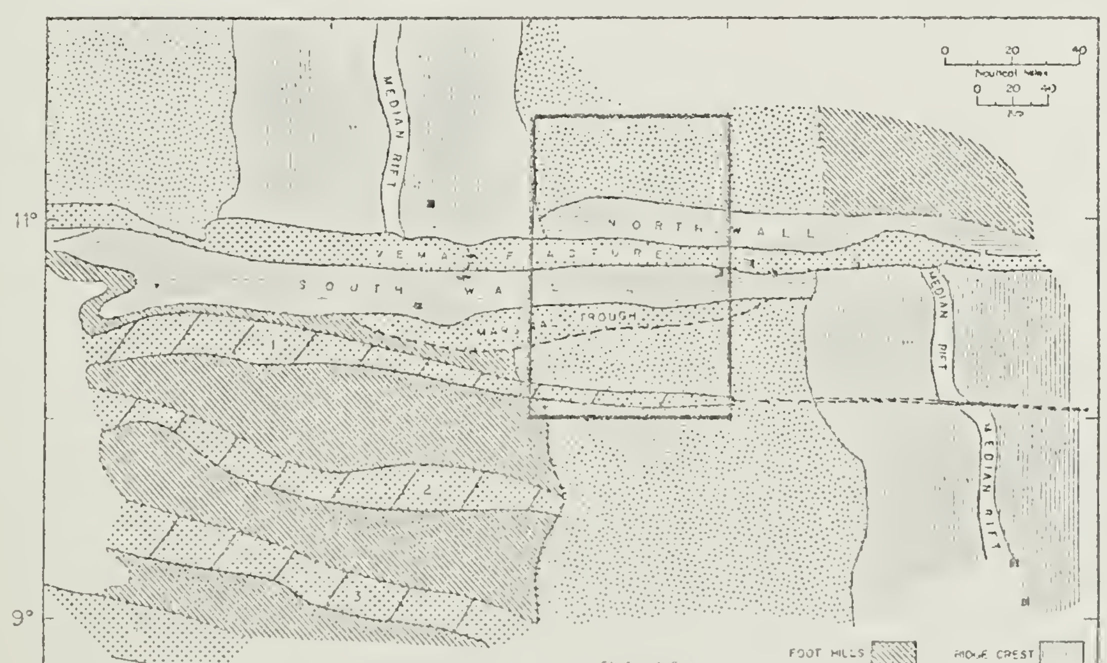

Fig. 2 Physiographic provinces of Vema fracture zone, from van Andel *et al.* (1971). Rectangular area is survey area.

Following Page

Fig. 3 Inset map of Figure 2. Ship's navigation. Date and time of day are indicated. Numbers 145-149 are ship stations. Heavy lines are seismic refraction profiles; circles and triangles denote the receiving position. SLF refers to Sonobuoy Low Frequency; R, to short-range airgun-sonobuoy profiles. The eight-arm star profile in the vicinity of station 146 was not successful. Circled numbers 1-4 mark the location of seismic reflection profiles shown in Figure 6.

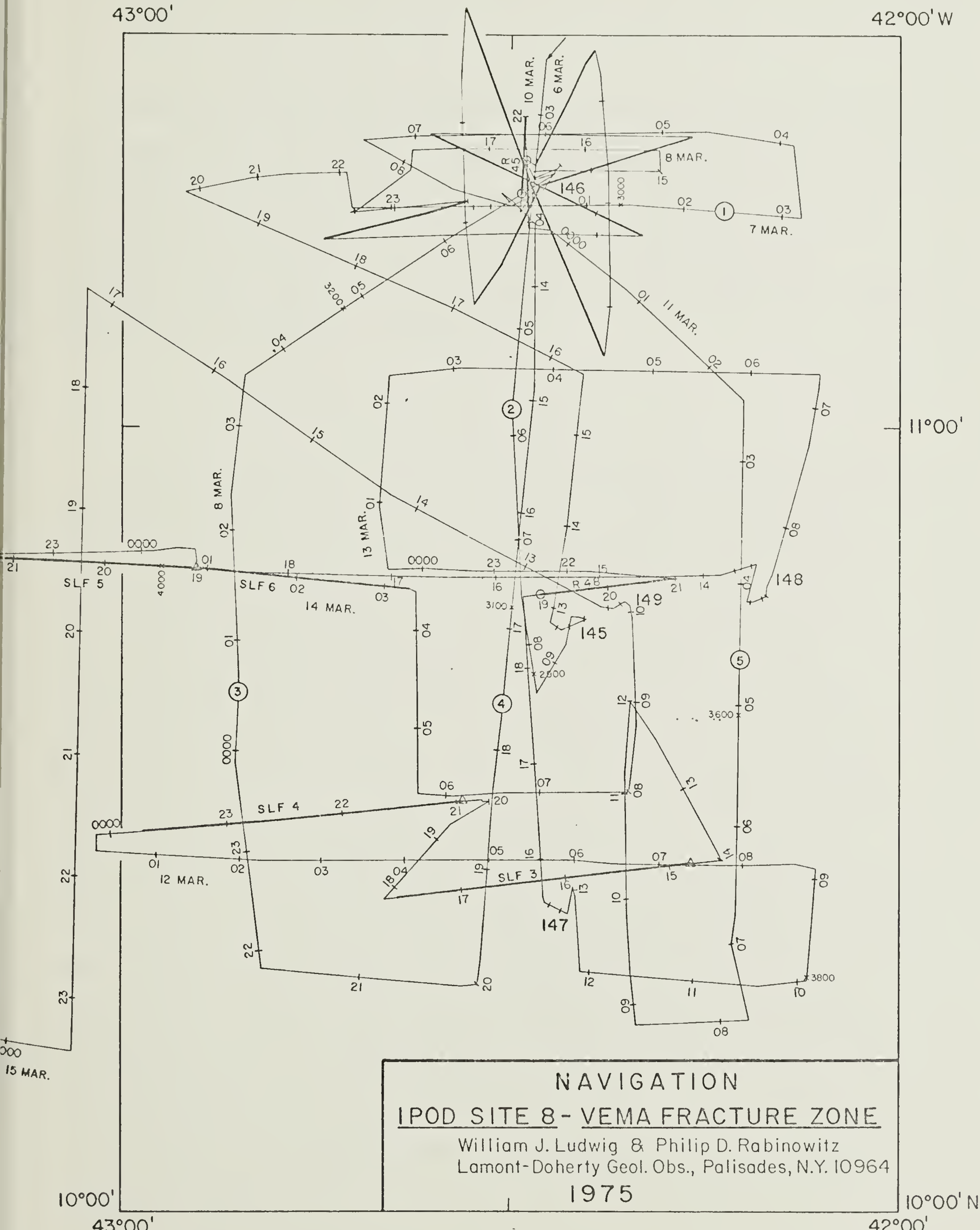
43°00'
42°00'W
11°00'
10°00'
10°00'N
43°00'
42°00'
NAVIGATION
IPOD SITE 8 - VEMA FRACTURE ZONE
William J. Ludwig & Philip D. Rabinowitz
Lamont-Doherty Geol. Obs., Palisades, N.Y. 10964
1975
6 MAR.
7 MAR.
8 MAR.
10 MAR.
11 MAR.
12 MAR.
13 MAR.
14 MAR.
15 MAR.
SLF 3
SLF 4
SLF 5
SLF 6
145
146
147
148
149

Fig. 3

Additional lines of geophysical data in the Vema fracture zone region were obtained on board R/V KURCHATOV (U.S.S.R.) and R/V GILLISS (U. of Miami). The combined results are expected to be portrayed in maps of the sediment distribution and bathymetry that will be made available through IPOD site survey management at L-DGO at a later date.

REGIONAL SETTING

The Vema fracture zone is very well known topographically and petrologically, through the studies of Heezen and Tharp (1961), Heezen *et al.* (1964), van Andel *et al.* (1967; 1969; 1971), Melson and Thompson (1971), and Bonatti *et al.* (1971; 1975). It is characterized by a deep seismically active trough between steep east-west trending ridges which offset left-laterally the crest of the mid-Atlantic ridge by 320 km. The axial trough has a thick sequence of flat-lying sediments found by deep-sea drilling at site 26 (10°54'N, 44°03'W) in 5169 m water depth to be mainly Pleistocene turbidites derived from the Amazon cone and transported across the Demerara abyssal plain (Bader *et al.*, 1970). An abrupt disturbance of these sediments, as seen in the seismic profiler records of Eittreim and Ewing (1975), is interpreted by them to be the trace of an active transform fault, representing relative plate motion over at least the past 500,000 yrs. Uniform high values of heat

flow are associated with the axial trough.

Other transverse features (relict fracture zones?) exist south of Vema fracture zone (Figure 2). Immediately south of the south wall, there is an elongate depression which consists of several en echelon sediment-filled troughs whose flat upper surfaces are tilted to the west. According to van Andel (1969), sediments filling the depressions were laid down in a nearly horizontal position by turbidity currents and were later tilted in response to uplift of the mid-Atlantic ridge crest.

Vema fracture zone and others are thought to be 'windows' into the lower oceanic crust. Rocks thought to be layer 3 material (gabbro, metagabbro, and serpentinized peridotite) have been dredged from the lower slopes of the north wall; basalt (layer 2?) was recovered from the upper slopes. The precipitous south wall (or ridge) is prevalently ultramafic rock that may represent diapirically emplaced upper mantle material (see Bonatti and Honnorez, 1976).

The main objectives of drilling in the axial trough of Vema fracture zone close to the northern and southern walls to obtain sections of the lower oceanic crust and upper mantle were not realized on leg 39 of DSDP. Drilling at site 353 (10°55'N, 44°02'W; 5165 m water depth) was terminated in basaltic cobbles (Scientific Staff, 1975).

SITE 8 DATA

The bathymetry[1] of the survey area is shown in Figure 4. The dominant features of the topography are the east-west trending trough and bordering ridges which make up the graben-shaped Vema fracture zone. Details of the bathymetry have been discussed by van Andel et al. (1971).

Parallelism of the bathymetry to the free-air gravity anomalies[1] is quite evident from the gravity map of Figure 5. The axial trough has the largest free-air gravity anomaly centered over it, with values about 130 mgal lower than those of the bordering ridges. Particularly noticeable are the low values of gravity anomalies associated with the ridges, indicating that they are nearly in isostatic equilibrium; otherwise, a positive free-air anomaly of over +250 mgal would have been observed.

Not all of the gravity anomaly can be accounted for by the topographic relief, implying that excess mass underlies the fracture zone or that densities in the crust and(or) upper mantle are not uniform. In order to account for the gravity anomalies, Robb and Kane (1975) introduced excess (high density) mass immediately under the lower slope of the south wall and a smaller body of excess mass at shallow depth under the north

---

[1] Data from all L-DGO ships' cruises in the area were included.

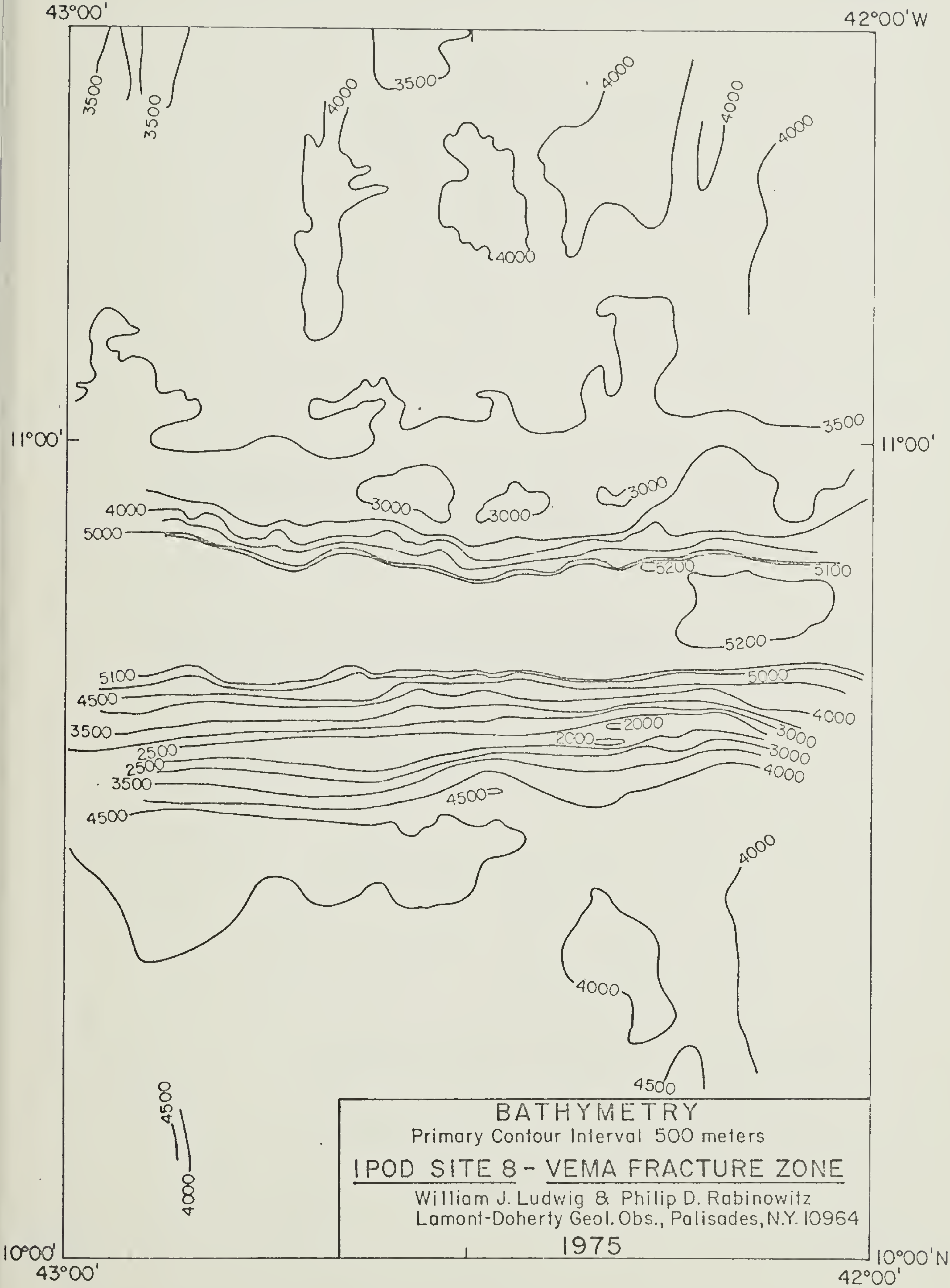

Fig. 4 Inset map of Figure 2: Bathymetric map. Primary contour interval 500 meters (corrected).

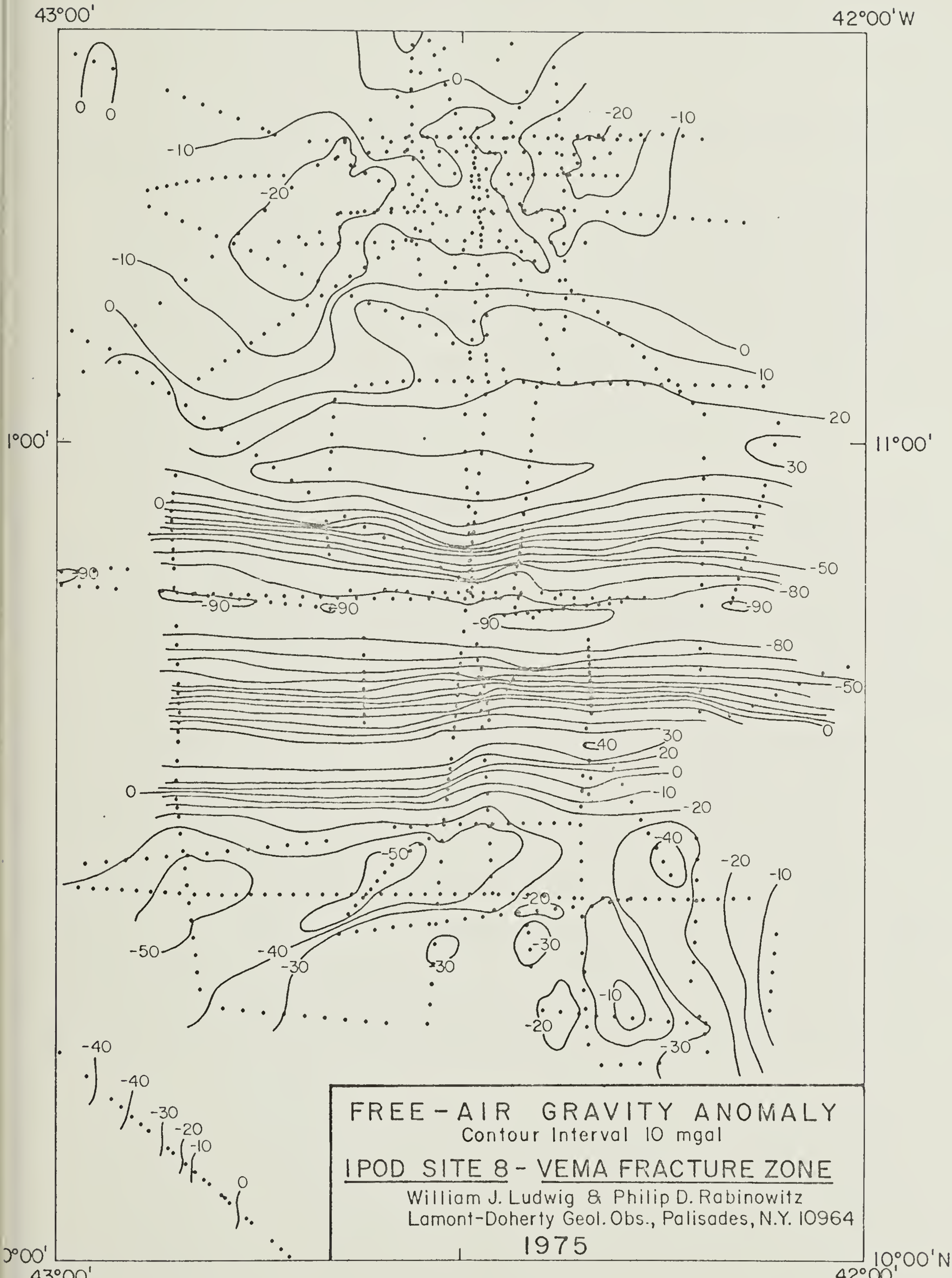

Fig. 5 Inset map of Figure 2: Free-air gravity map. Contour interval 10 mgal. Control for the map is indicated by dotted lines. Estimated error is less than 2 mgal.

wall. Their general scheme would seem to be supported by the exposures of ultrabasic rock.

Our east-west trending magnetic lines are not long enough to enable the characteristic shape and amplitude of the sea floor spreading magnetic anomalies to be determined. Long lines for magnetics were scheduled to be run by another IPOD survey vessel; unfortunately, equipment trouble prevented their acquisition.

Seismic reflection profiles of Vema fracture zone (Figure 6) illustrate its asymmetric cross-section and general pattern of sediment distribution. The axial trough is valley-shaped and is filled with sediment to slightly above the 5200 meter level. Reflection profile 5 revealed the sediment thickness in the valley to be 0.6 sec (or 1146 m, converted from the results of R-48; see Figure 7). Extrapolation of the side slopes in profiles where the valley floor was not detected suggests that the sediments may be, in places, up to 1500 m thick; i.e., the depth to basement in the center of the trough is 6200-6700 m below sea level. Obviously, the valley floor, both in longitudinal and transverse profile, consists of a

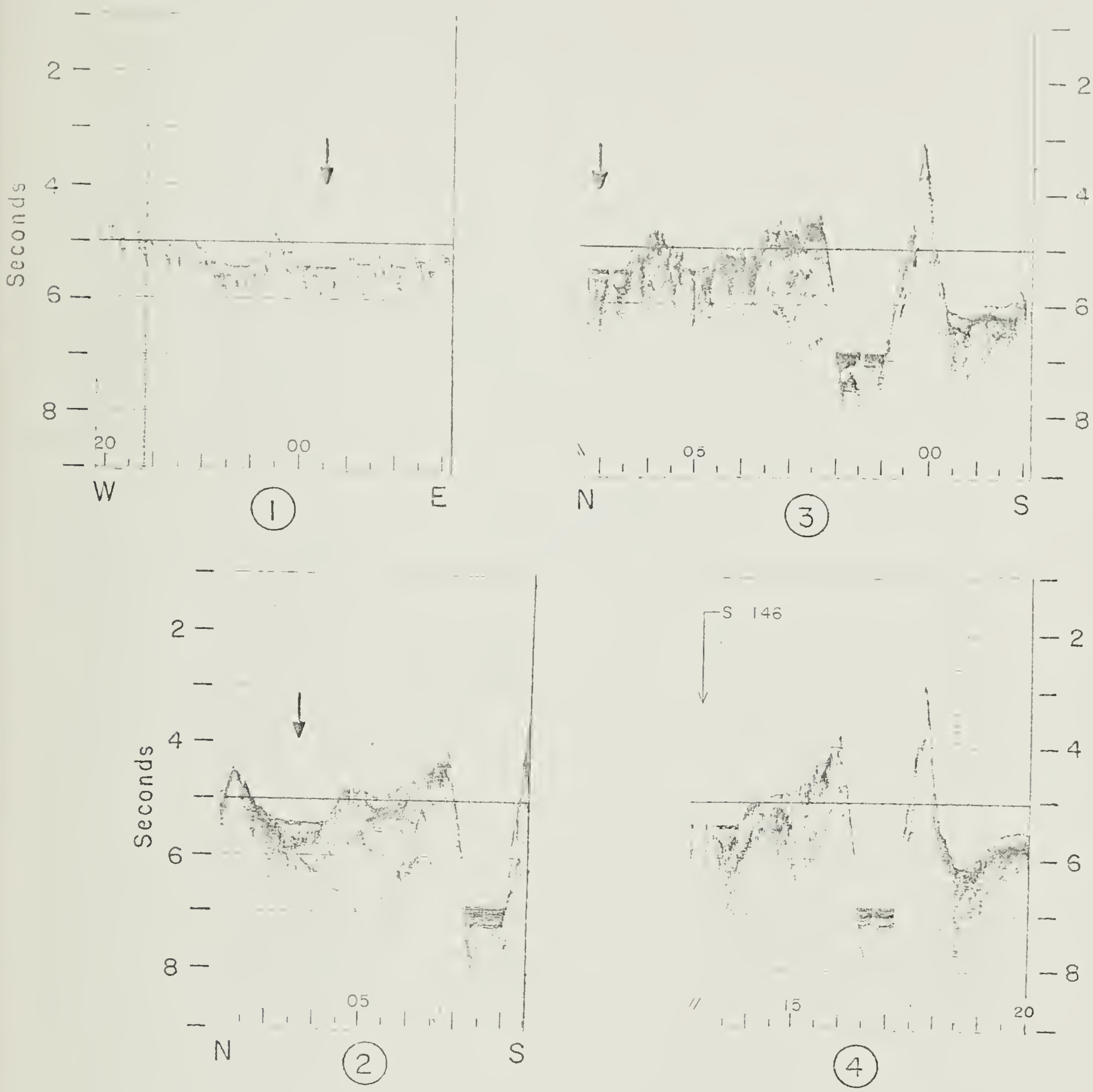

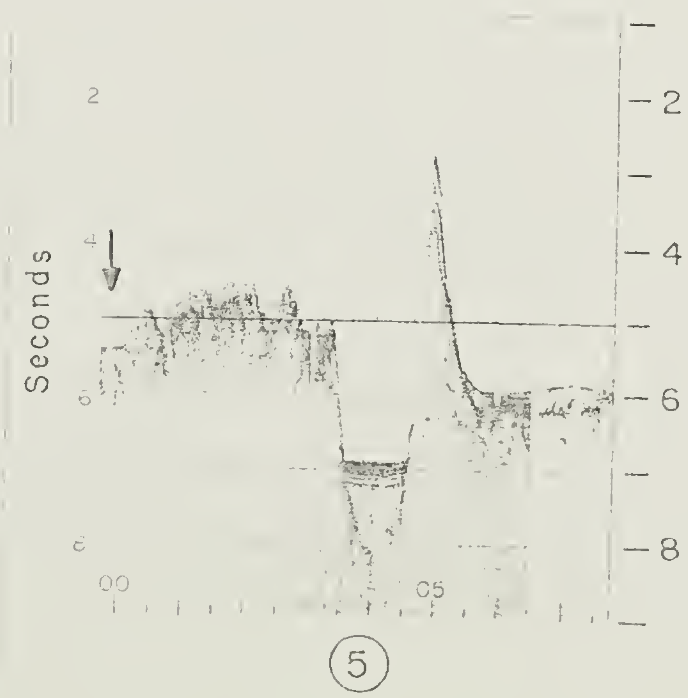

g. 6 Seismic reflection profiles. Local ship's time is given for keying to navigation map of Figure 3. Arrows designate the sediment pond at station 146 (sonobuoys R45 and 46); the optimum site for drilling 30 miles north of the fracture zone. The north ridge of the fracture zone has a positive magnetic anomaly greater than 200 gammas; the south ridge is partially non-magnetic.

number of hills and troughs (cf. van Andel et al., 1971).

North and south of the fracture zone the sediments are uniformly thin (generally not greater than 200 m) and are confined to depressions between topographic highs. There seems to be little or no draping of the sediments over the highs. Stations 146 and 147 occupied two sediment ponds; piston cores taken of the sediment are predominantly foraminiferal ooze.

The results of three airgun-sonobuoy profiles in the survey area are tabulated by Ludwig and Rabinowitz (1975) and are shown in the seismic structure section of Figure 7. Profiles 45 and 46 were recorded in opposite directions over the sediment pond near station 146 (see Figure 3); the results of profile 46 are open to question. Profile 48 was recorded in the axial trough of the fracture zone.

In profile 45, a line of refracted arrivals from a layer of apparent velocity 4.50 km/sec cuts the curve formed by variable-angle reflections from the base of the sediments, indicating that there is a layer of velocity intermediate between it and the top of the 4.5 km/sec layer. This value was assumed to be 3.5 km/sec (cf. Houtz and Ewing, 1976).

Sonobuoy profile 45 yielded an interval velocity of 5.75 km/sec from the top of acoustic basement down to a deep reflector that seems to be represented by 7.94 (?) km/sec arrivals,

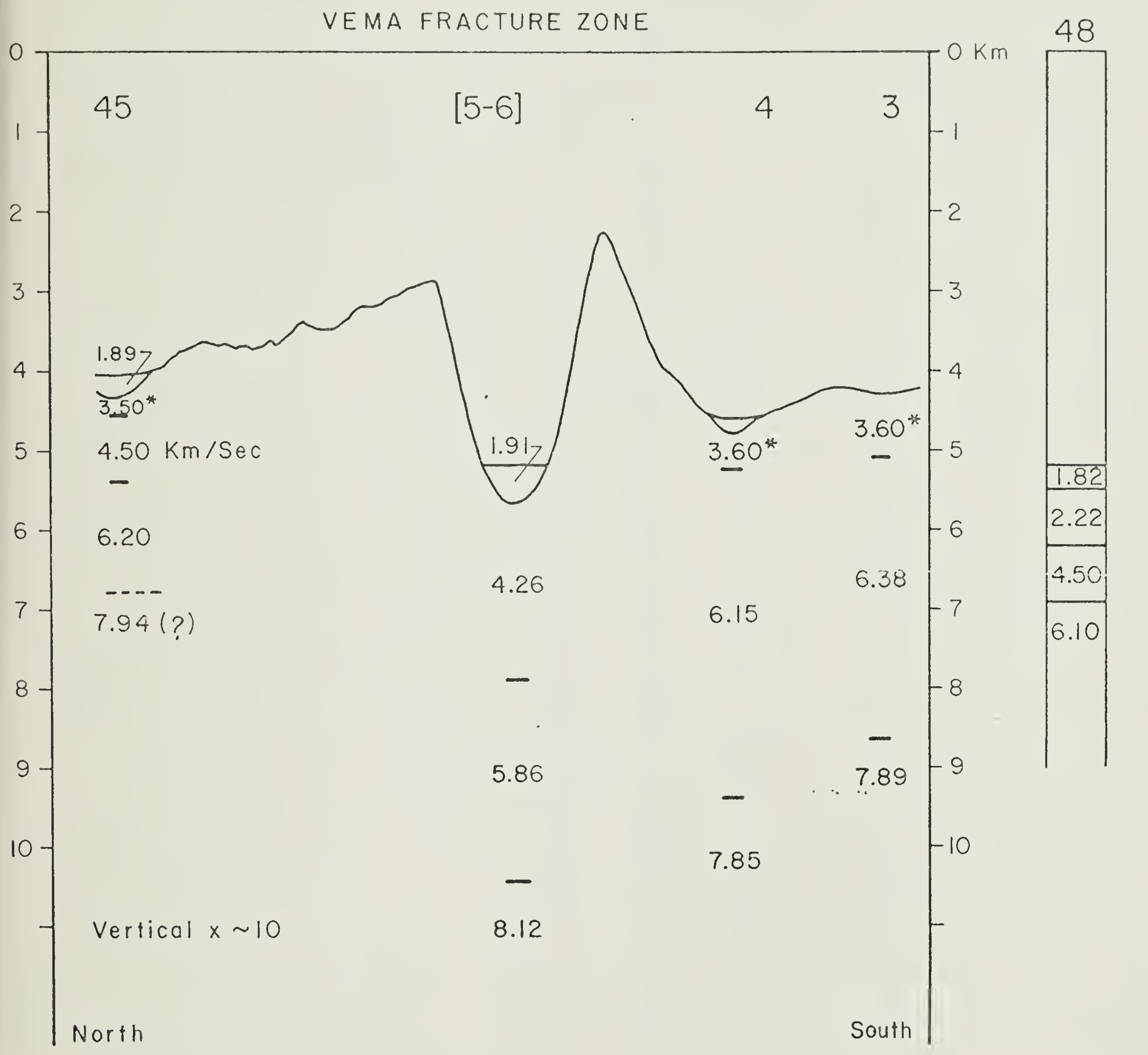

Fig. 7 Seismic structure of Vema fracture zone along 42°30'W. Explanation same as for Table 1. The results of airgun-sonobuoy profile 48 in the axial trough are included for comparison. Buoy 48 indicated that the mean velocity in the sediment is 1.91 km/sec.

[illegible] Thicknesses of layers, IPOD Candidate Site 8, VEMA Fracture Zone.

Profile	Velocity, km/sec				Thickness, km				Locations	
	b	c	d	e	Water	b	c	d	Lat. (N)	Long. (W)
3W		3.60*	6.38	7.89	4.30		0.80	3.55	10°23.9'	42°39.5'
E†									10°26.8'	42°14.7'
4W	1.80*	3.60*	6.15	7.85	4.57	0.20	0.49	4.12	10°29.0'	42°58.9'
E†									10°31.5'	42°32.6'
5W									10°50.3'	43°15.3'
E†									10°49.2'	42°54.2'
	1.91	4.26	5.86	8.12	5.18	0.51	2.20	2.56		
6W†									10°49.2'	42°54.2'
E									10°47.7'	42°37.8'

Notes:

Asterisks denote assumed velocity

Profiles 3 and 4 are unreversed profiles. They were computed by assuming that the layers are horizontal.

Profiles 5 and 6 are end-to-end unreversed profiles and were computed by using the average velocity of the apparent velocities observed in each direction as the true velocity and assuming horizontal layers.

The velocity 1.91 km/sec of profiles 5 and 6 is the computed mean velocity in the sediments from airgun-sonobuoy 48 recorded nearby.

Daggers indicate the location that the sonobuoy was launched; i.e., the receiving position of the profile.

Water thickness refers to the depth to the base line used for topographic corrections.

SLF refers to sonobuoy, low frequency.

which break from the 6.20 km/sec refraction line near the end of the profile. The refraction results (Σh=2.49 km, $\bar{V}$=5.24 km/sec, T=.48 sec) and the X^2-T^2 results (h=2.86 km, V=5.75 km/sec, T=.50) yield nearly the same one-way travel times (T), indicating that the deep reflector is real. Unfortunately, the velocity in the reflecting layers cannot determine accurately because of lack of information on dip and because associated refractions were recorded only over a short distance.

In Figures 8, 9, and 10 it can be seen that where no refracted arrivals are recorded from the sediments and(or) acoustic basement, a velocity must be assumed to compute the thickness of the layer. In profiles 3 and 4, the velocity in the basement is assumed to be 3.6 km/sec.

Houtz and Ewing (1976) examined sonobuoy data from the Atlantic Ocean and showed that seismic layer 2 may be a two- or three-component layer, depending on age of the sea floor with distance from a center of sea floor spreading. Near the crest of the mid-Atlantic ridge, layer 2 is a three-component layer with velocities 3.3 km/sec (2A), 5.2 km/sec (2B), and 6.1 km/sec (2C). The velocity of layer 2A increases from 3.3 km/sec to that of layer 2B on crust about 40 m.y. or older (cf. Christensen and Salisbury, 1972; 1973) while the thickness of layer 2A decreases from about 1.5 km at the ridge crest to about 100 m as the crust ages to about 40 m.y. According

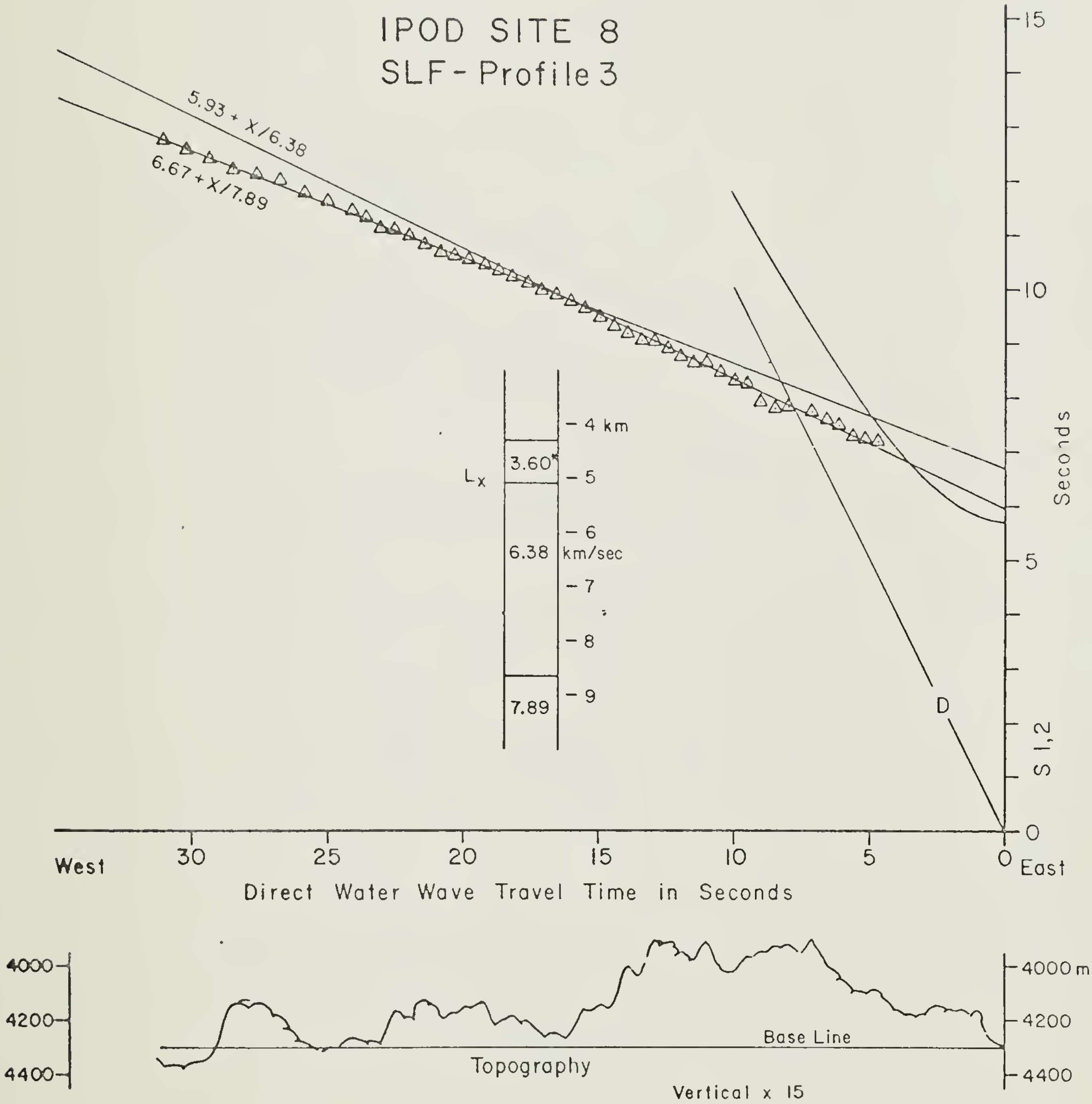
IPOD SITE 8
SLF-Profile 3
5.93 + X/6.38
6.67 + X/7.89
4 km
3.60*
Lx
5
6
6.38
km/sec
7
8
7.89
9
D
Seconds
S 1,2
15
10
5
0
West
30
25
20
15
10
5
0
East
Direct Water Wave Travel Time in Seconds
4000
4200
4400
4000 m
4200
4400
Base Line
Topography
Vertical x 15

Fig. 8

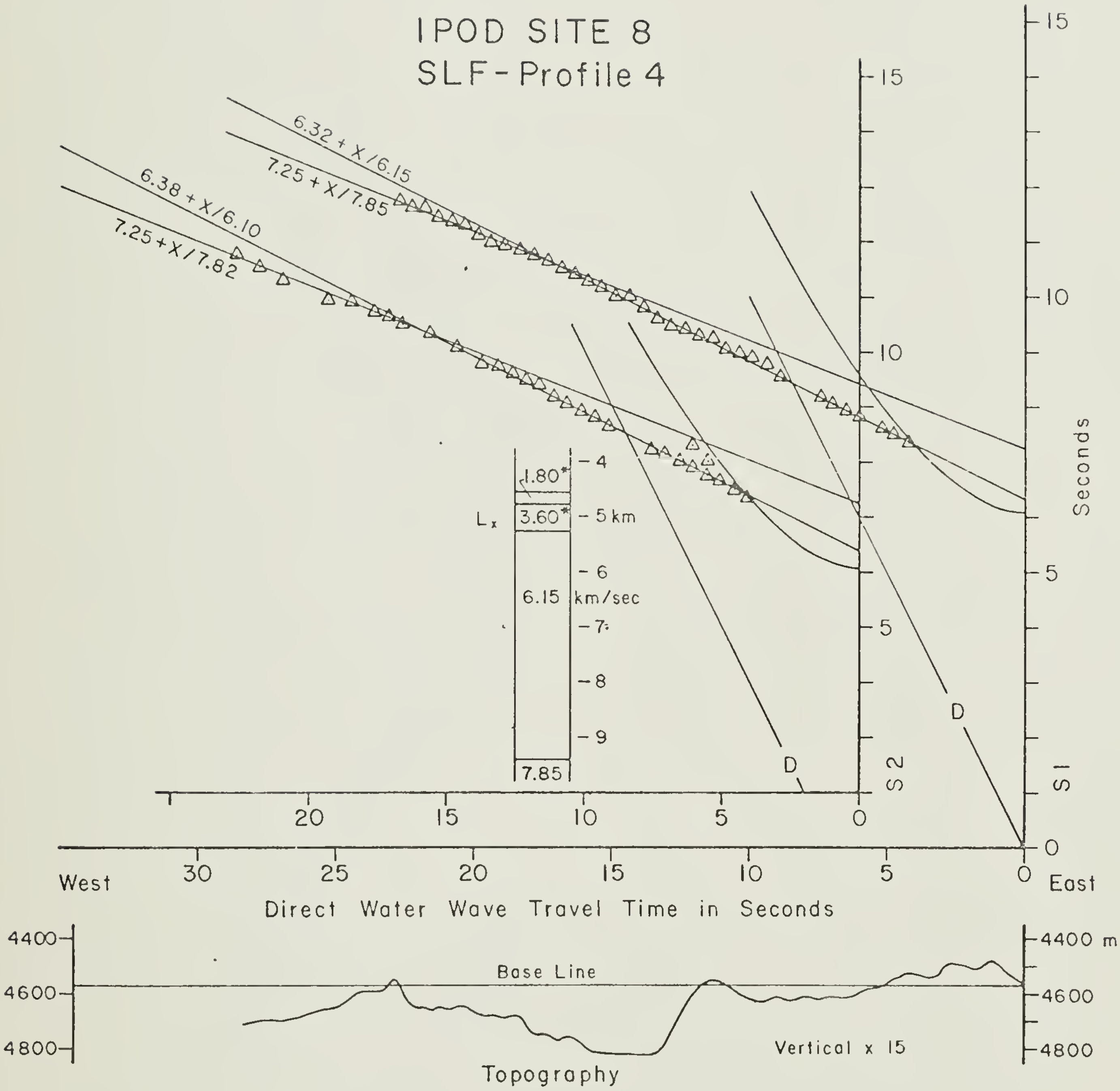
IPOD SITE 8
SLF-Profile 4
6.32 + X/6.15
7.25 + X/7.85
6.38 + X/6.10
7.25 + X/7.82
1.80*
Lx
3.60*
6.15
7.85
4
5 km
6
km/sec
7
8
9
D
D
S 2
S 1
Seconds
West
East
Direct Water Wave Travel Time in Seconds
4400
4600
4800
4400 m
Base Line
Vertical x 15
Topography

Fig. 9

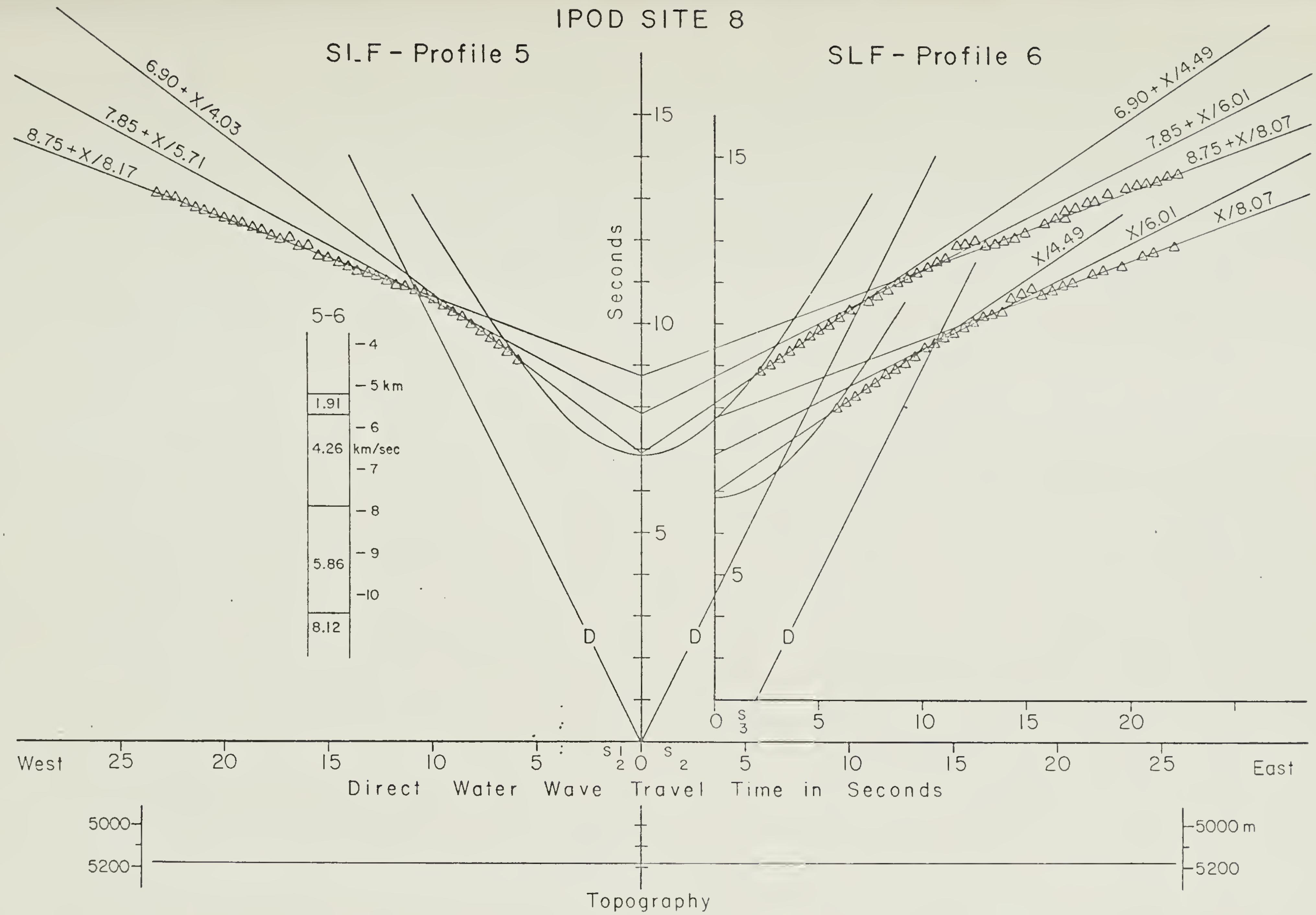
IPOD SITE 8
SI.F - Profile 5
SLF - Profile 6
6.90 + X/4.03
7.85 + X/5.71
8.75 + X/8.17
6.90 + X/4.49
7.85 + X/6.01
8.75 + X/8.07
X/4.49
X/6.01
X/8.07
Seconds
5-6
1.91
4.26
5.86
8.12
km/sec
5 km
D
West
East
Direct Water Wave Travel Time in Seconds
5000
5200
5000 m
Topography

Fig. 10

to Houtz and Ewing, there is no corresponding distal increase of velocity with age in layers 2B and 2C.

The age of the sea floor in the survey area has not been determined but may be estimated to be about 13 m.y. from the crustal age vs. sea floor depth curve of Sclater <u>et al.</u> (1971) and magnetic anomaly profiles of van Andel <u>et al.</u> (1971). Hence, the velocity in the basement (layer 2A) should be slightly higher than 3.3 km/sec, or about 3.6 km/sec, if layer 2A is a ubiquitous layer in crust less than 40 m.y. old, as is maintained by Houtz and Ewing.

A typical three-component layer 2 structure may be indicated by sonobuoy profile 45 north of the fracture zone, whereas, in the axial trough and area to the south, the velocities and thicknesses of the layers measured do not fit a simple three- or four-layer model of the earth's structure. There, our long-range sonobuoy profiles have established the presence of a 3-4 km thick crustal layer of velocity between 5.7 and 6.3 km/sec over a layer with normal mantle velocity (Figure 7; Table 1). The mean velocity may be attributed to layer 2C, but the thickness of the layer is more representative of that of layer 3 (velocity 6.7 km/sec). Of course, it must be remembered that profiles 3 and 4 were shot unreversed in a westerly direction, away from the central zone of the ridge. If the refractor dips down from the crestal zone, then the

apparent velocities measured are on the low side of the actual true velocity; i.e., a 6.7 km/sec layer dipping down at about 4° would give an apparent velocity of 6.2 km/sec.

Aumento et al. (1971) measured layer 2A and 2B velocities over a 7.5 km/sec refractor beneath the median valley of the mid-Atlantic ridge at 45°N. Nearby, in the crestal zone, Keen and Tramontini (1970) recorded layer 2B and layer 3 velocities. Poehls (1974) similarly measured layer 2A and 2B velocities in the median valley of the ridge at 37°N, but over a 6.3 km/sec refractor. His nearby western ridge flank profile revealed layer 2A and 2B over a 6.7 km/sec layer 3. Whitmarsh (1973) also recorded a 6.3 km/sec layer beneath the median valley at 37°N, but did not detect layer 2A or 2B. Elsewhere, Tramontini and Davis (1969) measured a 6.4 km/sec layer beneath the axial trough of the Red Sea; Talwani et al. (1971) measured velocities of less than 4.7 km/sec and of approximately 7.4 km/sec in the crestal zone of the Reykjanes ridge.

The above citations and the present work illustrate the amount of scatter in the velocities measured in and near the crestal zone of the mid-ocean ridge system. We believe that this attests to complexities in the structure and petrologic makeup of the rocks (see Christensen and Salisbury, 1972, 1973; Fox et al., 1973).

The velocities measured for serpentinized peridotite (density 2.4 gm/cm^3) range between 3.55 and 3.95 km/sec at 0.5 kb confining pressure (Fox et al., 1973); hence, exposure of both basalt and peridotite on the walls of the axial trough is in agreement with the velocities measured by (and inferred from) the seismic refraction technique. The requirement for excess mass (high velocity, high density) material at shallow depth beneath the fracture zone to balance the gravity data of Robb and Kane (1975) may be eliminated by assigning local increases in mantle density beneath the fracture zone.

Three measurements of the geothermal gradient were measured in the axial trough of Vema fracture zone, and three measurements were made on the ridge flanks to the north and south of the fracture zone (Table 2). These heat flow stations were all taken in areas having locally thick sediments. The measurements in the axial trough confirm the previously reported values of high heat flow there (Table 3). Heat flow values in the trough range from about 2 to 6 HFU; the mean value is 3.50 HFU. The two highest values of heat flow are 6.0 and 6.2 HFU, obtained near the walls of the fracture, which may be high due to topographic disturbances.

TABLE 2. R/V VEMA Cruise 32 Heat Flow Values at IPOD Site #8

Latitude (N)	Longitude (W)	Depth (corr m)	P (cm)	N	Gradient (°C/10m)	Conductivity	Heat Flow (HFU)	Evaluat.	Station
10°44.5'	42°26.0'	5206	450	2	1.26	2.45A	3.09	4	4
11°17.5'	42°30.3'	4091	275	3	N. L.	-	-	5	5
10°22.9'	42°25.5'	4231	573	5	0.208	2.30A	0.48	5	6
10°46.7'	42°11.2'	5212	548	5	1.14	2.45A	2.79	6	7
10°46.4'	42°21.5'	5188	423	4	1.50	2.45A	3.68	8	8
10°27.1'	44°40.2'	4954	578	5	N. L.	-	-	5	9

P = penetration into sediment
N = number of probes in mud

N. L. = Non linear
A = Assumed conductivity

TABLE 3. Other Heat Flow Values Near Site #8

	Latitude (N)	Longitude (W)	Depth (corr m)	P (cm)	N	Gradient (°C/10m)	Conductivity (mcal/°Csec cm)	Heat Flow (HFU)	Evaluation	Station
VEMA 15[1]										
	10°48'	43°12'	5002	-	-	1.51	2.45A	3.70	8	8
CONRAD 8[2]										
	10°48'	43°12'	5178	572	3	1.27	2.11	2.68	6	3
CONRAD 17*										
	10°43.3'	41°34.7'	5204	640	3	1.03	2.63	2.72	10	12
	10°47.1'	41°16.4'	5175	575	2	1.50	2.55	3.82	7	13
	10°49.1'	41°37.7'	5206	338	2	1.32	2.70	3.57	6	14
	10°47.6'	42°34.3'	5193	283	2	1.66	2.52	4.18	6	15
	10°49.1'	42°34.1'	5185	401	2	2.28	2.72	6.20	7	16
	10°43.2'	42°39.8'	5165	337	3	2.43	2.47	6.00	8	17
	10°49.2'	43°57.5'	5116	640	4	1.35	2.26	3.05	10	18
	10°51.8'	44°34.8'	5163	945	5	0.69	2.28	1.58	10	19
	10°51.4'	43°56.6'	5171	1001	4	1.23	2.39	2.94	10	20
	10°50.5'	43°38.5'	5189	625	4	1.27	2.41	3.06	9	21
	10°55.8'	44° 3.3'	5161	896	4	1.66	2.44	4.05	9	22
	10°55.7'	43°40.5'	5318	Core Fell Over			Lava Flow			23
	10°52.2'	43°40.4'	5380	484	3	1.22	2.26	2.76	8	24
	10°49.9'	42°38.8'	5195	-	-	-	-	-	-	25
	10°47.5'	41°15.6'	5122	610	4	1.70	2.35	4.00	10	26
	10°44.8'	41°35.0'	5204	430	4	0.82	2.56	2.86	7	27

TABLE 3 (Continued)

	Latitude (N)	Longitude (W)	Depth (corr m)	P (cm)	N	Gradient (°C/10m)	Conductivity (mcal/°Csec cm)	Heat Flow (HFU)	Evaluation	Station
ATLANTIS II 31[3]										
	10°50'	44°10'	5155	600	3	1.30	2.21	2.88	-	VFZ 4
	10°22'	44°18'	4950	300	2	0.38	2.45	0.93	-	5
	10°48'	42°56'	5180	300	3	1.23	2.53	3.00	-	8
	10°21'	41°19'	3180	600	3	0.30/0.60NL	2.4	-	-	12
	11°21'	41°52'	4205	600	3	0.09/0.50NL	2.31	-	-	13
	11°32'	42°43'	3735	600	4	0.52	2.55	1.32	-	14
	10°55'	44°08'	5165	200	3	1.30	2.27	2.95	-	SP 2
	10°51'	44°08'	5160	200	3	1.43	2.24A	3.22	-	3
	11°05'	42°50'	3700	200	3	0.21	2.40A	0.53	-	5
	10°22'	42°51'	4450	200	3	2.27	2.23A	5.06	-	6
	10°00'	40°34'	3620	200	3	1.68	2.57A	4.31	-	7
	11°06'	41°17'	3840	200	3	0.43	2.40A	1.03	-	8
	11°21'	42°02'	3825	200	3	1.00	2.30A	2.30	-	9
LSDA[4]										
	11°35'	44°03'	2755	-	-	-	2.28A	2.4	-	130

P = penetration into sediment; N = number of probes in mud: NL = non-linear; A = assumed conductivity.
* unpublished Lamont-Doherty Geological Observatory data.
1 Gerard et al., 1962.
2 Langseth et al., 1966.
3 Von Herzen et al., 1970
4 Vacquier and Von Herzen, 1964.

Heat flow station 5 is in the small sediment pond about 3 miles north of the fracture zone (ship station 146). The temperature profile measured there shows a reversal in temperature gradient at about 2 meters (see Figure 11).

Heat flow station 6 (at ship station 147) was taken in relatively rough terrain with uneven sedimentary cover. The temperature record is not of good quality but the low gradient observed in the upper 6 m is well established.

Heat flow station 9 was taken just before leaving the Vema fracture zone region. It is in a broad thickly sedimented trough running parallel to the main axial trough, approximately 30 miles south of it. The station is located very near some steeply dipping basement features which do not return reflections and appear as acoustically transparent portions of the profiler record. Temperature measurements at this station also show a reversal in gradient in the upper 2-3 m of sediment. The profile is similar to that obtained at station 5 (see Figure 11). One explanation for such a reversal of gradient is that these sites contained a layer of warm bottom water for a period of a few months prior to these measurements. In Figure 11 we show how such a gradient could evolve.

The measurements north and south of the fracture zone at stations 5, 6 and 9 appear to be disturbed by near-surface effects, such as transient variations in bottom water tempera-

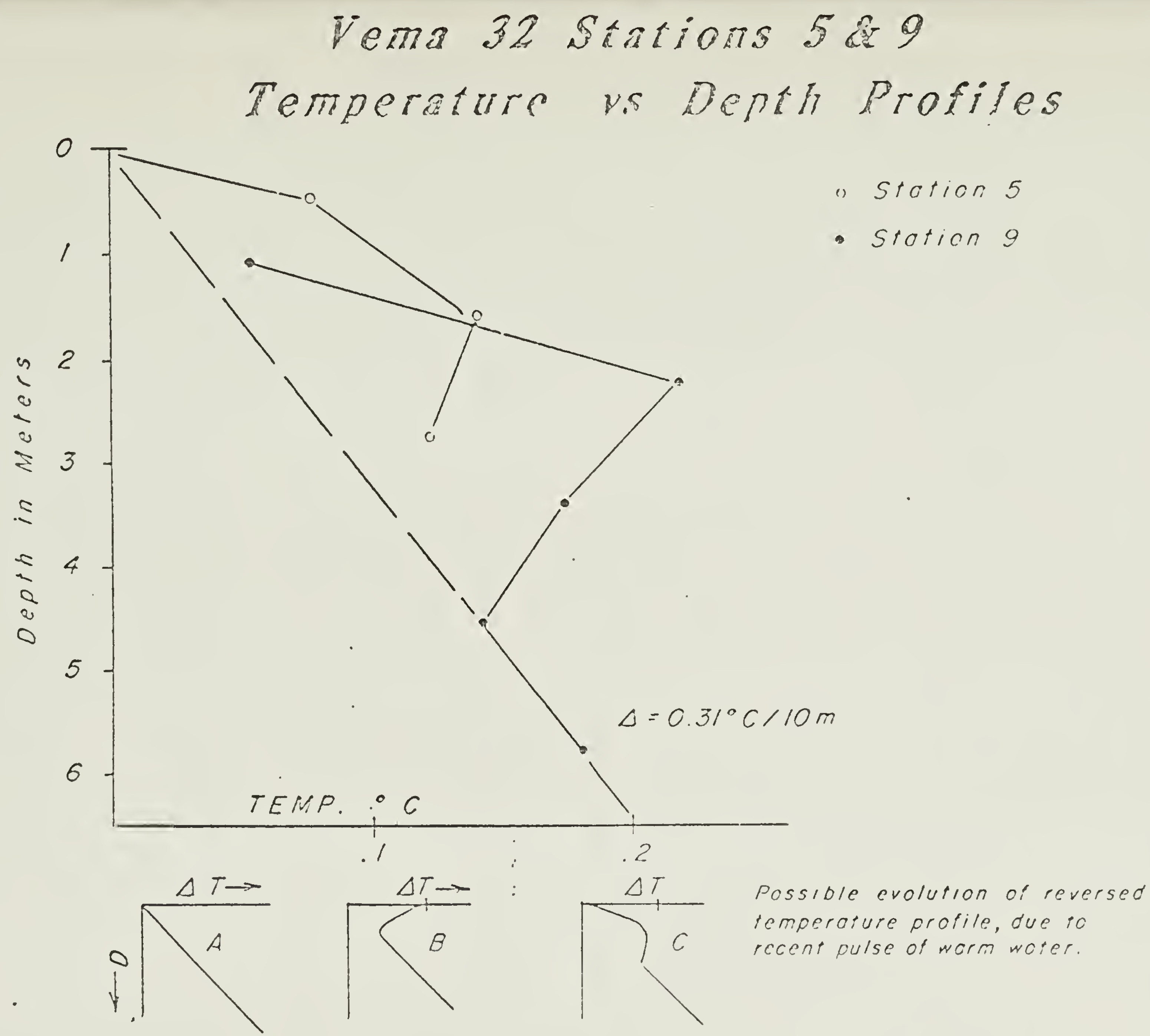

Vema 32 Stations 5 & 9
Temperature vs Depth Profiles
Station 5
Station 9
Depth in Meters
0
1
2
3
4
5
6
TEMP. °C
.1
.2
Δ = 0.31°C/10m
ΔT→
ΔT→
ΔT
D→
A
B
C
Possible evolution of reversed temperature profile, due to recent pulse of warm water.

Fig. 11

ture, or refraction of heat flow in the uppermost crust; consequently, they are not thought to be representative of the true heat flow (at the locations where they were made).

RECOMMENDATIONS FOR DRILLING

The velocity structure beneath a ridge crest and along a fracture zone which offsets it cannot be reconciled with the velocity structure in a typical ocean basin. Furthermore, from comparisons of our refraction results with measurements of seismic velocities of oceanic rocks in the laboratory, it is not possible to infer the composition of the crustal layers. Undoubtedly much more refraction work is needed, followed by deep-sea drilling. It seems probable that Vema fracture zone (and others) is the site of narrow dike-like intrusions of upper mantle materials, manifested by exposures of layer 2 basalts and ultrabasic rocks along lower sections of the north and south walls (Bonatti and Honnorez, 1976).

On the basis of the available data, three sites are recommended for drilling:

1. A re-entry hole in the trough immediately south of the south ridge in 4570 m of water (profile 4 vicinity) where the thicknesses of the sediments and basement layer (200 m and 500 m, respectively) are such to allow penetration of the basement layer(s) and deep drilling into the 6.2 km/sec crustal layer below.

2. A single bit hole in the axial trough of the fracture zone to sample the basement rocks. However, a modest amount of additional site surveying may be needed to locate the site. The site should be located in the center of the trough to avoid talus slumps, but over a basement high to minimize the section of turbidites to be drilled. Sonobuoy 48 measured 1000 m of sediment over a 4.5 basement layer in 5160 m of water. Nearby, the section, as measured by sonobuoys 5 and 6, consists of about 500 m of sediment over a 4.3 km basement layer.

3. A re-entry hole in normal (?) oceanic crust north of the fracture zone in 4050 m of water (within the sediment pond occupied by station 146 and sonobuoy profile 45). Here, the sediments are about 250 m thick and cover a basement layer (2A) with (assumed) velocity of 3.50 km/sec and a thickness of about 250 m. The next deeper layer (2B) has a velocity near 4.5 km/sec and a thickness of about 850 m. Below this is the main crustal layer (2C or 3) of velocity 6.2 km/sec.

ACKNOWLEDGMENTS

This study was supported by the IPOD Site Survey Management, under subcontract with the Deep Sea Drilling Project (UC-NSF-C842-2).

We thank the officers, crew, and scientific staff of R/V VEMA 32-06 for their assistance in gathering the data. The section on heat flow measurements was taken in part from a report "Geothermal Measurements at Sites 7 and 8," by L. Ongley and M. Langseth.

APPENDIX

Seismic Refraction Measurements

For the survey work in Vema fracture zone VEMA was equipped with three ocean-bottom seismographs, furnished by L-DGO through IPOD Site Survey Management. The OBS employed is a 3-component (vertical and horizontal seismometers and hydrophone) self-recording pop-up system that is contained in a buoyant sphere with a time-release mechanism (Carmichael et al., 1973). Explosives used as the sound source consisted of tetrytol and a two-component explosive purchased from EXCOA, called SAF-T-PAK. One component of the explosive is a 5-lb package of pellets in a plastic bag (cartridge) sealed at each end with a metal clip; the other is a bottle of activator fluid. The cartridges were packed five to a cardboard carton in vermiculite packing material for shipment by air cargo to VEMA at Dakar.

Our experiment with the OBS called for shooting an 8-arm star-shaped pattern of shots to three OBS in a triangular array positioned in the sediment pond north of the fracture zone (Figure 3). The instruments were spaced three miles apart. A fourth OBS, tethered to a radar-reflecting buoy at the sea surface, was positioned in the center of the L-DGO array by scientists aboard R/V KURCHATOV.

Aboard VEMA, we shot 5 to 15 lb charges of the SAF-T-PAK every 2-5 minutes over a 24-hour period. Here, and at Site 7, the clips used to seal the cartridges did not provide a watertight seal. After activation, we had to seal both ends by twisting and tie-wrapping the plastic closed. In reclosing, we could not always let out the same amount of air; hence, the sinking rates varied considerably. Most important, initiation of the SAF-T-PAK with a No. 9 engineer's special blasting cap was not reliable. We experienced considerable DUDS, unless a 1/2 lb TNT block was used as a booster (and to effect a more uniform sinking rate). We also had far too many partial explosions of the SAF-T-PAK charge.

Upon completion of the experiment, one L-DGO OBS failed to surface, another experienced a shorted power supply, and the third gave seismograms with poor signal-to-noise characteristics (due in part to partial explosions and instrument noise). The Soviet OBS worked satisfactorily; preliminary analysis of the data gives a 2.5 km thick basement layer of velocity 5.0 km/sec resting on a crustal layer with a velocity of 6.6 km/sec measured parallel to the crestal zone of the ridge and a velocity of 6.2 km/sec measured transverse to it (Y. Neprochnov, personal communication). A layer of velocity 3.5 km/sec was not observed.

Analysis of the Soviet OBS data is expected to be completed

in late 1976. It may be possible to salvage some data from the L-DGO instrument by post-filtering techniques, but the prognosis is not good.

VEMA was also equipped with low-frequency sonobuoys for long-range refraction work. Data from the buoys (Select International SLF73-5) were recorded wiggly-line on a Dresser SIE 12-channel amplifier-oscillograph recording system and were analyzed and interpreted in conventional manners. Explosives charges of tetrytol, ranging from 3 to 24 lbs, were used as the sound source.

There are no ambiguities in the SLF data. All the arrivals plotted on the travel-time graphs of Figures 8-10 are from strong events. For each profile, two sonobuoys telemetering at different frequencies were launched, either very close together (Profiles 3 and 5) or 2-5 miles apart (Profiles 4 and 6). In the latter instance, seismic signals originating from one shot point were received at two detector locations.

Profiles 3 and 4 are not reversed and were computed on the assumption of horizontal layers. Profiles 5 and 6 are split profiles; i.e., they were recorded unreversed in opposite directions from a central receiving point. The average of the apparent velocities measured in each direction is a close approximation of the true velocity if the dip of the layers remains uniform over the combined length of the profiles.

Obviously, there is dip in the layers observed and the assumption of horizontal layers used in the calculation of layer thickness results only in an approximation.

REFERENCES

Aumento, F., B.D. Loncarevic, and D.I. Ross, Hudston Geotraverse: geology of the mid-Atlantic ridge at 45°N, _Phil. Trans. Roy. Soc. A_, _268_, 623-650, 1971.

Bader, R.G., and others, _Initial Reports of the Deep Sea Drilling Project_, vol. 4, U.S. Gov't. Printing Office, Washington, 1970.

Bonatti, E., J. Honnorez, and G. Ferrara, I. Ultramafic rocks: Peridotite-gabbro-basalt complex from the equatorial mid-Atlantic ridge, _Phil. Trans. Roy. Soc._, _A_, _268_, 385-402, 1971.

Bonatti, E., J. Honnorez, and I. Innocenti, Basalts from the Vema fracture zone, _Earth Planet. Sci. Lttrs._, in press, 1975.

Carmichael, D., G. Carpenter, A. Hubbard, K. McCamy, and W. McDonald, A recording ocean bottom seismograph, _J. Geophys. Res._, _78_(35), 8748-8750, 1973.

Christensen, N.I., and M.H. Salisbury, Sea floor spreading, progressive alteration of layer 2 basalts, and associated changes in seismic velocities, _Earth Planet. Sci. Lttrs._, _15_, 367-375, 1972.

Christensen, N.I., and M.H. Salisbury, Velocities, elastic moduli and weathering-age relations for Pacific layer 2, _Earth Planet. Sci. Lttrs._, _19_, 461-470, 1973.

Eittreim, S., and J. Ewing, Vema fracture zone transform fault, Geology, 3(10), 555-559, 1975.

Fox, P.J., E. Schreiber, and J.J. Peterson, The geology of the oceanic crust: Compressional wave velocities of oceanic rocks, J. Geophys. Res., 78, 5155-5172, 1973.

Gerard, R., M. Langseth, and M. Ewing, Thermal gradient measurements in the water and bottom sediment of the western Atlantic, J. Geophys. Res., 67, 785-803, 1962.

Heezen, B.C., R.D. Gerard, and M. Tharp, The Vema fracture zone in the equatorial Atlantic, J. Geophys. Res., 69, 733-739, 1964.

Heezen, B.C., and M. Tharp, The physiographic diagram of the South Atlantic, the Caribbean, the Scotia Sea, and the eastern margin of the South Pacific Ocean, The Geological Society of America, New York, 1961.

Houtz, R., and J. Ewing, Upper crustal structure as a function of plate age, J. Geophys. Res., in press, 1976.

Keen, C., and C. Tramontini, A seismic refraction survey on the mid-Atlantic ridge, Geophys. J. Roy. Astr. Soc., 20, 473-491, 1970.

Langseth, M.G., Jr., X. Le Pichon, and M. Ewing, Heat flow through the Atlantic Ocean floor and convection currents, J. Geophys. Res., 71, 5321-5355, 1966.

Melson, W.G., and G. Thompson, Petrology of a transform fault zone and adjacent ridge segments, Phil. Trans. Roy. Soc., A, 268, 423-441, 1971.

Poehls, K., Seismic refraction on the mid-Atlantic ridge at 37°N, J. Geophys. Res., 79, 3370-3373, 1974.

Robb, J.M., and M.F. Kane, Structure of the Vema fracture zone from gravity and magnetic intensity profiles, J. Geophys. Res., 80, 4441-4445, 1975.

Scientific Staff, Leg 39 examines facies changes in South Atlantic, Geotimes, 20(3), 26-29, 1975.

Sclater, J.G., R.N. Anderson, and M.L. Bell, Elevation of ridges and evolution of the central eastern Pacific, J. Geophys. Res., 76, 7888, 1971.

Talwani, M., C.C. Windisch, and M.G. Langseth, Reykjanes ridge crest: A detailed geophysical study, J. Geophys. Res., 76 (2), 473-517, 1971.

Vacquier, V., and R.P. von Herzen, Evidence for connection between heat flow and the mid-Atlantic ridge magnetic anomaly, J. Geophys. Res., 69, 1093-1101, 1964.

van Andel, Tj. H., Recent uplift of the mid-Atlantic ridge south of the Vema fracture zone, Earth Planet. Sci. Lttrs., 7, 228-230, 1969.

van Andel, Tj. H., J.B. Corliss, and V.T. Bowen, The intersection between the mid-Atlantic ridge and the Vema fracture zone in the North Atlantic, J. Marine Res., 25, 343-351, 1967.

van Andel, Tj. H., J.D. Phillips, and R.P. von Herzen, Rifting origin for the Vema fracture in the North Atlantic, Earth Planet. Sci. Lttrs., 5, 296-300, 1969.

van Andel, Tj. H., R.P. von Herzen, and J.D. Phillips, The Vema fracture zone and the tectonics of transverse shear zones in oceanic crustal plates, Marine Geophys. Researches, 1, 261-283, 1971.

von Herzen, R.P., and G. Simmons, Two heat flow profiles across the Atlantic Ocean, Earth Planet. Sci. Lettrs., 15, 19-27, 1972.

Whitmarsh, R., Median valley refraction line, mid-Atlantic ridge at 37°N, Nature, 246, 297-298, 1973.

Whitmarsh, R.B., Axial intrusion zone beneath the median valley of the mid-Atlantic ridge at 37°N detected by explosion seismology, Geophys. J. Roy. Astr. Soc., 42, 189, 1975.

Bonatti, E., and J. Honnorez, Sections of the earth's crust in the equatorial Atlantic, preprint, 1976.

Ludwig, W.J., and P.D. Rabinowitz, Results of IPOD site surveys aboard R/V VEMA cruise 32-06: Part A. Data report, Lamont-Doherty Geological Observatory, Tech. Rept. CU-1-75, 70 pp., 1975.

Tramontini, C., and D. Davies, A seismic refraction survey in the Red Sea, Geophys. J. Roy. Astr. Soc., 17, 225-241, 1969.